

Summer 2022

Using Geochemical Composition to Determine Paleo Environmental Conditions and Source Inputs In Paleozoic Rocks Within The Central Kansas Uplift USA

Christiana Fumnanya Eziashi
Fort Hays State University, christyeziashi@gmail.com

Follow this and additional works at: <https://scholars.fhsu.edu/theses>



Part of the [Geochemistry Commons](#), [Geology Commons](#), [Sedimentology Commons](#), and the [Stratigraphy Commons](#)

Recommended Citation

Eziashi, Christiana Fumnanya, "Using Geochemical Composition to Determine Paleo Environmental Conditions and Source Inputs In Paleozoic Rocks Within The Central Kansas Uplift USA" (2022). *Master's Theses*. 3204.

DOI: 10.58809/TBUB8539

Available at: <https://scholars.fhsu.edu/theses/3204>

This Thesis is brought to you for free and open access by FHSU Scholars Repository. It has been accepted for inclusion in Master's Theses by an authorized administrator of FHSU Scholars Repository. For more information, please contact ScholarsRepository@fhsu.edu.

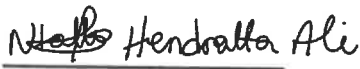
USING GEOCHEMICAL COMPOSITION TO
DETERMINE PALEO ENVIRONMENTAL AND
SOURCE INPUTS IN PALEOZOIC ROCKS
WITHIN THE CENTRAL KANSAS UPLIFT,
USA

A Thesis Presented to the Graduate Faculty of the
Fort Hays State University, in Partial Fulfilment of
the Requirements for the Degree of Master of
Science

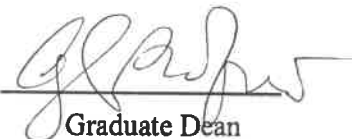
By

Christiana Fumnanya Eziashi
B.Sc. Delta State University
FHSU Graduate College

Date July 18, 2022

Approved 
Major Professor

Date 07/21/2022

Approved 
Graduate Dean

GRADUATE COMMITTEE APPROVAL

The Graduate Committee of Christiana Fumnanya Eziashi hereby approves his thesis as meeting partial fulfilment of the requirements for the Degree of Master of Science in Geosciences.


Chair, Supervisory Committee

Tom C. Schafer
Supervisory Committee


Supervisory Committee

DR. PRIDE ABONGWA

Supervisory Committee

July 8, 2022

On this day of

ABSTRACT

Paleoenvironmental conditions, sediment characteristics and lateral continuity using chemostratigraphy are not well established for stratigraphic units associated with some small fields within the Central Kansas Uplift (CKU). Samples of drill cuttings recovered from six wells (Hottman #1, and Hottman-Furthmeyer#1, Yocemento #1, Mong Benno #2, Rhian #3 and Worcester #1) at 10 ft intervals between 3150 ft and 3900 ft below ground level, were processed and analyzed using X-ray fluorescence (XRF) and X-Ray diffraction (XRD). The XRF technique was used to determine elemental compositions, and XRD was used to determine mineral content. The composition of the rock cuttings was used to characterize sediments and assess paleoenvironmental conditions and source inputs.

Cross plots of detrital elements which includes Titanium (Ti), Potassium (K), and Zirconium (Zr) against Aluminum (Al), show a strong positive relation, which account for about 30% of the total elemental composition. Carbonate proxies, Magnesium (Mg), Calcium (Ca), and Strontium (Sr) show strong positive correlations with each other indicating a common source, and collectively account for 70% elemental composition. This observation supports the XRD data that shows that the analyzed interval is mainly carbonate with minor amounts of detrital inputs. Principal component Analysis (PCA) shows clusters of various elements which supports the cross plots of the carbonate and detrital proxies. Phosphorous (P), a measure of paleo-productivity ranged from 0.18% to 0.36% with a mean of 0.25% across six wells, well above crustal abundance of 0.01%. This significant enrichment of P is interpreted to indicate relatively high paleo-productivity. An analysis of downhole variation in Zr/Rb ratio across the six wells revealed two distinct zones, a coarse-grained zone and a fine-grained zone which suggest the presence of two major energy regimes (high and low) during deposition.

ACKNOWLEDGMENT

I sincerely want to say a very big thank you to my Advisor Dr. Hendratta Ali for giving me the opportunity to work under her tutelage. This has set a milestone for my journey as a researcher and seasoned geoscientist. I would like to thank Dr Henry Agbogun, Dr Thomas Schafer and Dr Pride Abongwa, for serving in my supervisory committee and taking out time to review my thesis. Also, I would like to thank Dr. Keith Bremer and Dr Todd Moore for their guidance and support throughout this research process.

I would like to thank the Department of Geosciences, Fort Hays State University for the privilege accorded to me to become a graduate student and work as a teaching assistant in the department. I also express gratitude to the Atoka Geochemical Services for analyzing my data.

Finally, I would like to thank my family and friends for their moral support and all the people who have shown interest in my research especially Dr. Jude Ogala who gave me insights on how to carry out this research. Most importantly, I would like to thank God almighty for his Grace, Strength, and mercies throughout my graduate school journey.

TABLE OF CONTENT

ABSTRACT	i
ACKNOWLEDGMENT	ii
TABLE OF CONTENT	iii
LIST OF FIGURES	v
LIST OF TABLES	vi
1.0 INTRODUCTION	1
1.1. Background	2
2.0 PREVIOUS WORK.....	4
2.1 Geochemical Proxies	4
2.1.1. Grain Size Proxies	4
2.1.2. Detrital Proxies	5
2.1.3. Carbonate Proxies	5
2.1.4. Paleo Productivity proxy.....	6
2.1.5. Chemostratigraphy.....	7
2.1.6. Paleoenvironmental Conditions.....	8
2.2. Study Area.....	9
2.3 Geological Background of Study Area.....	10
2.3.2. Stratigraphy and Sedimentary Geology	11
2.3.3. The Arbuckle Group	11
2.3.4. The Simpson Group	11
2.3.5. The Lansing-Kansas City Group	12
3.0 MATERIALS AND METHODS	13
3.1. Materials.....	13
3.2. Analytical Methods.....	13
3.2.1. Sample Analysis	13
3.2.2. Basic Principles of X-Ray Florescence and X-Ray Diffraction Techniques	13

3.2.2.1. X-Ray Florescence (XRF) Technique.....	13
3.2.3. X-Ray Diffraction (XRD)	14
3.2.4. Data Processing	14
3.3. Statistical Analysis.....	15
4.0 RESULTS AND INTERPRETATION.....	16
4.1 Results.....	16
4.1.1 Variation in Elemental Content	16
4.1.2. Variation of major elements across wells	17
4.1.3 Downhole variation of trace elements	18
5.0. Discussion	22
5.1. Source Inputs.....	22
5.2.1. Paleo environmental Conditions.....	23
6.0 CONCLUSION	30
7.0 REFERENCES	31
8.0 APPENDIX	1

LIST OF FIGURES

Figure 1: The figure above shows the study area and the subsurface structures within the state of Kansas. The red shaded squares show the location of Graham County with Rhian #3 and Worcester #1, red box shows Trego County with Mong Benno #2, Ellis County with Yocemento Benno #1, Hottman #1, and Hottman- Furthmeyer #1, and Graham County with Rhian and Worcester wells 10

Figure 2: Stratigraphic column of Paleozoic interval in the study area. Enlarged section show the intervals present in the study location adapted from Cansler and Carr (2002). 12

Figure 4: Map showing Location of Study Area..... 16

Figure 5: Distribution of elemental content of rock samples from a Paleozoic interval in the CKU (a): Hottman #1; (b): Hottman-Furthmeyer #1; (c): Mong Benno #2; (d): Yocemento #1; (e): Rhian #3 (f): Worcester #1. 17

Figure 6: Downhole variation of major elemental distribution of sediments within the Paleozoic interval (a): Hottman #1; (b): Hottman-Furthmeyer #1; (c): Mong Benno #2; (d): Yocemento #1; (e): Rhian #3 (f): Worcester #1..... 18

Figure 7: Downhole plots illustrating variation of trace elemental distribution of sediments within the Paleozoic interval (a): Hottman #1; (b): Hottman-Furthmeyer #1; (c): Mong Benno #2; (d): Yocemento #1; (e): Rhian #3 (f): Worcester #1. 19

Figure 8: Chart showing the distribution of mineral content of sediments within the Paleozoic interval (a): Hottman #1; (b): Hottman-Furthmeyer #1; (c): Mong Benno #2; (d): Yocemento #1; (e): Rhian #3 (f): Worcester #1. 20

Figure 9: Downhole plots showing variation in mineralogical content of selected minerals plotted against depth from Paleozoic interval within the CKU. a: Hottman #1 minerals; b: Hottman-Furthmeyer #; c: Mong Benno #1 minerals; d: Rhian #3 minerals; e: Yocemento minerals; f: Worcester minerals. 21

Figure 10: Cross plots of Al against detrital element illustrating the presence of detrital input within the formation in the Paleozoic interval (a): Hottman #1; (b): Hottman-Furthmeyer #1; (c): Mong Benno #2; (d): Yocemento #1; (e): Rhian #3 (f): Worcester #1. Aluminum is on the X axis in all plots, values of elements increase as Aluminum increases upwards. 23

Figure 11: Cross plots of Mg/Ca; Mg/Al against Ca/Al; Sr/Ca, Sr/Al against Ca/Al illustrating the presence of Carbonate input within the formation in the Paleozoic interval (a): Hottman #1; (b): Hottman-Furthmeyer #1; (c): Mong Benno #2; (d): Yocemento #1; (e): Rhian #3 (f): Worcester #1. 24

Figure 12: Paleo productivity proxies within the Paleozoic interval illustrating the amount of paleo productivity in the formation (a): Hottman #1; (b): Hottman-Furthmeyer #1; (c): Mong Benno #2; (d): Yocemento #1; (e): Rhian #3 (f): Worcester #1 25

Figure 13: Grain size proxies within the Paleozoic interval illustrating the grain size of the sediments in the formation. An increase in Zr/Rb shows a coarser grain size and vice versa... 27

Figure 14: Principal component analysis using major elements in the formation 28

LIST OF TABLES

Table 1: Showing the Latitude and Longitude locations of the wells.....4

1.0 INTRODUCTION

The study of elemental composition and mineral content is crucial in understanding the composition of the rocks which they formed from, the processes and environments which the sediments formed. The understanding of the information about rocks, processes, and the environments in which formed can be used to describe and interpret paleoenvironmental conditions, source inputs and provenance. The elemental composition and mineral content of a known lithostratigraphic units add further insights about unique characteristics such as how the rock types were deposited, source inputs and conditions present during deposition and how these conditions have changed over time.

Within the CKU, the Paleozoic interval is mostly composed of cyclotherms made of succession of majorly carbonate rocks with intercalations of the siliciclastic (sands and shale) rocks of varying thickness. Therefore, chemostratigraphic characterization of well data within the CKU using XRF and XRD analysis will generate a rich source of information about the detailed chemical composition of the rocks in the area (CKU) and contribute to a better understanding of the stratigraphy for the subsurface applications such as energy and groundwater exploration.

Studies have focused on the geology and lithostratigraphy, but a few have involved a study of the chemostratigraphy of the CKU. For examples, Jewett and Marriam, 1959; studied the geological framework of Kansas and based on their studies, the sedimentary rocks in CKU have a thickness of about 5,000 feet over the Precambrian basement structure and are truncated on the flanks by pre-Pennsylvanian strata and entirely removed locally on crest and overstepped by the Pennsylvanian beds. However, other studies focused on Chemical stratigraphy using geochemical proxies such as Rogala et al., 2007 who carried out lithostratigraphic and chemostratigraphic characterization of core samples from the Mesoproterozoic Sibley Group.

Various authors interpreted geochemical trends based on the elemental and mineralogical compositions of sedimentary rocks. For example, Liu et al., 2002; Driskill et al., 2018;

Tribovillard et al., 2006. Liu et al., (2002) used Zr/Rb ratio as a grainsize proxy to study loess plateau of central China during the last 130000 years and its implications for winter monsoon. Based on their research, Zr/Rb ratio increases when grain size is coarser and decreases when grain size is finer. The ratio can also be used to eliminate the effect of weather and pedogenesis. Driskill et al., (2018) described the chemical stratigraphy of a complex, heterolytic section which comprises of cycles that are basically at or below log scale using core observation, high-resolution XRF geochemical data and supplemental datasets. Driskill et al., (2018) employed detrital proxies such as Al, Si, Fe and K, carbonate proxies such as Ca and Mg and grain size proxies such as Zr/Rb to investigate source characteristics. Based on the studies of Driskill et al, Al, Si, Fe and K were identified as detrital elements and they correlate positively with each other, elements associated with carbonate minerals correlate positive with other, Zr/Rb ratio which was used as the grainsize proxies show two coarser grainsize as the ratio increases and finer grainsize as the ratio decreases. Tribovillard et al., (2006) used the composition selected trace element to interpret reconstruct paleo productivity and paleo redox conditions. Based on their research, enrichment of U, V and Mo suggests anoxic-euxinic environments and depletion suggests oxic environment.

The goal of the study is to assess the characteristics and conditions of deposition of a Paleozoic Interval of rocks within the CKU. The objective is to describe the elemental composition and mineral content of a Paleozoic sequence to investigate the conditions under which the sediments were deposited, to determine source inputs, and sedimentary processes.

Although several studies have been done to investigate the sedimentary geology and stratigraphy within the CKU, there is still a need to explore the use of elemental composition and mineral content to study the conditions of depositions of rocks within the CKU.

1.1. Background

Paleozoic rocks within the CKU are of great significance in the state of Kansas because all commercial oil and gas within the state comes from these rocks (Hilpman, 1958; Goebel, 1958; Merriam and Goebel, 1959a, 1959b, 1960) except for a part of the Precambrian rocks that

originated from the Paleozoic. The Permian and Pennsylvanian units comprise of thin bedded, alternating marine and non-marine sediments which could be sand and shale intercalations. To interpret Paleoenvironmental conditions, geochemical proxies are employed as indirect methods. These proxies have been used by recent researchers to indirectly interpret paleoenvironmental conditions, describe and characterize sediments (Tribovillard et al., 2006). The use of geochemical proxies necessitates chemical analysis of geological samples and these proxies have been used in various parts of the world to investigate paleoenvironmental conditions and sediments characteristics during deposition. However, describing sediments characteristics and assessing the paleo environmental conditions within the CKU using geochemical proxies needs to be explored.

2.0 PREVIOUS WORK

Elemental ratios and abundances can be used as proxies to interpret chemical stratigraphy, paleo productivity, and paleoenvironmental conditions.

2.1 Geochemical Proxies

Geochemical proxies are distinct elements and elemental ratios that indicate a particular geologic events or processes in geologic history. Some proxies are indirect indicators for the reconstruction of paleo environments, Gornitz, 2009, such as grain size proxies (Zr and Rb) which are elements that are associated and persistent where sediments with fine or coarse grainsizes are found. Detrital proxies (Al, Ti, K, Si, and Fe) comprise of elements that are associated with minerals that are conservative, persistent, and ubiquitous in the environment.

Organic proxies include paleo-redox which comprises of Uranium, Thorium, and Molybdenum which are enriched or depleted in either oxidizing or reducing environment Tribovillard et al., 2006. Paleo productivity proxies such as P is used because it is part of the nutrients living organism need to survive. Hence, an environment that is enriched in P indicates that living organism thrived at some point.

2.1.1. Grain Size Proxies

Grain size proxies are indicators of a particular grainsize, they comprise of elements that are used to indirectly interpret the grainsize of sediments. Although, Petrographic and thin section analysis can be used to study grainsizes as well as their textural characteristics, the studies of grainsize using elements using geochemical proxies gives an insight to the overall grain size pattern in a formation as such zones with finer grainsize and be distinguished from zones with coarser grain sizes. According to Rothwell 2015, Zr/Rb and Ti/Al are grain-size proxies because Zr resides mainly in coarser grains and Rb in clays. Zr/Rb has been used to reconstruct river flood histories, as floods carry greater coarse-grain sediment loads, Zr/Rb increases in flood events (Wang et al. 2011). The higher the Zr/Rb peaks, the more significant coarse particles deposited by saltation processes. Grainsize variations were analyzed using Zr/Rb ratios on the Loess Plateau of Central China during the last 130000 years and its

implication for winter monsoon (Liu et al., 2002). An increase in Zr/Rb ratio showed a coarser grain size, and a decrease in the ratio showed a finer grain size. Due to the immobility of the two elements during the post-depositional process, Zr/Rb can eliminate the effect of weathering and pedogenesis (Liu et al., 2002). The conservative nature of Zr and Rb makes them resistant to post-depositional process. Furthermore, Rothwell and Croudence 2015a, explained that silicon (Si), Aluminum (Al), Potassium (K), Iron (Fe), and Titanium (Ti) are commonly used as proxies for basinal terrigenous materials and grain sizes. They are also commonly found in minerals that comprise primarily detrital materials that are shed into basins regardless of grain size.

2.1.2. Detrital Proxies

Detrital proxies are inorganic indicators of detrital materials in sediments. Elements used for the interpretation and measurement of detrital proxies include Ti, Si, K, Fe, and Al. Other detrital elements, including Uranium, Rubidium, Sodium, and Chromium, are less significant but very useful in interpreting detrital input in a basin because they are associated with clay minerals.

Silicon (Si) and Sodium may be detrital, derived from mechanical weathering of crustal rocks, or biogenic, derived from siliceous phytoplankton (diatoms, silicoflagellates), protozoans and protists (radiolarians and ebridians), plant phytoliths, some scolecodonts (polychaete worm jaws), and sponge spicules (Blanchet et al. 2007; Kleiven et al. 2007). Normalization using a detrital divisor can distinguish detrital or biogenic origin.

2.1.3. Carbonate Proxies

Carbonate proxies are indirect methods of measuring the presence of carbonate input in sediments examples of carbonate proxies include Mg, Ca, and Sr. Interpreting carbonate proxies helps to distinguish the source of the carbonate minerals present in the sediment for example minerals that are low in Mg and high calcite may not correlate with each other. Also, there could be an impact of detrital materials in a carbonate mineral and normalization helps to remove the influence of the detrital materials. Mario et al 2020 used Mg/Ca and Sr/Ca ratios to correct for Global variability in seawater. Results of the analysis suggest that modern variability should be

considered. Based on their research, Mg/Ca and Sr/Ca ratios show a positive correlation with each other, indicating a substantial seawater interaction with biogeochemical processes.

In another study by Stephen. et al., 2004, They reconstructed temperature for the Last Glacial Maximum (LGM) based on planktonic Mg/Ca ratios were interpreted. Mg/Ca ratio thermometry was described to illustrate the state of the method used. Foraminifera Mg/Ca ratios with temperature, including culture, trap, and core top, were analyzed. Based on the study, the dissolution of foraminiferal calcite at the seafloor caused the lowering of Mg/Ca ratios. Advantages of Mg/Ca thermometry over paleotemperature proxies, including its use to investigate changes in the oxygen isotopic composition of seawater, were also highlighted.

According to Huber et al. 2017, carbonate minerals such as aragonite or calcite are included in the marine sedimentary record at the seawater-sediments interface. Carbonate elements such as Ca and Mg associating with carbonate rocks may have a biogenic origin and hence are used as proxies to interpret the carbonate and biogenic input in the sediments. In this study, Mg, Ca, and Sr was used to interpret diagenetic reactions in marine sediments, such as recrystallization of carbonates. Results showed that there is significant siliciclastic input than the carbonate input as indicated by the significantly lower carbonate-rich sediments.

2.1.4. Paleo Productivity proxy

Paleo- productivity proxies are indicators such as elements that are used to interpret and measure the presence of organic matter in a sediment and environment. Phosphorus, like nitrogen, is an essential nutrient needed by all forms of life on Earth. According to Tribovillard et al., 2006, elements that have only one oxidation state, such as Phosphorus (P), are used to interpret the level of paleo productivity in sediments because it suggests that the sediments were deposited in a conducive environment that allowed organic matter to thrive and this impacts the sedimentary record of rocks generally because it gives an insight to the conditions present during deposition.

P is soluble under reducing conditions and may be lost from oxygen-deprived sediment. The primary source of Phosphorus in sediments is the Phytoplankton necromass which gets to the sediment-water interface. The crustal abundance of Phosphorus is 0.01%, but this abundance can be higher in most marine sediments and sedimentary rocks (Mackenzie et al., 1993). The abundance of P could be attributed to the presence of organic matter in the sedimentary rocks. Furthermore, the amount of Phosphorus in sediments is dependent on the amount of organic matter present in that sediment which also suggests the amount of productivity in that sediment. Organic matter dies and decay in sediments, and a measure of the amount of P present in that sediments gives an idea of ancient (paleo) productivity in that sediment.

2.1.5. Chemostratigraphy

Chemostratigraphy is a relatively new branch of stratigraphy. It is the study of strata based on variations in elemental composition. Chemostratigraphy uses temporal and spatial variations in geochemical attributes (elemental compositions, ratios, isotopic ratios, and elemental oxide ratios) to study sedimentary rocks. However, within the CKU, only a few works have been done using chemostratigraphic principles. Chemostratigraphic study is an important aspect of stratigraphy because it gives an insight of the temporal and spatial variations of geochemical attributes such as compositions, isotopic ratio, elemental and or elemental oxide ratios (Stratigraphy lecture note, Agbogun H.M., 2022). Chemostratigraphy helps to identify areas with distinct geochemical signatures that can be correlated on a spatial and temporal scale, these areas are referred to as chemofacies. Cyclic, secular, and irregular trends and patterns which are seen in lithostratigraphic studies can also be identified based on variations in geochemical profiles.

Chemostratigraphy variability of the eagle ford shale, South Texas, gave insights into the paleo redox and sedimentary facies changes. Variability in elemental compositions was used to interpret sediment source, mineralogy, depositional environment, and lateral continuity when

integrated with other datasets such as Total Organic Carbon (TOC) (Beau M.T. et al. 2016, Ratcliffe et al.).

Chemostratigraphy of the Eagle Ford and woodbine groups, Brazos Basin, Texas, was done and used in a sequential analysis to characterize five chemofacies across ten core samples. Based on their interpretation, the chemofacies identified includes argillaceous, organic matter poor, transitional-organic matter poor, transitional-organic matter moderate, calcareous, organic matter rich and calcareous, organic matter-moderate (Melissa, 2019).

Lithostratigraphic and chemostratigraphic characterization of core samples from the Mesoproterozoic Sibley Group was established to interpret geochemical trends using the elemental and mineralogical compositions of the core data (Rogala et al. 2007).

2.1.6. Paleoenvironmental Conditions

Paleo environmental conditions the biological, chemical, and physical conditions that have been preserved in rocks found environments of past geologic ages (Paleoenvironmental analysis, AAPG Wiki., 2022). These conditions include the energy of deposition, weathering, productivity, and oxidation state and the indicators that infer paleoenvironmental conditions include grain size, source characteristics and inputs of the sedimentary rocks.

Paleoenvironmental conditions are commonly studied by interpreting geochemical attributes. However, they can also be studied by interpreting other characteristics in rocks such as the sedimentary structure and rock type. Algeo and Tribollivard 2009, used U and Mo covariation to carry out environmental analysis of palaeoceanographic system. Based on their study, U and Mo were abundant which suggests the prevalence of anoxic condition. Driskill et al., 2018 used grain size proxy as a tool to study paleoenvironmental condition during deposition. Based on their study, coarser grain size zone suggests the prevalence of high energy and vice versa.

Environmental parameters that control trace-element distributions in modern and ancient sediments have been studied to analyze the enrichment mechanism of some elements and their

associated advantages and disadvantages using paleo redox proxies (Tribollivard et al., 2006). The authors integrated how trace-element such as Rubidium, Molybdenum and Uranium enrichment/depletion could reconstruct paleo depositional conditions, emphasizing paleo-productivity and paleo-redox. According to their research, Mo and U are enriched in anoxic/reduced environment and depleted in oxic/oxidizing environment (oxygen rich) which invariably suggests that the enrichment of Mo and U may be common in marine environments and depletions mainly occur in oxic environments.

Past geologic conditions such as the energy of deposition, weathering, productivity, and oxidation state have been identified using geochemical proxies such as redox proxies to determine the geochemistry of modern oxic and anoxic marine sediments and infer their implications relating to geological records (Calvert, 2010). In addition, these proxies give an insight into the amount of oxygen present and how it affects the system.

Geochemical analytical methods and petrographic studies were used to interpret variations in sediment fluxes, redox conditions, and productivity of outcrop samples from the Permian-Triassic Panthalassic Ocean (Algeo et al., 2011).

2.2. Study Area

The study area covers three counties in Central Kansas (USA). These counties include Graham, Trego, and Ellis, as shown in Figure 1. The three counties are located between Latitude 38.98469 and -99.432347 to 39.040603 and -99.321157). For this research, six Southeast-Northwest trending wells (Hottman #1 and Hottman-Furthmeryer #2, Mong Benno #2 Yocemento Benno # 1, Rhian #3, and Worcester #1,) from which the drill cutting samples were obtained. These six wells are within the Central Kansas Uplift.

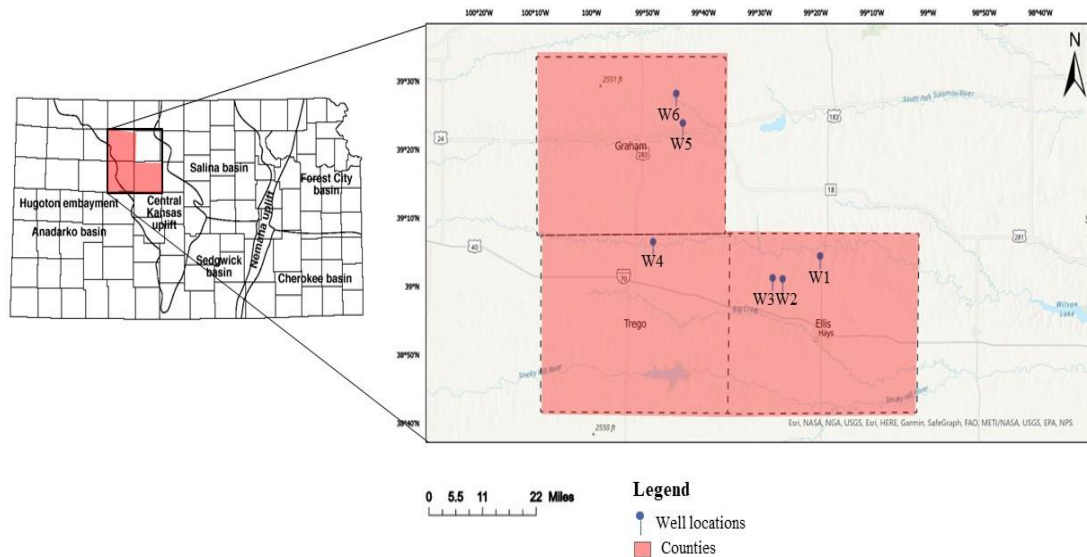


Figure 1: The figure above shows the study area and the subsurface structures within the state of Kansas. The red shaded squares show the location of Graham County with Rhian #3 and Worcester #1, red box shows Trego County with Mong Benno #2, Ellis County with Yocemento Benno #1, Hottman #1, and Hottman- Furthmeyer #1, and Graham County with Rhian and Worcester wells

2.3. Geological Background of Study Area

Rocks within the Paleozoic interval are associated with the Permian, Pennsylvanian, Mississippian, Devonian, Silurian, Ordovician, and Cambrian systems. These Paleozoic systems are represented in Kansas although some the series are not completely developed or entirely absent. The CKU consists of Permian and Pennsylvanian deposits which comprise of thin bedded marine and non-marine sediments deposited mainly in shelf-type marine environments. The Permian and Pennsylvanian rocks consist of the cyclic Lansing-Kansas City group which are made up limestones, dolomites, shales, and sandstones. The Mississippian-Devonian systems are seen mostly in the entire state, consisting of majorly carbonates sequences. The Mississippian-Devonian rocks have the smallest areal distribution unit because they were eroded from the CKU during the tectonic activities that occurred during that age. Cambrian and Ordovician rocks which include Dolomite and sandstone unconformably overlies the Precambrian rocks are found throughout the state of Kansas, except at the higher parts of the Uplift.

2.3.2. Stratigraphy and Sedimentary Geology

Rocks of the Central Kansas Uplift are five series (in descending order): Virgilian, Missourian, Desmoinesian, Atokan, and Morrowian have been identified as shown in figure 2, and the lithologic units consists of alternating limestone, and non-marine deposits (Moore, 1949a).

Three major unconformities have been identified with the CKU. First, the unconformity between the late Precambrian and early Cambrian, marked the nonconformity between the Precambrian basement rocks and the Arbuckle. Second, the unconformity marked by an erosional surface between the late Devonian and early Mississippian resulted in a disconformity between Simpson and the Arbuckle group. Third, the unconformity between the late Mississippian and early Pennsylvanian resulted from an erosional surface between them, marking the disconformity between the Simpson and Lansing- Kansas City groups (Merriam, 1963).

2.3.3. The Arbuckle Group

The Arbuckle group is found primarily in the western part of Kansas. The Arbuckle is Ordovician- Cambrian in age and the thickness ranges from 3200 to 4600 feet. The group consists mainly of dolomite and is white, light grey, and brown in color (Frenseen et al., 2004). Rocks found within the Arbuckle group are dense and crystalline and their thickness increases towards the eastern and southwestern part of Oklahoma.

2.3.4. The Simpson Group

The Simpson Group unconformably overlies the Arbuckle group. Within Kansas, the group is in the south-central region with thinner layers in a few areas of the CKU (Newell et al., 1987). The Simpson group is divided into the upper Platteville formation and the lower St. Peters Sandstone formation. During the Late Mississippian to Early Pennsylvanian tectonism, most of the Simpson group was removed from the CKU (Merriam, 1963) and the tectonism resulted in erosional truncation fault reactivation.

2.3.5. The Lansing-Kansas City Group

The Lansing- Kansas City (LKC) Group is part of the Missourian series, which conformably overlies the Pleasanton Group consisting mainly of alternating limestone and shale beds (Kansas Geological Survey, 2002). LKC can be identified either as a separate group or as a single group because they both have similar characteristics. However, there is an unconformable contact at the upper part of the Lansing group, removed by erosion. The thickness of the LKC ranges between 20 to 350 feet, they contain 12 formations and 27 members comprising marine limestone and non-marine clastics and most of the limestones are algal, cross-bedded, and oolitic (Parkhurst,1959b).

2.3.6. The Shawnee groups

The Shawnee group is part of the Virgilian series. It consists mainly of seven formations; four limestone packs separated by three shales. The Heebner shale is the most important of the three shales because it is a marker bed that is laterally continuous over a large area. This marker bed is used for structural and stratigraphic interpretations (Merriam and Jewett, 1956).

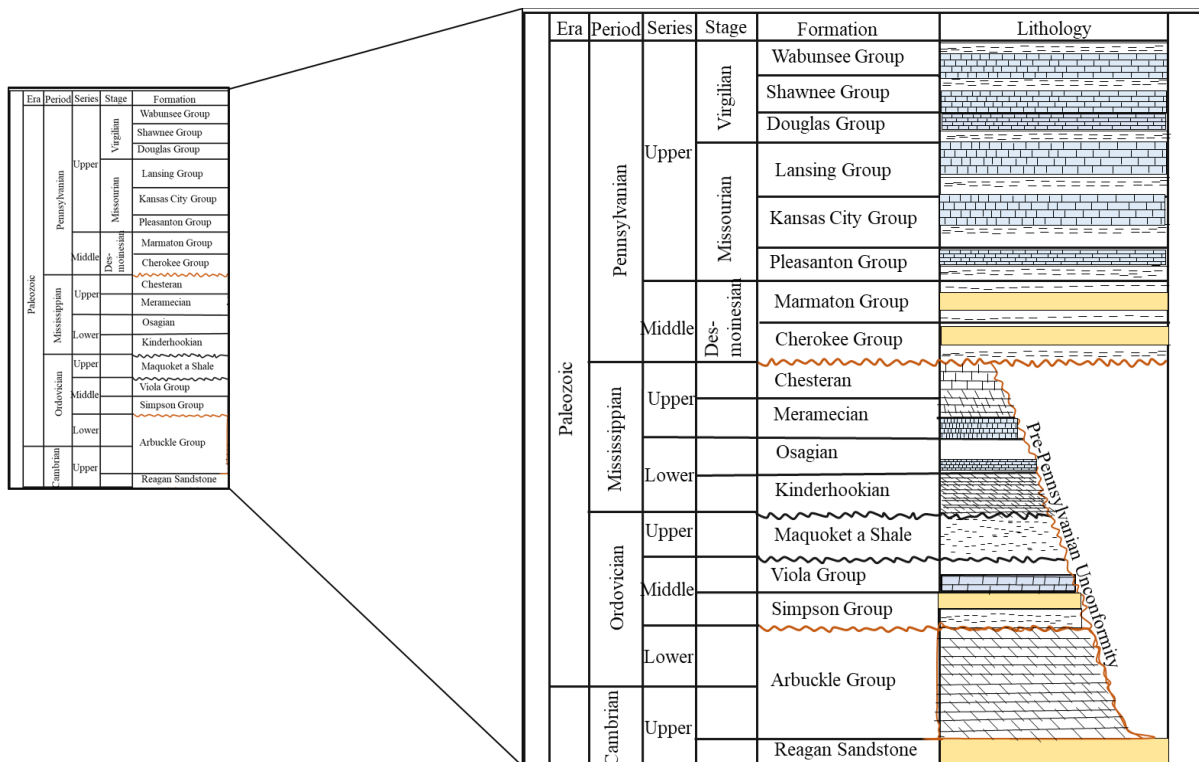


Figure 2: Stratigraphic column of Paleozoic interval in the study area. Enlarged section show the intervals present in the study location adapted from Cansler and Carr

3.0 MATERIALS AND METHODS

3.1. Materials

Materials include drill cuttings samples that were obtained from six (Hottman #1, Hottman-Furthmeyer #1, Mong Benno #3, Yocemento #1, Rhian #3 and Worcester #1) wells which are 3 – 10 miles apart at an interval of 10ft within the Central Kansas Uplift. The Spatial distribution of the Southeast-Northwest trending wells which includes the Hottman #1 well, which is about 5miles away from the Hottman-Furthmeyer #1 well, followed by the Yocemento #2 well, Mong Benno #2 well, Rhian #3 and then the Worcester #1 well. The drill cutting sampling interval ranges from 3100ft-3870ft, 3310ft-3530ft, 3600ft-4285ft, 3150ft-3870ft, 3150ft-3800ft, 3150ft-3890ft, 3150ft-3890ft, for Worcester #1, Rhian #3, Mong Benno #2, Yocemento Benno #, Hottman #1 and Hottman-Furthmeyer #2 respectively.

3.2. Analytical Methods

The analytical methods used in this research involve X-ray diffraction and X-ray florescence techniques used in analyzing the drill cutting samples and the statistical techniques used in analyzing the data.

3.2.1. *Sample Analysis*

The drill cutting samples were analyzed by the Atoka Geochemical Services (AGS) using standard laboratory measurements to decipher the elemental and mineral content of the sediments using X-ray fluorescence (XRF) and X-ray diffraction (XRD) techniques.

3.2.2. *Basic Principles of X-Ray Florescence and X-Ray Diffraction Techniques*

3.2.2.1. X-Ray Florescence (XRF) Technique

XRF is a technique that is used to determine the elemental composition of rocks. When samples are analyzed, X-rays are emitted when excited by a primary X-ray source, the emitted X-rays are detected by a detector. X-rays detected show a characteristic florescent X-ray or a specific signature which is peculiar to a particular element. XRF is a good option for gathering

multi-elemental data because it is fast, inexpensive, non-destructive. In addition, XRF has advantages for collecting high-resolution data from the core (Löwemark et al., 2011). This technique is also applicable when using drill cuttings and other suitable data for analysis using elemental concentrations to model mineralogy, brittleness, and organic content in mudstone-dominated sequences.

In this study, XRF was used to determine the elemental compositions of the samples. The XRF analysis results were reported in values that showed abundances and amounts of the major and trace elements in percentages and Parts Per Million (PPM), respectively.

3.2.3. X-Ray Diffraction (XRD)

X-ray diffraction (XRD) technique is used to determine the mineralogical composition of rocks. The analysis is done by irradiating a sample or material with incident X-rays resulting to scattering angles of the X-rays that emanates from the sample. The intensities of a scattering angle are measured, these intensities are specific to a particular crystallographic structure which gives an idea of the mineralogical composition of the sample. In other words, every mineral has a particular crystal structure and symmetry, therefore when a mineral is subjected to an X-ray diffraction analysis technique, a diffraction of a beam in a specific direction takes place. The measurement of the direction of the constructive beams allows an individual to determine the fundamental properties of the crystalline state, the magnitude of the fundamental unit cell of the crystals and its symmetry.

In this research, XRD was used to carry out an analysis of the mineral phases and concentrations of samples in percentages. The analyzed minerals include Quartz, chlorite, illite calcite, dolomite, feldspar, albite, SiO₂ and the unidentifiable. The unidentifiable includes the minerals that were not detected during the analysis.

3.2.4. Data Processing

Data Quality assurance/Quality control (QA/QC) was done by averaging repeated intervals and taking out extreme outliers. In addition, the depths were corrected to the datum by

the subtraction of the higher ground level values from the lowest ground level value. The QA/QC was done to improve the data quality for proper analysis and interpretation of the results.

3.3. Statistical Analysis

The depths were corrected to the datum, and three major data analytical methods were employed: downhole plots, cross plots, and Principal Component Analysis (PCA). The downhole and cross plots were carried out using Microsoft Excel to interpret paleoenvironmental conditions and investigate lateral continuity in order to assess the conditions present during deposition. Different geochemical proxies were interpreted using elements that are specific to those proxies. Zr/Rb plot was used for grain size proxies (Liu et al., 2002). Ti/Al, Si/Al, K/Al, and Fe/Al plots were used as detrital proxies to interpret detrital input (Driskill et al., 2018). P/Al, and Ca/Al plots were used to decipher paleo-productivity, and Mg/Ca and Sr/Ca plots were used to determine the amount of carbonate in the rock (Mario, 2020). Principal component analysis (PCA) is a multivariate plot used in extracting important information from the data by removing the redundancy to simplify interpretations (Jolliffe, 2002; Gil et al., 2008). PCA allows grouping variables depending on their covariation, thereby reducing the dataset, and revealing the underlying factors affecting the distribution of elements in the drill cuttings. In this study, PCA used group elements to interpret detrital and carbonate source inputs. Elements associated with detrital minerals (Al, K, Ti, Si and Fe) plotted together which indicate that they are from the same source and elements associated with carbonate minerals which includes (Sr, P, Mg and Ca) which suggests that they are from the same source.

4.0 RESULTS AND INTERPRETATION

4.1 Results

This section highlights the X-ray fluorescence and X-ray diffraction analysis results, which consists of major, trace and rare earth elemental abundances, and mineral phases and concentrations of the samples in percentages from the Southeast - Northwest trending wells (one to six) as shown in figure 4.

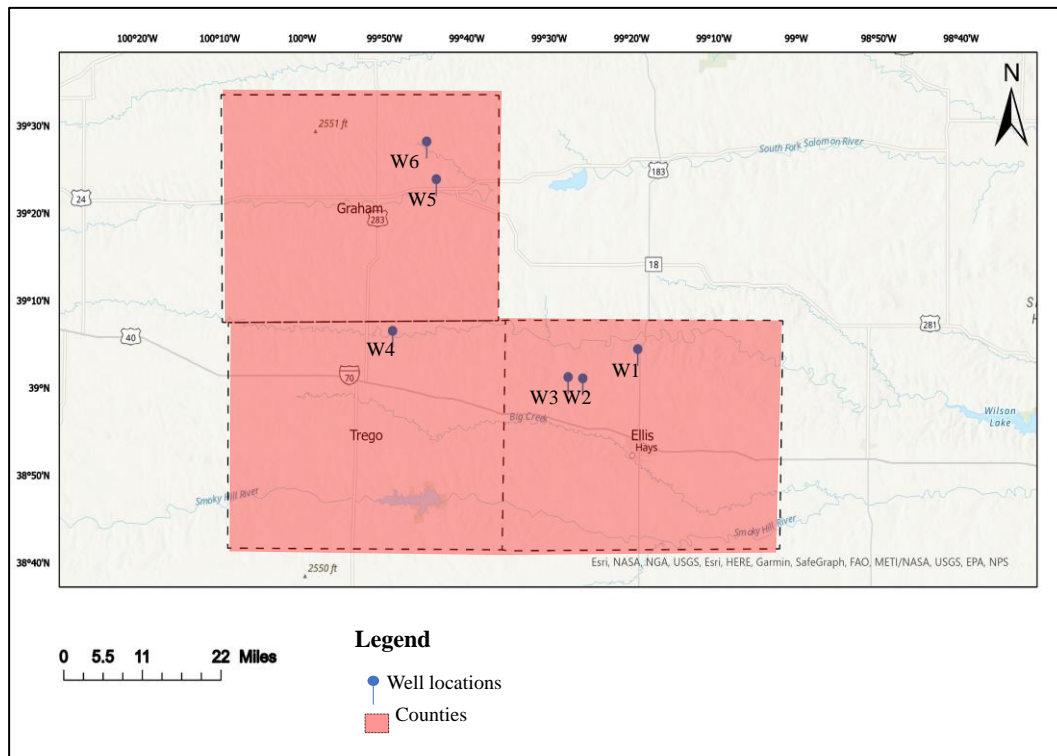


Figure 4: Map showing Location of Study Area

4.1.1 Variation in Elemental Content

The full suite of major, trace and rare earth element analysis for the tables showing the results of the Hottman #1, Hottman-Furthmeyer #1, Yocemento #1, Mong Benno #2, and Rhian #3 (well two to six) are in the appendix. The most abundant elements are Calcium (Ca), Aluminum (Al) and Silicon (S). However, other elements include Magnesium (Mg), Phosphorus (P), Potassium (K), Iron (Fe), Chromium (Cr), Titanium (Ti), Sulfur (S), Manganese (Mn), Zinc (Zn), Arsenic (As), Strontium (Sr), Zirconium (Zr), Molybdenum (Mo), Lead (Pb), Thorium

(Th), Yttrium (Y), and Niobium (Nb). Across the six wells, Ca content ranged from 1 - 39 wt.%, Al content ranged from 1 – 7 wt. %, and Si content ranged from 2 – 26 wt.% as shown in table 1.

Table 1: Showing range of elemental abundances in percentages across the six wells

	W1	W2	W3	W4	W5	W6
Ca	3 - 34	8 - 38	11 - 33	1 - 39	11 - 29	2 - 31
Al	1 - 6	1 - 5	1 - 4	1 - 6	1 - 5	2 - 7
Si	5 - 20	3 - 12	3 - 10	2 - 26	6 - 14	7 - 22

4.1.2. Variation of major elements across wells

Distribution Across Wells

The percentage distribution of the major elements as shown in figure 5 suggests that in all the wells, Ca show a relatively higher content and K show a relatively lower content which suggests the CKU is dominated by carbonate rocks as supported by the general sedimentary geology (Merriam and Jewett, 1956).

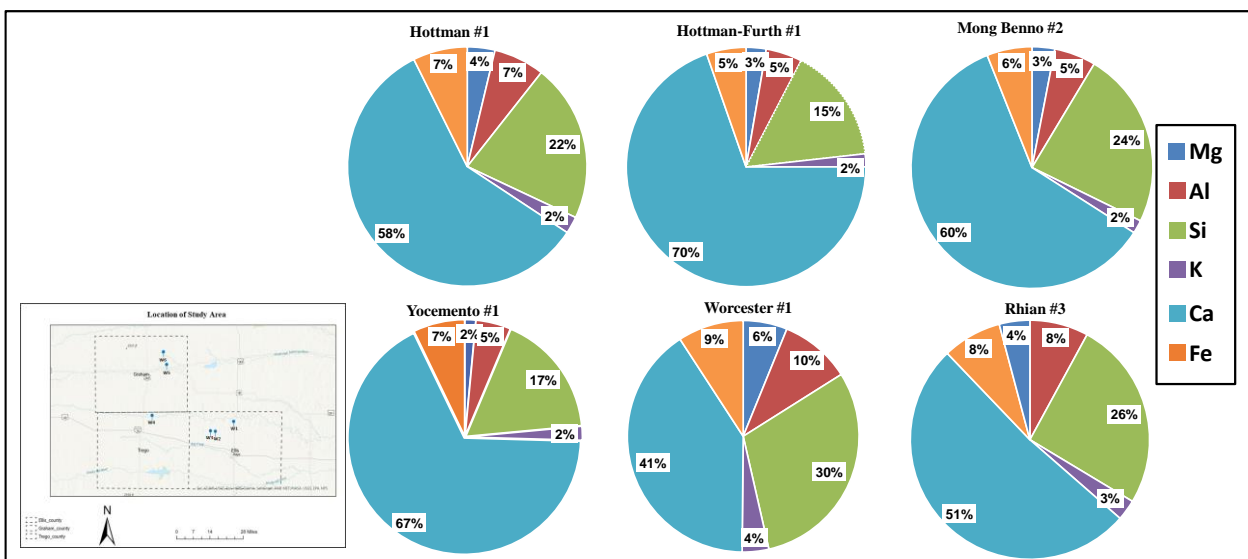


Figure 5: Distribution of elemental content of rock samples from a Paleozoic interval in the CKU (a): Hottman #1; (b): Hottman-Furthmeyer #1; (c): Mong Benno #2; (d): Yocemento #1; (e): Rhian #3 (f): Worcester #1.

Downhole Variation Across wells

Downhole plots of major elemental content (%) against depth in ft are shown in figure 6. Based on these results, Ca shows a relatively higher content compared to other elements while Potassium (K) shows a relatively lowest content. Other elements include Silicon (Si), Magnesium (Mg), and Aluminum (Al). Downhole variations of elements across the wells show

similar trends and pattern. However, Si show a different pattern in the lower part of the well D. Magnesium also shows a different trend in C and E (Mong Benno and Rhian well).

Based on the downhole variations, as Ca, and Mg which are associated with carbonate minerals increases, Al, K and Si which is associated with clay and detrital minerals decreases. Hence, the variation of the carbonate minerals is inversely proportional to the variation of the detrital elements. These variations suggest that at a particular interval what is promoting the supply of carbonate elements is inhibiting the supply of clay elements.

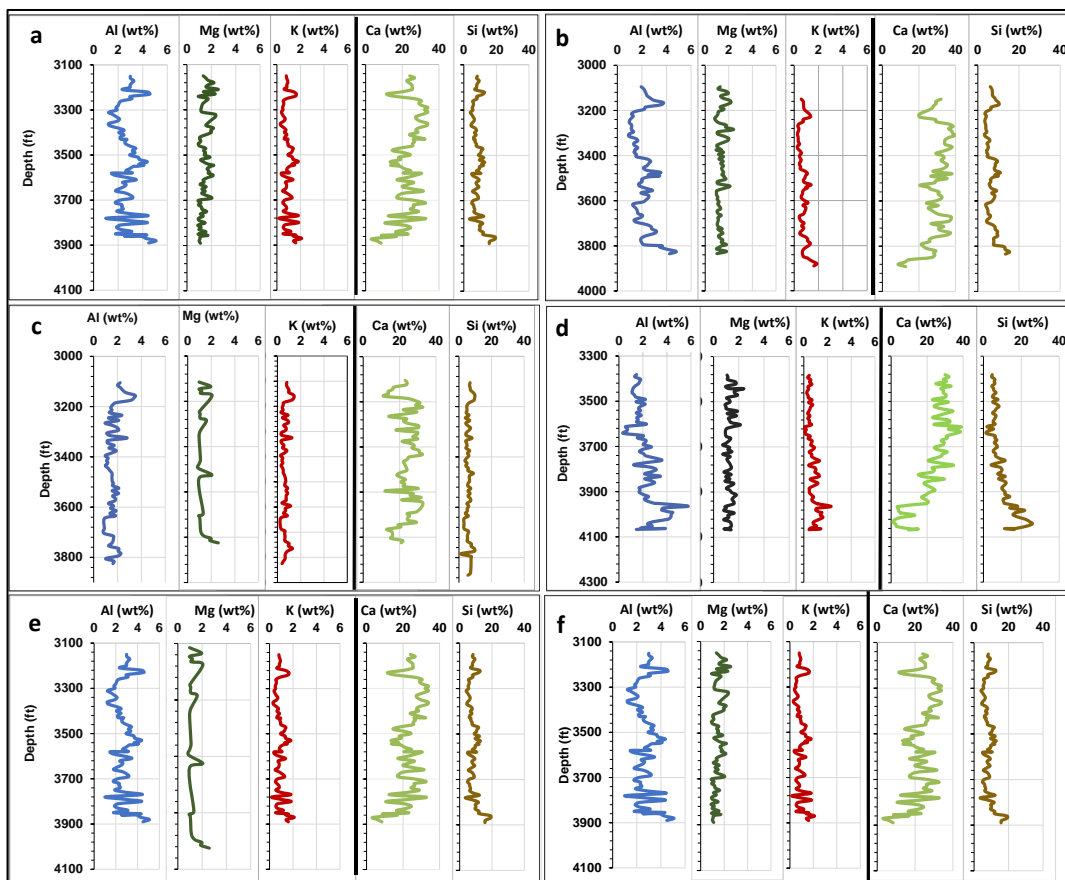


Figure 6: Downhole variation of major elemental distribution of sediments within the Paleozoic interval (a): Hottman #1; (b): Hottman-Furthmeyer #1; (c): Mong Benno #2; (d): Yocemento #1;

4.1.3 Downhole variation of trace elements

Figure 7 shows the downhole plots of selected trace elements in parts per million (ppm) against depth in ft. These trace elements were selected because they are the most abundant trace elements in the sample. The downhole plots show variation in trace elemental content in the six

wells. Based on the analysis of the sample, Phosphorous (P) show a relatively high content and this suggests that there could be presence of organic matter when the sediments were deposited. Rubidium (Rb) shows a relatively low content.

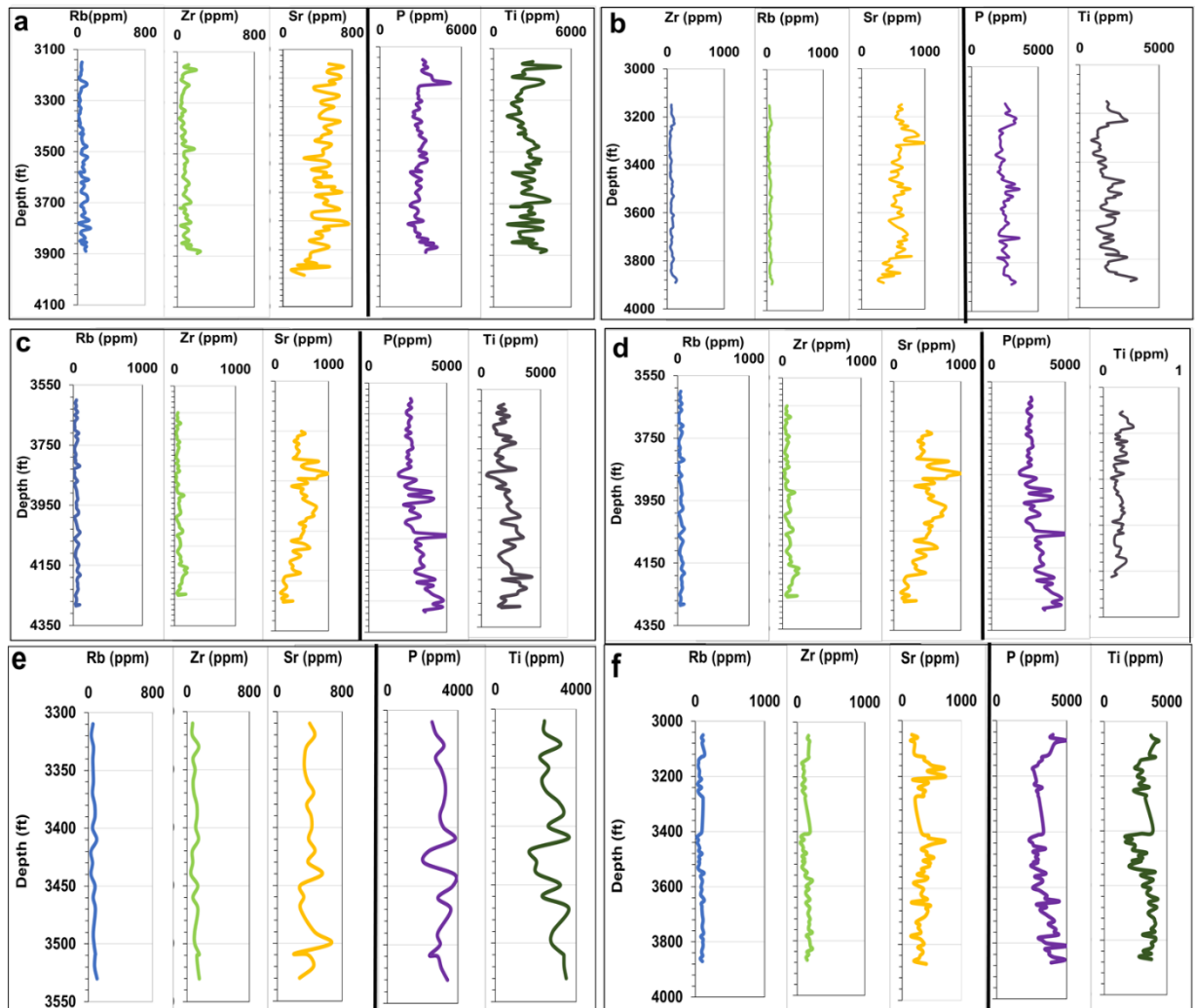


Figure 7: Downhole plots illustrating variation of trace elemental distribution of sediments within the Paleozoic interval (a): Hottman #1; (b): Hottman-Furthmeyer #1; (c): Mong Benno #2; (d): Yocemento #1; (e): Rhian #3 (f): Worcester #1.

4.1.4. Variation of Mineral content across wells

Based on the XRD analyses of the sample, the most abundant minerals are Calcite, Quartz, Illite and Dolomite. However, other minerals include Feldspar, Chlorite, SiO₂ and albite. Across the six wells, Calcite elemental content range from 2 - 29 wt.%, Quartz content range from 12 – 33 wt.%, illite content values ranges from 13 - 32 wt. %, and dolomite content values

ranges from 1 - 27 wt. %, as shown in table 2. Table 2 shows the complete suite of results of the Hottman #1, Hottman-Furthmeyer #1, Yocemento #1, Mong Benno #2, and Rhian #3 are in the appendix.

Table 2: Showing range of mineral concentration in percentages across the six wells

	W1	W2	W3	W4	W5	W6
Calcite	6 - 22	10 - 27	7 - 29	3 - 20	3 - 7	2 - 17
Quartz	14 - 26	15 - 25	12 - 25	13 - 29	18 -25	15 - 33
Illite	15 - 30	17 - 27	13 - 25	15 - 34	20 - 29	14 - 32
Dolomite	2 - 8	1 - 9	2 - 27	2 - 18	2 - 6	2 - 16

4.2.2. Mineral distribution across cells

The percentage distribution of the minerals as shown in figure 8 suggests that in all the wells, calcite, quartz and illite show a relatively higher content while dolomite show a relatively lower content compared to chlorite and dolomite. This also supports that CKU is dominated by carbonate rocks and contains intercalation of siliciclastic rocks based the sedimentary geology.

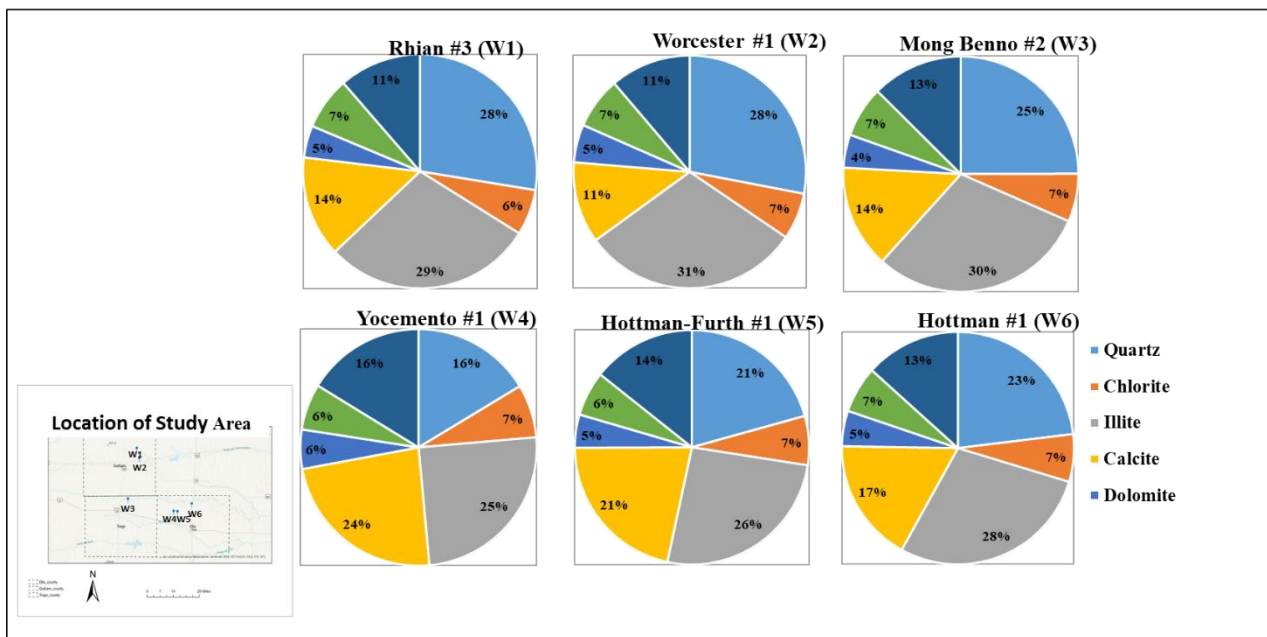


Figure 8: Chart showing the distribution of mineral content of sediments within the Paleozoic interval (a): Hottman #1; (b): Hottman-Furthmeyer #1; (c): Mong Benno #2; (d): Yocemento #1; (e): Rhian #3 (f): Worcester #1.

4.2.3. Downhole variation across wells

Figure 9 shows the downhole plots of selected minerals plotted against depth. These minerals were selected because they are the most abundant minerals in the formations within the

Paleozoic interval. The downhole plots show variation in the mineralogical composition of the samples in Hottman #1, Hottman-Furthmeyers #1, Yocemento #1, Mong Benno #2, Rhian #3, and Worcester, respectively. The percentage distribution of the minerals as shown in figure 9 suggests that in all the wells, quartz, calcite and illite show a relatively high composition. However, the variation of the carbonate minerals is inversely proportional to the variation of the clay minerals hence, as calcite is increasing illite is decreasing and vice versa. This suggests that what is promoting the supply of Carbonate minerals is inhibiting the supply of clay minerals.

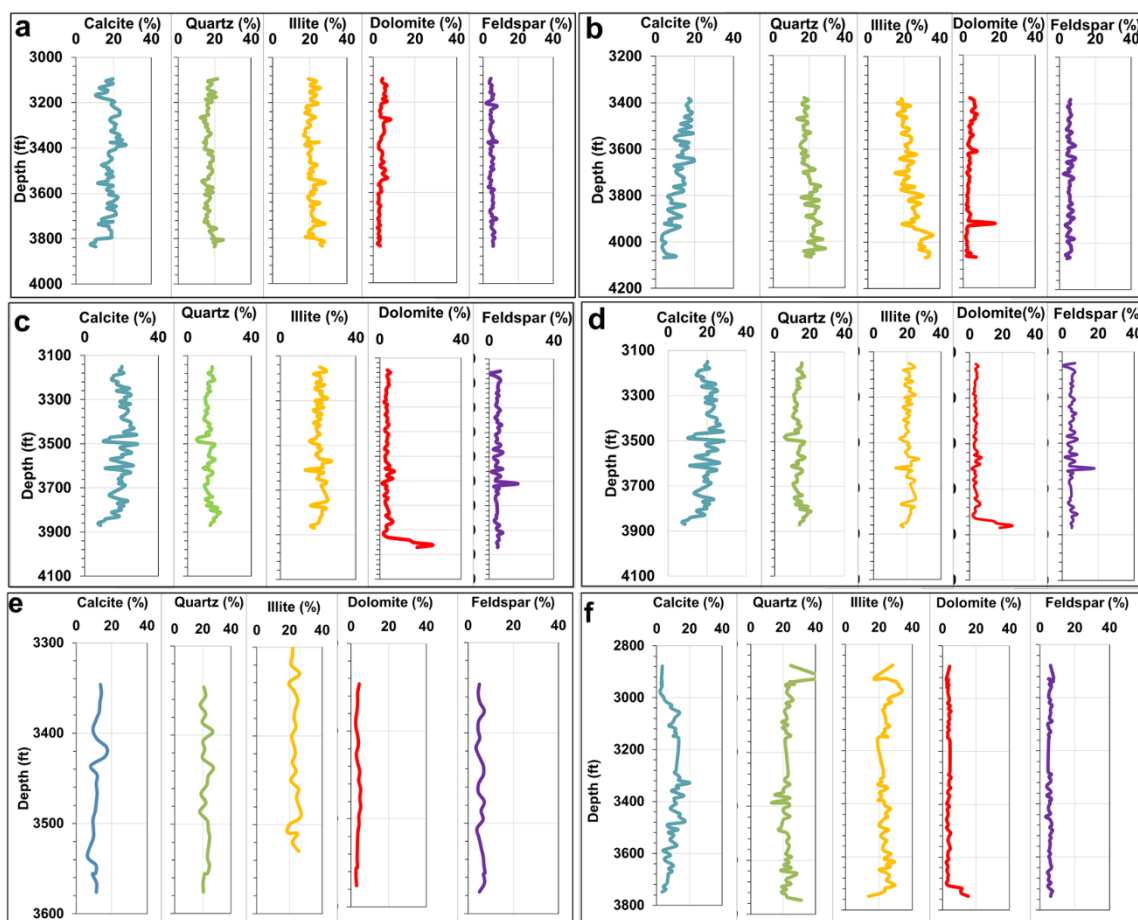


Figure 9: Downhole plots showing variation in mineralogical content of selected minerals plotted against depth from Paleozoic interval within the CKU. a: Hottman #1 minerals; b: Hottman-Furthmeyer #; c: Mong Benno #1 minerals; d: Rhian #3 minerals; e: Yocemento minerals; f: Worcester minerals.

5.0. Discussion

Carbonate rocks are the major hydrocarbon-bearing reservoirs in CKU. However, there are inputs of detrital materials and other sources. Hence, assessing the source characteristics and inputs, geologic processes, and conditions of deposition of the Paleozoic rocks within the CKU are critical to understanding the energy of deposition and the amount of organic matter present within the CKU. To assess these parameters, geochemical proxies will be used. The different pattern observed for Mg in Mong Benno & Rhian wells (figure 6) and the lower part of Si in Rhian well is as a result of outliers which not consistent across other wells. In figure 6 above, the observed increase in Ca with depth and the corresponding decrease in elements associated with clay minerals (Al, Si, and K) with depth shows that reduction in detrital input increases the supply of Ca and decreases the occurrence of elements that makes up a clay mineral.

5.1. Source Inputs

Source inputs involve the type of sediments and the environment the sediments were supplied during deposition. Detrital proxies are used to interpret source input in sediment. Elements such as Silicon (Si), Aluminium (Al), Potassium (K), Iron (Fe) and Titanium (Ti) are associated with sediment deposited into basins regardless of grain size (Rothwell and Croudace, 2015a). These elements can be used as detrital proxies (Driskill et al., 2018) which means that they are used to indirectly interpret the grain size of sediments within a formation. Plots of elements against Al show positive correlation and suggests that the elements are from the same source as shown in figure 10. However, the R^2 values indicates that there is a stronger correlation between potassium (K) and Al compared to Silicon (Si) and Al, Titanium (Ti). The least positive correlation occurs between Iron (Fe) and Al plots which could be as a result of a non-detrital influence affecting the level of correlation between the elements. In figure 11, elements (Mg, Ca, and Sr) peculiar to carbonate rocks (carbonate proxies) were plotted against each other. Positive correlation between the elements suggests that they are from the same source. Magnesium (Mg) against Ca plots show no correlation, Sr against Ca show a weak

positive correlation. This could be as a result of detrital influence in the formation. However, Al was used to normalise the analysis and this normalization improved the plots by removing detrital influence thereby producing a strong positive correlation.

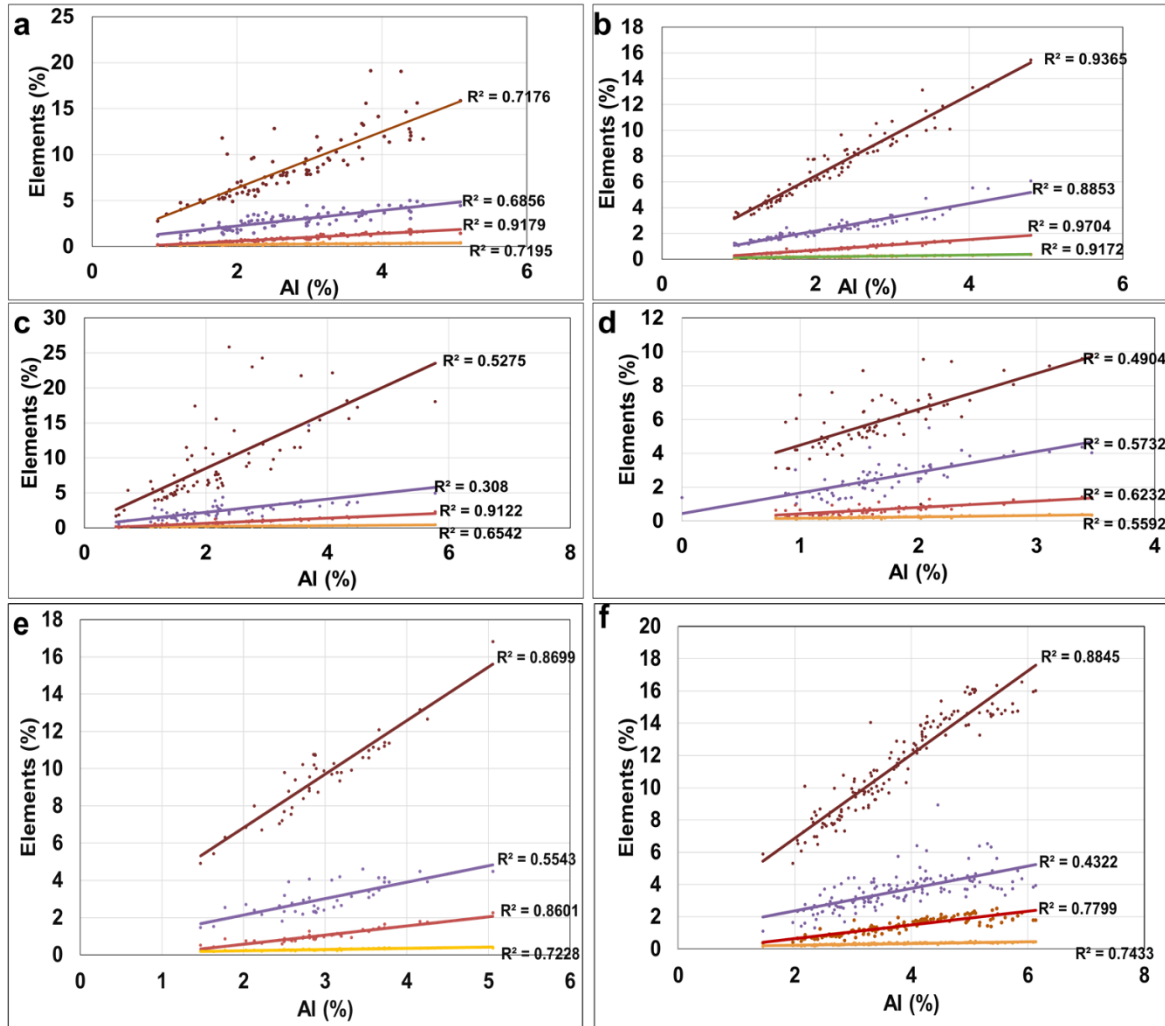


Figure 10: Cross plots of Al against detrital element illustrating the presence of detrital input within the formation in the Paleozoic interval (a): Hottman #1; (b): Hottman-Furthmeyer #1; (c): Mong Benno #2; (d): Yocemento #1; (e): Rhian #3 (f): Worcester #1. Aluminum is on the X axis in all plots, values of elements increase as Aluminum increases upwards.

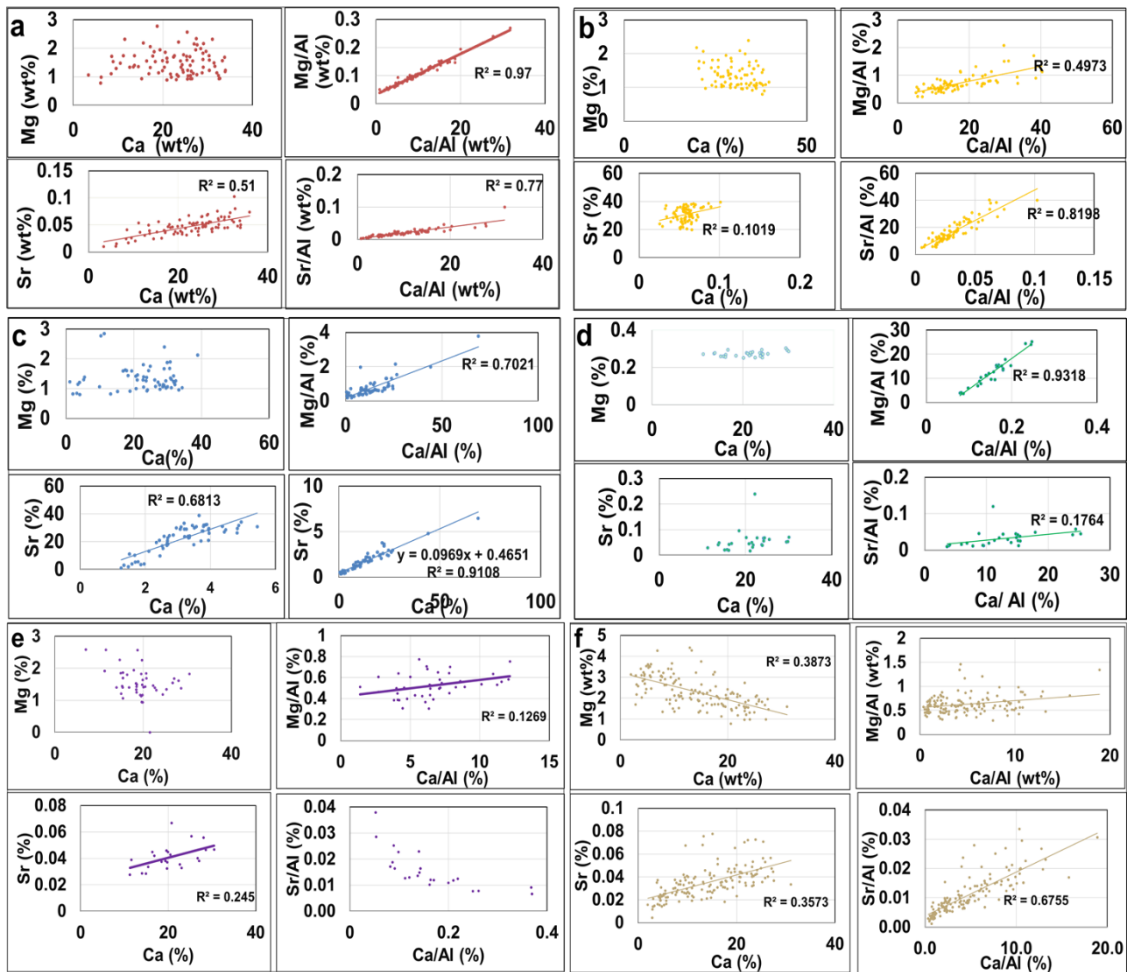


Figure 11: Cross plots of Mg/Ca; Mg/Al against Ca/Al; Sr/Ca, Sr/Al against Ca/Al illustrating the presence of Carbonate input within the formation in the Paleozoic interval (a): Hottman #1; (b): Hottman-Furthmeyer #1; (c): Mong Benno #2; (d): Yocemento #1; (e): Rhian #3 (f): Worcester #1.

5.2.1. Paleo Environmental Conditions

Presence of organic matter

Organic matter absorb Phosphorus (P) as part of the nutrients they need for survival and when they die the sediments they lived in contains the nutrient they absorbed when they were alive Hence, the presence of organic matter are investigated using P. P has been identified as a good paleo-productivity proxy because it is stored in ancient times as nutrients in life forms (Schenau et al., 2004). Organisms secrete Ca and when they die their shells accumulate to form Carbonate rock. Hence, calcium and phosphorus are used to investigate the presence of organic matter in a sediment. In figure 12, elements (P, Ca) were used as proxies to interpret paleo

productivity in the formation. Plots of P against Ca show a negative correlation but when Al was used to normalise the analysis, the P/Al and Ca/Al plots show a positive correlation. Furthermore, the average amount of P in the formation is greater than the crustal abundance of P (indicated with the red line) in the formation.

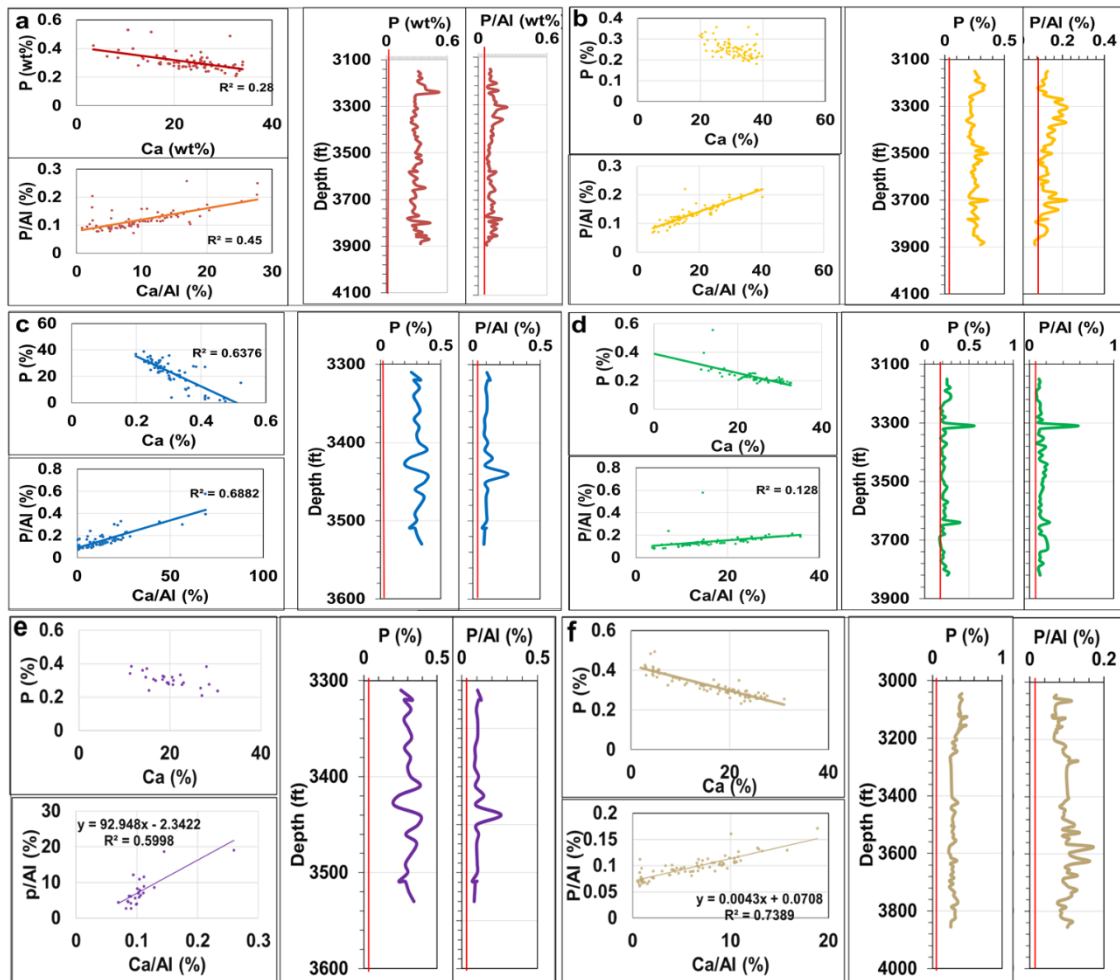


Figure 12: Paleoproductivity proxies within the Paleozoic interval illustrating the amount of paleo productivity in the formation (a): Hottman #1; (b): Hottman-Furthmeyer #1; (c): Mong Benno #2; (d): Yocemento #1; (e): Rhian #3 (f): Worcester #1

Energy of the Environment

Zr is enriched in areas where there are more coarse-grain sized sediments, while Rubidium (Rb) is enriched in areas where there are finer grain size sediments. Zr/Rb ratios reflect the grain size distribution in the formation and eliminate the effect of weathering and pedogenesis (Liu et al., 2002). Since there is significant amount of detrital materials in the formation, Zr and Rb ratio

were used to interpret grain size within the formation. Cross plots of Zr/Rb ratio show positive correlation which indicates that they may be from the same source (figure 13). An increase in Zr/Rb ratio indicates a coarser grain size sediment and a decrease in the ratio suggests the presence of finer grain size sediments as shown in figure 13. The standard deviation of Zr/Rb and their mean values support that there are two zones: a (coarse) and zone b (fine). Grain sizes in the two different zones give an insight to the amount of energy present during deposition. During a high energy regime, coarse grain size sediments are deposited and when the energy begins to drop a finer grain size sediments will be deposited. Therefore, the Zr/Rb ratio suggests that there are two major energy regimes. The high energy regimes illustrated by the coarse sediments in Zone A and a low energy regime supported by the finer sediments in Zone B.

Weathering

Zr is enriched in areas where there are more coarse grain size sediments while Rubidium (Rb) is enriched in areas where there are finer grain size sediments. Zr/Rb ratios reflect the grain size distribution in the formation and eliminate the effect of weathering and pedogenesis (Liu et al., 2002). Since there are no Zr and Rb in carbonates, their ratio can be used to remove influence of carbonate content in the formation. An increase in Zr/Rb ratio indicates a coarser grain size sediment and a decrease in the ratio suggests the presence of finer grain size sediments as shown in figure 13.

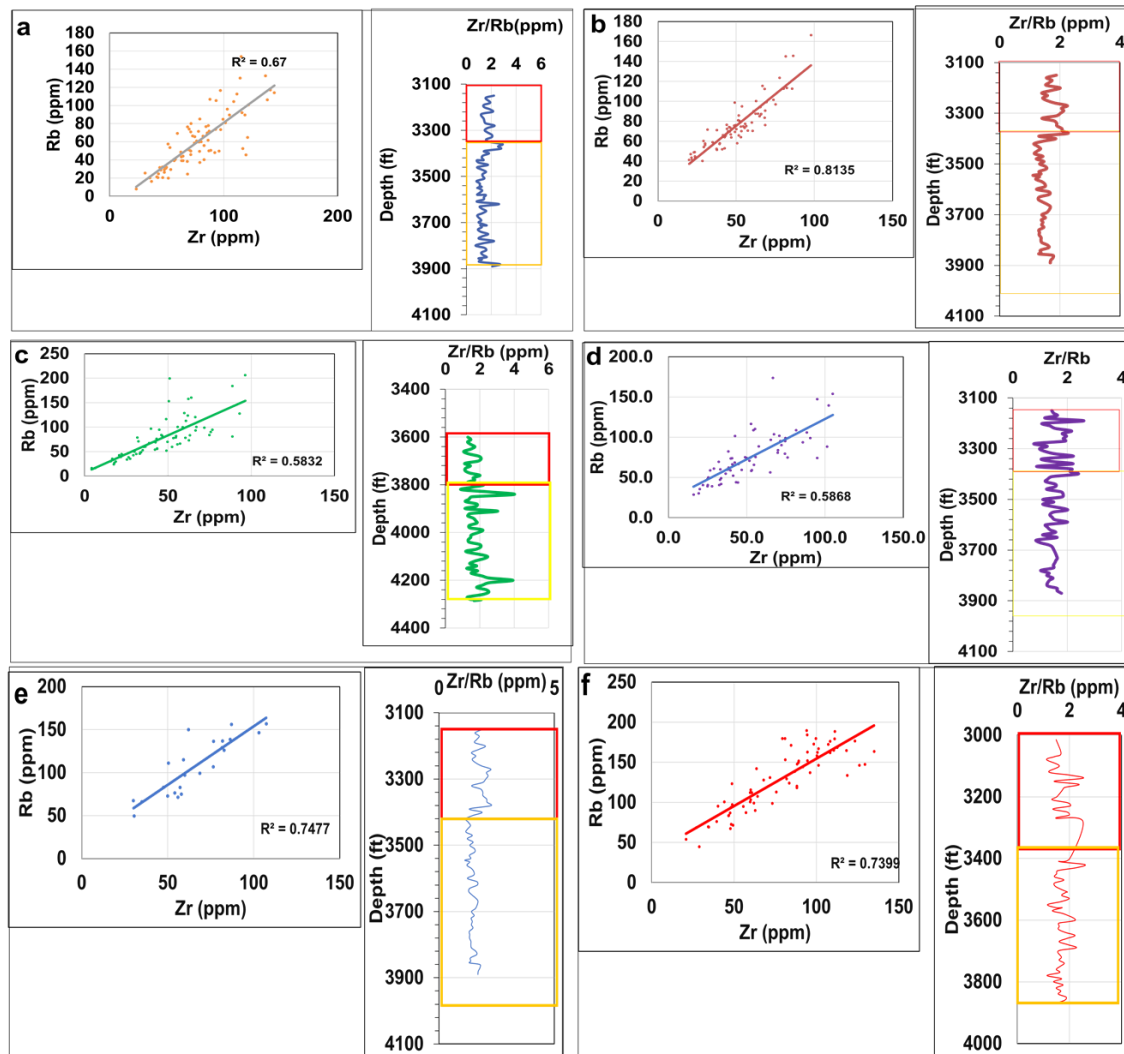


Figure 13: Grain size proxies within the Paleozoic interval illustrating the grain size of the sediments in the formation. An increase in Zr/Rb shows a coarser grain size and vice versa.
 (a): Hottman #1; (b): Hottman-Furthmeyer #1; (c): Mong Benno #2; (d): Yocemento #1; (e): Rhian #3 (f): Worcester #1.

4.2.1.4. Principal Component Analysis

In this study, major elements in Hottman #1 are presented and discussed as defined by the PCA (See appendix for the PCA of other wells). Positive and negative correlations of variables are summarized into principal components, which are used to interpret why element associations exist and what that may indicate (figure 14). Ideally, detrital elements (Al, Si, K, Fe, and Ti) should plot together, and elements associated with carbonate minerals (Ca, Sr, Mg, Mn, and P) should also plot together (Javid et al., 2018). PC-1 of the Eigen analysis of the

correlation matrix indicates the highest variability in the samples. Eigen vectors of the principal component indicates that all the major elements are important in accounting for the variability in the data (distribution of sources). The variable Al, Si, K, Fe, and Ti are negatively correlated with the PC-1 which Sr/Al, Mg/Al, Ca/Al, P/Al, and Mn/Al are positively correlated with the first principal component (figure 14). The PC-1 accounts for a cumulative of 68% and PC-1 and PC-2 accounts for 78.6% of the variability in the data (Table 4). Furthermore, the first three PC's accounts for the 83.1% of the variability in the data. All the variables are positively correlated with the second PC except for Ca/Al. In this study, PC-1, PC-2, and PC-3 will be considered because they account for most of the variability in the data (83.1%). Based on the plot (figure 14) elements that cluster together have a strong correlation index with each other. The close relationship between Ca, Sr, Mn, and P after normalization to remove the detrital influence, might be attributed to the presence of carbonate inputs and organic matter richness and correlation between Mg and Mn might be attributed to dolomitization.

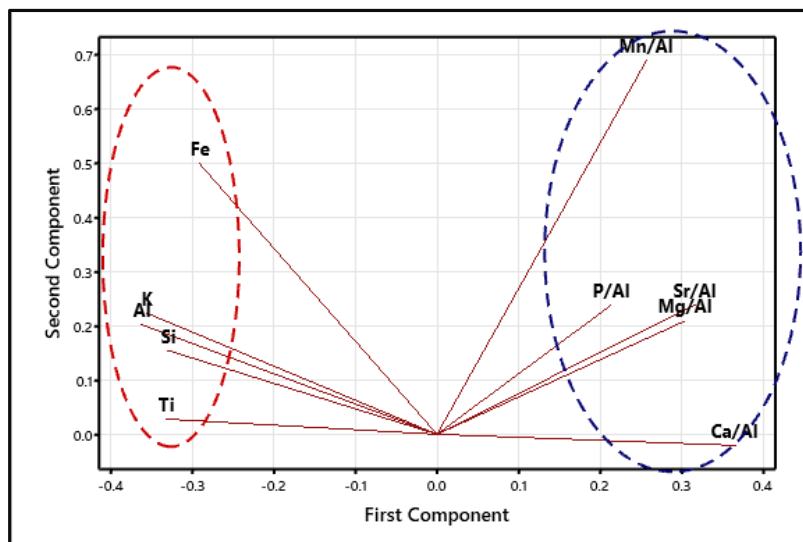


Figure 14: Principal component analysis using major elements in the formation

Table 4 : Principal component analyses values

Eigen Analysis of the Correlation Matrix										
Variable	PC1	PC2	PC3	PC4	PC5	PC6	PC7	PC8	PC9	PC10
Eigenvalue	6.80	0.76	0.75	0.58	0.37	0.32	0.22	0.12	0.05	0.04
Proportion	0.68	0.076	0.08	0.06	0.04	0.03	0.02	0.01	0.01	0.004
Cumulative	0.68	0.76	0.83	0.89	0.92	0.96	0.98	0.99	0.99	1
Eigen Vectors										
Variable	PC1	PC2	PC3	PC4	PC5	PC6	PC7	PC8	PC9	PC10
Sr/Al	0.32	0.24	0.01	-0.52	-0.18	-0.50	-0.29	0.03	-0.35	0.29
Al	-0.36	0.20	0.07	0.11	-0.03	-0.15	-0.31	-0.34	-0.41	-0.64
Si	-0.33	0.16	-0.03	0.37	-0.39	-0.43	0.01	0.62	0.11	0.10
K	-0.36	0.22	-0.09	0.12	-0.002	-0.29	-0.02	-0.61	0.41	0.43
Fe	-0.29	0.5	-0.10	-0.49	0.12	0.07	0.60	0.12	0.02	-0.16
Ti	-0.33	0.03	-0.06	-0.21	0.61	0.06	-0.55	0.35	0.18	0.08
Mg/Al	0.30	0.21	0.19	0.42	0.63	-0.39	0.27	0.02	-0.18	0.01
Ca/Al	0.37	-0.02	-0.05	-0.17	-0.01	-0.32	-0.07	-0.03	0.66	-0.54
P/Al	0.21	0.24	-0.90	0.21	0.03	0.11	-0.10	-0.004	-0.10	-0.02
Mn/Al	0.26	0.69	0.34	0.18	-0.15	0.43	-0.26	0.04	0.17	0.05

5.0 CONCLUSION

The detrital proxies (Ti, Al, K, and Fe) and the carbonate proxies (Mg, Ca, and Sr) show a positive correlation suggesting that they are from the same source. In cases where they showed negative correlations or no correlation, the element Al was used to normalize proxies which resulted to the dilution of the detrital input. The correlation was also supported by the PCA plot. The analysis showed a set of clusters for the detrital elements and another cluster for the carbonate elements indicating that they are from the same source. Based on the analysis, there are two major source inputs: detrital and carbonate sources. Zr/Rb ratios are good proxies that demonstrated variation in grain size based on their trends. An increase in this ratio suggests the presence of coarser grained sediments, and a decrease in this ratio suggests the presence of finer grained sediments. The coarse and fine grainsizes suggest the presence of two major energy regimes: the high energy and the low energy regime. Phosphorus, which has a crustal abundance of 0.01%, has been identified as a paleo-productivity proxy. The average amount of phosphorus is greater than the crustal abundance of phosphorous which suggests relatively high paleo-productivity in the formation and presence of organic matter in the sediments. The chemostratigraphic relationship between Trego and Ellis counties showed lateral continuity which suggests a lateral continuity in stratigraphic sequence between the two counties.

6.0 REFERENCES

- Algeo, J.T., Kiyoko, k., Sano, H., Bates, S., Lyons, T., Elswick, E., Hinnov, L., Ellwood, B., Moser, J., Maynard, J.B., 2011, Spatial variation in sediment fluxes, redox co0itions, and productivity in the Permian–Triassic Panthalassic Ocean. *Palaeogeography, Palaeoclimatology, Palaeoecology* 308, p. 65–83.
- Blanchet C., L., Thouveny N., Vidal L., Leduc G., 2007, Terrigenous input response to glacial/interglacial climatic variations over southern Baja California: A rock magnetic approach, DOI: 10.1016/j.quascirev.2007.07.008 *Quaternary Science Reviews* 26 (2007) 3118–3133
- Calvert, S.E., and Pedersen, T.F., 2010, *Geochemistry of Recent oxic anoxic marine sediments: Implications for the geological record*. Department of Oceanography, University of British Columbia, Vancouver, B.C., V6T 1Z4, Canada.
- Cansler, J. R., aand T. R. Carr, 2002, Paleogeomorphology of the sub-Pennsylvanian unconformity of the Arbuckle Group (Cambrian–Lower Ordovician): Kansas Geological Survey Open-File Report 2001-55, 3.
- Driskill, B., Pickering, J., Rowem, H., 2018, Interpretation of High-Resolution XRF data from the Bone Spring and Upper Wolfcamp, Delaware Basin, USA. Unconventional resource Technology Conference. p. 1-27, DOI 10.15530/urtec-2018-2901968.
- Edward A., K., 1935, Geology of Central Kansas Uplift Bulletin of the American Association of Petroleum Geologist. <https://doi.org/10.1306/3D932D70-16B1-11D7-8645000102C1865D> AAPG Bulletin 19 (10): pp1405–1426.
- Franseen, E.K., Byrnes, A.P., Cansler, J.R., Steinhauff, D. M., Carr, T.R., 2004, The Geology of Kansas Arbuckle Group, Current Research in Earth Sciences, Bulletin 250, part 2 (<http://www.kgs.ku.edu/Current/2004/franseen/franseen1.html>) Pp 1-43.
- Gorntiz V., 2009, Proxies, An introduction. In Gornitz V. (eds) *Encyclopedia of Paleoclimatology and Ancient Environments*. Encyclopedia of Earth Sciences Series. Springer, Dordrecht. https://doi.org/10.1007/978-1-4020-4411-3_171
- Higginson M.J., 2009, Geochemical Proxies (Non-Isotopic). In: Gornitz V. (eds) *Encyclopedia of Paleoclimatology and Ancient Environments*. Encyclopedia of Earth Sciences Series. Springer, Dordrecht. https://doi.org/10.1007/978-1-4020-4411-3_89.
- Hilpman, P. L., 1958, Producing zones of Kansas oil and gas fields: Kansas Geol. Survey, Oil and Gas Inv. 16, p. 1-10
- Huber. C., Druhan. J., L., Fantle. M., S., 2017, Perspectives on geochemical proxies: The impact of model and parameter selection on the quantification of carbonate recrystallization rates.

- Geochimica et Cosmochimica Acta, Elsevier, <https://doi.org/10.1016/j.gca.>, Vol 217, pp 171-192.
- Jewett, J. M., 1951, Geologic structures in Kansas: Kansas Geological Survey Bulletin, 90, part 6.
- Kansas Geological Survey, 2022, Geologic History of Kansas--stratigraphy—Paleozoic. from http://www.science.earthjay.com/instruction/HSU/2015_fall/GEOL_332/labs/lab_11/KGS--Geologic%20History%20of%20Kansas--Stratigraphy--Paleozoic.html
- Kansas Geological survey, 1987, Subsurface Geology series 9, Energy Research
- Mario L., 2020, Global variability in seawater Mg: Ca and Sr:Ca ratios in the modern ocean www.pnas.org/cgi/doi/10.1073/pnas.1918943117. Vol 117, no36, pp 22281-22292.
- Merriam, D. F., 1963, The geologic history of Kansas: Kansas Geological Survey Bulletin, 162, 317.
- Merriam, D. F., 1955, Structural patterns in western Kansas: Kansas Geological Society Annual Field Conference, 18, 80-87.
- Merriam, D. F., and Jewett, J. M., 1956, Pennsylvanian rocks in the subsurface along the Kansas Turnpike, Lawrence to Emporia: Kansas Geol. Soc. 19th Field Conf. Guidebook, p. 22-24.
- Newell, D.K., and Hatch, J.R., 2006, Petroleum geology and Geochemistry of a production tre0 along the McPherson Anticline in Central Kansas, with Implication for long- and short-Distance Oil Migration. Transaction of the 1999 AAPG Midcontinent Section Meeting (Geoscience for the 21st Century). Kansas Geological Survey, Lawrence. p. 22-28.
- Newell, K.D., Watney W. L., Cheng W. L., and Brownrigg R. L., 1987, Stratigraphic and spatial distribution of oil and gas production in Kansas: Kansas Geological Survey, Subsurface Geology Series, 9, 86.
- Parkhurst, R. W., 1959a, Surface to subsurface correlation and oil entrapment in the Lansing Kansas City Groups (Pennsylvanian) in northwestern Kansas: Unpub. master's thesis, Kansas Univ., p. 1-71.
- AAPG Wiki., 2022, Paleoenvironmental analysis https://wiki.aapg.org/Paleoenvironmental_analysis
- Löwemark, L., Chen, H.-F., Yang, T.-N., Kylander, M., Yu, E.-F., Hsu, Y.-W., Jarvis, S. 2011, Normalizing XRFscanner data: A cautionary note on the interpretation of high-resolution records from organic-rich lakes. Journal of Asian Earth Sciences, 40, 1250–1256.
- Liu, L., Chen, Y., Chen, J., Lu, H., 2002, Variation of Zr/Rb ratios on the Loess Plateau of Central China during the last 130000 years and its implications for winter monsoon. Chinese Science Bulletin 47(15), p. 1298-1302. DOI: 10.1360/02tb9288.

- Rogala, B., Fralick, P.W., Heaman, L.M., Metsaranta, R., 2007, Lithostratigraphy and Chemostratigraphy of the Mesoproterozoic Sibley Group, Northwestern Ontario Canada. *Canadian Journal of earth sciences*. Vol. 44, p. 1131-1148, DOI: 10.1139/E07-027.
- Rothwell R.G., 1989, *Minerals and mineraloids in marine sediments: an optical identification guide*, Elsevier Applied Science, London.
- Rothwell R.G., and Croudace I.W., 2015a, Micro-XRF studies of sediment cores: a perspective on capability and application in the environmental sciences, in Croudace I.W, and Rothwell R.G, (eds), *Micro-XRF Studies of Sediment Cores Applications of a non-destructive tool for the Environmental Sciences*, Springer, Heidelberg, Germany, p. 1-21, DOI: 10.1007/978-94-107-9849-5.
- Rothwell R.G., and Croudace I.W., 2015b, twenty years of XRF core scanning marine sediments: what do geochemical proxies tell us? in Croudace I.W, and Rothwell R.G, (eds), *Micro-XRF Studies of Sediment Cores Applications of a non-destructive Tool for the Environmental Sciences*, Springer, Heidelberg, Germany, pp 25-102, doi: 10.1007/978-94-107-9849-5.
- Tribovillard, N., Algeo, T., Lyons, T.W., Riboulleau, A., 2006, Trace metals as paleoredox and paleoproductivity proxies: an update. *Chemical Geology* 232, p. 12–32.
- Tinnin, B., Shariva D., 2016, Chemostratigraphic variability of the Eagle Ford Shale, south Texas: Insights into paleoredox and sedimentary facies changes, in J. A. Breyer, ed., *The Eagle Ford Shale: A renaissance in U.S. oil production: AAPG Memoir 110*, p. 259–283.
- Rana E., Steve S., 2021, A Principal Component Analysis Approach to Understanding Relationships Between Elemental Geochemistry Data and Deposition, Niobrara Formation, Denver Basin, CO. Paper presented at the SPE/AAPG/SEG Unconventional Resources Technology Conference, Houston, Texas, USA, July 2021. Paper Number: URTEC-2021-5440-MS, <https://doi.org/10.15530/urtec-2021-5440>
- Schenau, S. J., Reichart, G. J., De Lange, G. J., 2004, Phosphorus burial as a function of paleoproductivity and redox conditions in Arabian Sea sediments. *Geochimica et Cosmochimica Acta*, Vol. 69, No. 4, pp. 919–931, doi: 10.1016/j.gca.2004.05.044
- Wang, L. C.; Wu, J. T.; Lee, T. Q.; Lee, P. F.; and Chen, S. H. 2011. Climate changes inferred from integrated multi-site pollen data in northern Taiwan. *J. Asian Earth Sci.* 40:1164–1170

7.0 APPENDIX

1. Table 3: Results showing Major Elemental composition and concentrations of the samples in Hottman #1 within the Paleozoic interval between 3150 to 3890 ft

Depth (ft)	Mg (%)	Al (%)	Si (%)	P (%)	K (%)	Ca (%)	Ti (%)
3150	1.334	2.989	8.259	0.314	0.795	24.044	0.304
3160	1.557	3.010	7.879	0.336	0.826	26.661	0.232
3170	1.743	3.277	9.408	0.321	0.897	22.549	0.516
3180	2.216	3.110	8.594	0.350	0.923	23.494	0.255
3190	1.716	2.966	7.869	0.308	0.836	25.249	0.225
3200	1.587	2.958	7.862	0.325	0.840	25.339	0.240
3210	2.570	2.357	6.864	0.375	0.626	25.377	0.148
3220	1.340	4.394	12.429	0.384	1.379	20.309	0.354
3230	2.318	4.568	11.697	0.399	1.653	11.495	0.387
3240	0.931	2.965	7.977	0.516	1.563	15.241	0.344
3250	1.708	3.116	8.128	0.299	0.869	26.003	0.252
3260	1.584	2.246	5.503	0.281	0.541	30.384	0.217
3270	1.340	2.073	5.895	0.282	0.581	28.967	0.214
3280	1.233	1.999	5.762	0.278	0.554	30.368	0.189
3290	1.187	1.813	5.197	0.285	0.479	33.915	0.177
3300	1.138	1.897	5.509	0.282	0.515	32.044	0.219
3310	1.229	1.225	4.010	0.306	0.382	33.958	0.141
3320	2.316	1.551	4.877	0.268	0.456	31.030	0.157
3330	2.342	1.851	5.736	0.282	0.568	27.464	0.195
3340	2.123	2.108	6.471	0.290	0.708	27.622	0.194
3350	1.893	1.905	6.063	0.247	0.600	29.619	0.209
3360	1.690	1.220	4.765	0.255	0.311	33.734	0.107
3370	1.565	1.313	4.535	0.244	0.342	33.259	0.159
3380	2.164	2.004	6.978	0.289	0.595	29.040	0.201
3390	1.949	2.487	7.780	0.305	0.770	27.295	0.229
3400	1.989	2.050	6.576	0.262	0.628	28.431	0.192
3410	1.559	2.473	7.540	0.279	0.845	23.892	0.235
3420	1.072	2.165	6.067	0.277	0.692	27.575	0.242

3430	1.048	2.232	6.146	0.289	0.624	32.378	0.191
3430	1.040	2.707	6.954	0.308	0.935	26.138	0.249
3440	1.125	2.548	6.877	0.289	0.875	26.795	0.237
3450	0.923	2.599	7.770	0.313	0.945	25.486	0.262
3460	1.035	2.969	7.856	0.338	0.972	25.604	0.306
3470	1.535	3.432	11.599	0.324	1.370	18.299	0.318
3480	1.358	3.153	10.702	0.312	1.322	14.516	0.349
3490	1.523	3.368	10.287	0.302	1.226	20.921	0.297
3500	1.425	2.933	9.028	0.288	0.930	24.308	0.264
3510	1.879	3.637	12.218	0.341	1.317	18.015	0.289
3520	1.143	3.730	9.537	0.293	1.368	19.025	0.280
3530	1.349	4.377	12.796	0.343	1.819	13.399	0.366
3540	1.729	3.681	10.826	0.344	1.286	17.747	0.308
3545	2.191	4.034	11.999	0.329	1.506	15.650	0.356
3550	1.953	3.254	9.628	0.295	1.110	19.326	0.287
3560	1.658	2.949	9.556	0.279	0.876	20.897	0.269
3570	1.777	2.629	7.743	0.265	0.840	24.621	0.314
3580	1.858	3.126	10.473	0.305	1.053	20.515	0.300
3590	2.150	1.746	5.592	0.240	0.433	26.953	0.192
3600	1.694	2.783	8.200	0.272	0.853	22.349	0.279
3610	1.327	3.470	9.369	0.304	1.370	17.143	0.315
3620	1.403	2.384	7.553	0.270	0.744	26.072	0.224
3630	1.077	2.642	8.060	0.275	0.808	23.092	0.259
3640	1.570	2.492	9.244	0.302	0.816	19.909	0.295
3650	1.225	2.056	7.098	1.059	0.742	25.554	0.242
3660	1.493	1.800	5.331	0.263	0.473	31.379	0.222
3670	1.222	2.678	7.722	0.278	0.850	19.889	0.329
3690	2.052	3.190	8.950	0.290	1.290	17.141	0.435
3600	1.829	1.528	4.757	0.234	0.427	28.916	0.198
3700	0.934	2.149	5.700	0.239	0.680	26.441	0.255
3712	0.946	1.938	4.903	0.224	0.502	32.719	0.207
3720	0.936	2.293	6.018	0.265	0.622	26.173	0.295

3730	1.192	2.282	6.204	0.281	0.796	26.302	0.271
3740	1.235	2.402	6.739	0.275	0.807	24.397	0.316
3750	1.613	1.894	6.187	0.257	0.535	28.905	0.206
3760	1.100	2.958	8.351	0.272	1.003	21.663	0.285
3770	1.334	4.399	12.057	0.315	1.804	12.564	0.378
3780	0.936	1.025	3.533	0.209	0.186	32.539	0.109
3790	1.018	2.689	8.025	0.254	0.925	23.400	0.308
3800	1.485	4.383	11.609	0.730	1.847	10.451	0.377
3810	0.890	2.229	9.683	0.260	0.690	20.912	0.199
3820	1.160	1.863	10.046	0.294	0.539	24.554	0.205
3830	0.989	2.201	9.553	0.275	0.663	21.893	0.209
3840	1.555	3.104	11.940	0.352	1.184	16.338	0.307
3850	0.907	1.794	11.802	0.294	0.515	23.016	0.145
3855	1.531	3.780	15.572	0.394	1.560	8.873	0.331
3860	1.737	3.721	13.380	0.337	1.390	11.173	0.276
3870	1.067	4.261	19.045	0.420	2.104	3.386	0.299
3880	0.994	5.083	15.870	0.346	1.428	6.222	0.407
3890	1.108	4.487	15.628	0.337	1.598	8.413	0.364

2. Table 4: Results showing Trace and Rare Earth Elemental content of Hottman #1 within the Paleozoic interval between 3150 to 3890 ft

Depth (ft)	Cr (%)	Mn (%)	Ni (%)	Zn (%)	As (%)	Rb (%)	Sr (%)	S (%)	Y (%)	Zr (%)	Nb (%)	Mo (%)	Pb (%)	Th (%)
3150	-	0.059	0.003	0.004	0.001	0.005	0.053	0.123	0.002	0.012	0.001	-	0.003	0.002
3160	0.008	0.101	0.002	0.003	-	0.005	0.070	0.227	0.002	0.007	0.001	-	0.003	-
3170	0.009	0.046	0.003	0.004	-	0.004	0.054	0.095	0.003	0.020	0.001	-	0.001	0.001
3180	0.006	0.079	0.003	0.004	-	0.005	0.051	0.147	0.002	0.010	0.001	-	0.002	-
3190	0.008	0.070	-	0.003	0.001	0.004	0.065	0.096	0.001	0.006	0.001	-	0.001	0.001
3200	0.010	0.071	0.002	0.003	-	0.004	0.066	0.101	0.001	0.006	0.001	-	0.001	0.001
3210	-	0.160	-	0.002	-	0.002	0.053	0.123	0.001	0.004	-	-	0.001	-
3220	0.007	0.060	0.004	0.004	0.001	0.004	0.060	0.163	0.001	0.008	0.001	-	0.002	0.002
3230	0.008	0.061	0.003	0.005	0.001	0.010	0.036	0.121	0.002	0.012	0.001	-	0.001	0.002
3240	0.011	0.039	0.004	0.006	0.001	0.011	0.037	0.142	0.002	0.009	0.001	0.001	0.002	0.002
3250	-	0.053	-	0.003	0.001	0.005	0.049	0.186	0.001	0.007	0.001	-	0.001	-
3260	0.009	0.031	0.002	0.003	0.001	0.004	0.064	0.110	0.001	0.006	-	-	0.001	-
3270	0.008	0.060	0.003	0.003	0.001	0.003	0.060	0.124	0.001	0.005	0.001	-	0.001	0.001
3280	0.007	0.064	-	0.002	-	0.002	0.045	0.130	0.001	0.005	-	-	0.001	-
3290	0.006	0.029	0.003	0.002	-	0.002	0.045	0.068	0.001	0.004	-	-	0.001	0.002
3300	0.009	0.038	-	0.003	0.001	0.003	0.058	0.151	0.001	0.005	0.001	-	0.001	-
3310	0.009	0.029	-	0.002	-	0.002	0.050	0.084	0.001	0.004	-	0.001	0.001	0.001
3320	0.008	0.059	0.002	0.005	-	0.002	0.045	0.094	0.001	0.004	-	-	0.002	0.002
3330	-	0.036	0.003	0.003	-	0.004	0.042	0.137	0.001	0.008	0.001	-	0.002	0.002
3340	0.011	0.043	0.004	0.003	0.003	0.003	0.043	0.180	0.001	0.005	-	0.001	0.002	-
3350	-	0.036	-	0.004	0.001	0.003	0.065	0.091	0.001	0.005	-	-	0.001	-
3360	0.006	0.037	-	0.002	-	0.001	0.058	0.058	0.001	0.002	-	-	-	-
3370	0.006	0.028	0.002	0.002	0.001	0.002	0.048	0.080	0.001	0.005	-	0.001	0.003	-
3380	0.006	0.042	-	0.002	-	0.002	0.051	0.095	0.001	0.007	-	-	0.001	0.002
3390	0.008	0.032	-	0.002	0.001	0.003	0.055	0.131	0.001	0.005	-	-	0.001	0.002
3400	-	0.044	-	0.002	0.001	0.003	0.046	0.095	0.001	0.005	-	-	0.005	0.002
3410	0.010	0.037	0.004	0.003	-	0.006	0.043	0.172	0.001	0.008	0.001	-	0.001	-
3420	-	0.024	0.002	0.003	0.001	0.006	0.037	0.073	0.001	0.008	0.001	-	0.001	0.002
3430	0.010	0.020	0.003	0.003	0.001	0.003	0.055	0.072	0.001	0.004	-	-	0.003	-

3430	0.008	0.029	0.004	0.004	0.001	0.007	0.050	0.103	0.001	0.006	0.001	0.001	0.001	0.002
3440	0.007	0.024	0.003	0.005	0.001	0.005	0.053	0.095	0.001	0.005	0.001	0.001	0.002	0.001
3450	0.006	0.021	-	0.003	0.001	0.005	0.046	0.160	0.001	0.009	0.001	-	0.002	0.001
3460	0.008	0.028	0.003	0.005	0.001	0.006	0.046	0.193	0.001	0.005	0.001	-	0.002	0.001
3470	0.008	0.029	0.003	0.005	0.001	0.007	0.045	0.281	0.001	0.009	0.001	0.001	0.005	0.001
3480	-	0.024	0.004	0.005	-	0.011	0.024	0.101	0.002	0.018	0.001	-	0.001	0.002
3490	0.009	0.034	0.004	0.004	0.001	0.006	0.048	0.140	0.001	0.008	0.001	0.001	0.002	-
3500	0.009	0.032	0.003	0.004	0.001	0.005	0.054	0.093	0.001	0.007	0.001	-	0.001	0.002
3510	0.006	0.040	-	0.009	0.001	0.005	0.051	0.083	0.002	0.007	0.001	0.001	0.001	0.001
3520	0.009	0.028	0.004	0.005	0.001	0.012	0.033	0.091	0.001	0.010	0.001	-	0.001	0.001
3530	0.009	0.028	0.004	0.005	0.001	0.010	0.050	0.104	0.002	0.010	0.001	-	0.001	0.002
3540	0.008	0.030	0.003	0.004	0.001	0.007	0.046	0.085	0.001	0.007	0.001	-	0.001	0.002
3545	0.010	0.031	0.003	0.004	0.001	0.007	0.056	0.121	0.001	0.008	0.001	-	0.001	0.001
3550	0.007	0.037	0.004	0.005	0.001	0.009	0.037	0.119	0.002	0.008	0.001	-	0.001	-
3560	-	0.035	0.003	0.006	0.001	0.006	0.036	0.054	0.001	0.007	0.001	-	0.001	-
3570	0.006	0.030	0.003	0.004	0.001	0.008	0.044	0.047	0.002	0.008	0.001	-	0.001	0.001
3580	-	0.029	0.002	0.004	0.001	0.008	0.039	0.058	0.002	0.007	0.001	-	0.001	0.002
3590	-	0.033	-	0.003	0.001	0.004	0.056	0.046	0.001	0.006	-	-	-	-
3600	-	0.037	0.004	0.004	0.001	0.006	0.067	0.492	0.001	0.009	0.001	-	0.007	0.002
3610	0.005	0.016	0.004	0.006	0.001	0.013	0.038	0.273	0.002	0.011	0.001	0.001	0.003	0.002
3620	-	0.034	0.002	0.003	0.001	0.005	0.047	0.114	0.001	0.012	0.001	0.001	0.002	0.002
3630	0.008	0.026	0.003	0.004	0.001	0.008	0.051	0.189	0.002	0.009	0.001	-	0.002	0.002
3640	0.007	0.035	0.003	0.004	0.001	0.007	0.047	0.064	0.002	0.009	0.001	-	0.001	0.001
3650	0.015	0.025	0.011	0.015	0.001	0.005	0.049	0.281	0.002	0.008	0.001	0.001	0.001	0.002
3660	-	0.022	0.004	0.003	-	0.005	0.065	0.086	0.001	0.006	-	-	0.001	0.001
3670	0.010	0.026	0.004	0.006	0.001	0.011	0.035	0.291	0.002	0.009	0.001	-	0.001	0.001
3690	0.009	0.041	0.004	0.007	0.002	0.012	0.036	0.069	0.002	0.014	0.001	-	0.002	0.002
3600	-	0.031	-	0.003	0.001	0.004	0.061	0.044	0.001	0.006	0.001	-	-	-
3700	0.008	0.022	0.003	0.004	0.002	0.007	0.068	0.227	0.001	0.007	0.001	-	0.001	0.002
3712	0.007	0.020	-	0.002	-	0.004	0.080	0.020	0.001	0.006	-	-	0.001	-
3720	0.008	0.024	0.002	0.004	0.001	0.007	0.047	0.066	0.002	0.009	0.001	-	0.001	-

3730	0.007	0.027	0.002	0.004	0.001	0.007	0.053	0.084	0.001	0.007	0.001	0.001	0.001	0.002
3740	0.008	0.027	0.002	0.005	0.001	0.009	0.038	0.062	0.002	0.011	0.001	-	0.001	0.002
3750	0.007	0.028	-	0.003	0.001	0.005	0.045	0.123	0.001	0.009	0.001	-	0.001	-
3760	0.008	0.027	0.003	0.004	0.001	0.009	0.044	0.066	0.001	0.012	0.001	-	0.001	-
3770	0.009	0.021	0.003	0.005	0.001	0.013	0.030	0.103	0.002	0.014	0.001	-	0.001	0.002
3780	0.006	0.050	-	0.001	0.001	0.002	0.103	0.303	0.001	0.004	-	0.001	0.004	0.002
3790	0.006	0.035	0.002	0.003	0.001	0.007	0.053	0.149	0.001	0.010	0.001	-	0.001	0.002
3800	0.010	0.028	0.005	0.007	0.001	0.015	0.020	0.093	0.002	0.012	0.001	-	0.002	0.001
3810	-	0.046	0.002	0.002	0.001	0.006	0.033	0.122	0.001	0.008	0.001	0.001	0.001	-
3820	0.006	0.024	0.002	0.002	-	0.004	0.031	0.099	0.001	0.006	-	-	0.001	0.002
3830	0.011	0.031	0.003	0.003	-	0.007	0.031	0.101	0.002	0.009	0.001	0.001	0.001	0.001
3840	0.007	0.026	0.004	0.004	0.001	0.009	0.026	0.220	0.002	0.012	0.001	0.001	0.001	0.002
3850	-	0.026	-	0.003	0.001	0.003	0.039	0.133	0.001	0.005	0.001	-	0.001	0.002
3855	0.008	0.023	0.004	0.004	-	0.011	0.017	0.064	0.002	0.014	0.001	-	0.001	0.001
3860	0.009	0.037	0.003	0.004	0.001	0.008	0.054	1.546	0.001	0.010	0.001	-	0.004	-
3870	0.012	0.015	0.007	0.004	0.001	0.010	0.010	0.019	0.002	0.011	0.001	-	0.001	0.001
3880	0.007	0.026	0.006	0.004	-	0.009	0.015	0.044	0.002	0.023	0.001	-	0.005	0.002
3890	0.013	0.023	0.004	0.003	0.001	0.010	0.024	0.025	0.003	0.021	0.001	-	0.001	0.001

3. Table 5: Results Showing Mineral Content of the sediments in Hottman #1 within the Paleozoic interval between 3150 to 3890 ft

Depth (ft)	Qtz + Carbonates	Quartz (%)	Chlorite	Illite (%)	Calcite (%)	Dolomite (%)	Feldspar (%)	Albite (%)	SiO2 (%)	UNIDENTIFIABLE (%)	Total (%)
3150	34.7	18	4	25.9	12.7	4	6.5	10	9.6	9.3	100
3160	37.8	19.1	3.3	22.3	15.5	3.2	4.7	13.3	8.9	9.6	99.9
3170	34.3	17.9	5.2	25.6	11	5.4	4.4	11	9.5	10	100
3180	36.6	17.9	4.1	24.1	11.8	6.9	6.5	9.7	8.9	10.1	100
3190	36.7	20.2	3.8	27.1	9.7	6.8	4.9	8.4	10	9.1	100
3200	36.8	23.5	3.3	27.1	7.7	5.6	3.8	11.1	10	7.8	99.9
3210	34.5	23.4	5.1	25.2	7	4.1	3.8	14.6	9.3	7.5	100
3220	28.7	20.8	4.8	29.8	4.3	3.6	5.9	11.3	11	8.5	100
3230	31.1	19.1	5	29	7.1	4.9	3.9	11.8	10.8	8.6	100
3240	32.6	19.1	4.5	29.2	9.2	4.3	3.9	9.3	10.8	9.8	100

3250	35.1	18.5	4.2	26.6	12.2	4.4	4.5	10.3	9.8	9.4	99.9
3260	40.8	17.1	3.9	19.9	19	4.7	5.6	10.7	7.4	11.6	99.9
3270	36.3	15.8	4.7	22.6	17.5	3	4.5	12	8.4	11.5	100
3280	38.5	16.5	5.7	23.7	18.3	3.7	3.9	8	8.8	11.3	99.9
3290	37.3	17.1	5.7	22.8	16.9	3.3	4.7	9.5	8.5	11.6	100
3300	43.5	17.9	3.9	20.9	22.2	3.4	4.9	7.3	7.7	11.8	100
3310	36.2	15.1	5.4	20.2	17.7	3.4	4.9	13.6	7.5	12.2	100
3320	40.2	15.5	4.5	20.8	19.5	5.2	5	9.6	7.7	12.3	100
3330	41.8	17.1	3.7	18.3	17.1	7.6	6.9	11.8	6.8	10.7	100
3340	37	16.8	5.8	22.6	14.8	5.4	3.4	11.6	8.4	11.4	100
3350	38.9	17.3	3.8	21.7	14.7	6.9	3.5	13.1	8	11.1	100
3360	42.4	18.1	5.6	19.3	18.2	6.1	4.4	9.9	7.1	11.3	100
3370	42.7	16.8	5.1	19.6	20.6	5.3	4.1	9.3	7.3	11.2	100
3380	39.7	18.8	5.6	20.1	14.6	6.3	6.1	10.4	8	10.1	100
3390	35.9	17	5.3	24.3	14	4.9	4.8	10.6	9	10.3	100
3400	41.8	19.5	7.2	15.8	16.1	6.2	6.3	10.8	7.1	11	100
3410	38.2	18.8	6	21.8	15.2	4.2	6.1	10.2	7.4	10.3	100
3420	35.5	17.3	5	24.8	14.3	3.9	5.6	9.6	9.2	10.5	100
3430	34.9	17	4.9	21.4	13.8	4.1	6.8	13	7.9	11	99.9
3430	37.5	16.6	4.7	22.5	17.2	3.7	5.1	11	8.3	11	100
3440	24.3	12.1	10.2	22.7	9.9	2.3	5.3	10	8.4	19	99.9
3450	36.5	17.7	5.4	23.8	15.1	3.7	3.6	10.9	8.8	11.1	100
3460	40.9	20.9	4	18.8	16	4	5.8	11.6	9	10	100
3470	34.9	20.7	4.7	25.9	9.9	4.3	4.2	11.5	9.6	9.3	100
3480	36.7	20.1	4	25.2	12.7	3.9	4.9	11.2	9.3	8.7	100
3490	34.9	21.9	5.5	23.5	9.2	3.8	4.4	13.6	8.7	9.3	99.9
3500	35.1	20.1	5.8	25	10.5	4.5	4.7	10.9	10	8.4	99.9
3510	32.4	19.9	4.2	26.7	8.7	3.8	4.9	12.3	9.9	9.6	100
3520	35.9	21.3	5	24.9	10.2	4.4	4.5	10.4	9.9	9.4	100
3530	28.9	19.2	4.9	29.2	6	3.7	5.5	11.7	10.8	9	100

3540	34.1	21.2	5.7	24.7	9.2	3.7	6	11.7	9.1	8.8	100
3545	32.4	21.1	4.8	24.6	7.9	3.4	5.8	14.6	9.1	8.7	100
3550	35.4	20.4	6	23.8	10.1	4.9	4	12.7	8.8	9.4	100
3560	23.8	13.1	8.9	23.4	7.8	2.9	6.4	10.9	8.7	17.9	100
3570	36.6	17.3	3.8	21.7	14.3	5	5.6	13.2	8.1	11.1	100
3580	33.2	18.4	6.1	24.6	11.3	3.5	4.5	12.8	9.1	9.7	100
3580	39.7	19.8	5	21.3	14.5	5.4	4.8	10.9	7.9	10.3	99.9
3590	37.2	16.1	5.1	17.4	15.2	5.9	7.8	13.4	6.4	12.5	99.8
3600	39.1	21.3	5.2	21	13.7	4.1	6	10.2	7.8	10.6	99.9
3610	35.7	21.6	5.3	25.2	10.7	3.4	4.4	10.5	9.3	9.3	99.7
3620	40.4	20	4.7	21.6	16.2	4.2	4.1	11.1	8	10.2	100
3630	41.2	18.9	4	20.3	18.1	4.2	5.3	10.3	7.5	11.5	100
3640	38.2	18.8	4.3	23.7	15.8	3.6	6.1	7.5	8.8	11.4	100
3650	23.3	10.2	9.8	22.8	11.1	2	5	8.5	8.5	22.1	100
3660	37.7	15.6	5.4	22.3	19.1	3	5	7.6	9.2	12.7	99.9
3670	39.3	17.3	4.8	20.3	19.2	2.8	6.3	9.6	8.3	11.3	99.9
3680	40.2	15.3	6	17.8	22.2	2.7	6.2	10.5	6.6	12.9	100
3690	38	14.6	6	18.3	19.7	3.7	6.4	11.1	6.8	13.4	100
3600	36.3	15.7	6.3	23.9	16.6	4	5.1	7.6	8.8	12	100
3700	38	16.5	7.4	19.3	17.3	4.2	4.7	10.2	7.1	13.2	99.9
3712	37.3	15.3	4.6	22.1	19.8	2.2	6.9	8.4	8.2	12.5	100
3720	37.9	16.9	6.8	21.3	18	3	4.8	9.4	7.9	12.1	100
3730	37.1	17.5	6.2	21.9	17.1	2.5	4.8	9.6	8.1	12.1	99.8
3740	41.1	18.6	4.8	18.3	18.9	3.6	6.8	11.6	6.8	10.5	99.9
3750	41.5	20.2	5	21.5	18.1	3.2	5.6	8.2	8	10.2	100
3760	37.3	19	5.4	22.1	15.3	3	5.3	11.8	8.2	9.9	100
3770	33.5	18.7	4.3	26.9	11.8	3	5.3	10.4	10	9.7	100
3780	39.2	17.4	6.8	17.1	18.5	3.3	6.3	10.8	6.9	12.9	100
3790	35.5	20	5.6	25.1	12	3.5	4.1	11.1	9.3	9.5	100
3800	41.8	23.8	6.9	21.1	14.6	3.4	3.9	9.9	7.8	8.7	100

3810	39.4	22.6	5.2	22.3	13.2	3.6	5.5	9.4	8.9	9.4	100
3820	40.4	23	6.5	20.4	15.2	2.2	7.5	9.2	6.9	9.3	100
3830	40.3	21.7	6.2	21.3	15.9	2.7	4.4	10.3	7.9	9.6	100
3840	38.5	18.7	6	25.1	17.1	2.7	5.3	7.8	6.8	10.7	100
3850	39	19.1	4.6	24	16.6	3.3	5.3	7.7	8.9	10.5	100
3855	40.2	23.7	4.6	23.3	13.5	3	6.7	8.2	8.6	8.4	100
3860	28.6	19.9	12.3	21.2	6.2	2.5	5.6	9.6	7.8	14.9	100
3870	31.8	21.4	6	28.6	8	2.4	6	8.8	10.6	8.3	100
3880	36.1	25.1	3.7	26.9	7.9	3.1	7.1	8.3	10	7.8	99.9
3890	31.6	20	5.1	26.9	8.1	3.5	7.2	9.7	10	9.6	100

4. Table 1a: Results of Hottman-Furthmeyer #1 showing Major elements

Depth (ft)	Mg (%)	Al (%)	Si (%)	P (%)	S (%)	K (%)	Ca (%)	Ti (%)	Fe (%)
3150	1.270	1.938	6.041	0.251	0.158	0.577	32.101	0.170	2.064
3160	-	2.157	6.786	0.262	0.209	0.744	29.248	0.182	2.368
3170	1.776	2.253	7.033	0.274	0.208	0.764	29.424	0.176	2.343
3180	1.949	2.343	7.102	0.286	0.190	0.770	27.903	0.178	3.026
3190	1.323	2.424	7.147	0.254	0.153	0.790	27.159	0.197	2.673
3200	1.472	2.678	8.236	0.297	0.187	0.896	24.864	0.248	2.863
3210	2.070	2.975	8.819	0.334	0.196	1.126	21.656	0.259	3.422
3220	2.181	3.750	10.094	0.316	0.170	1.301	19.826	0.275	3.885
3230	1.772	3.556	10.186	0.325	0.175	1.322	20.557	0.297	3.848
3240	1.266	2.305	6.524	0.284	0.163	0.745	29.038	0.174	2.752
3250	1.597	2.187	6.301	0.242	0.168	0.745	29.362	0.180	2.675
3260	1.123	1.425	4.124	0.208	0.152	0.396	36.221	0.128	1.511
3270	1.087	1.160	3.443	0.234	0.120	0.297	38.760	0.113	1.493
3280	0.971	1.298	4.161	0.215	0.130	0.381	36.177	0.113	1.455
3290	-	1.130	3.737	0.210	0.093	0.351	37.886	0.111	1.182
3300	-	0.996	3.386	0.217	0.102	0.285	38.385	0.114	1.054
3310	1.159	0.989	3.537	0.217	0.122	0.277	39.691	0.073	1.129

3320	1.780	1.167	3.886	0.216	0.174	0.324	36.181	0.112	1.350
3330	1.742	1.154	3.856	0.220	0.146	0.327	34.263	0.129	1.467
3340	2.393	1.149	3.976	0.230	0.153	0.349	34.059	0.122	1.481
3350	1.061	1.325	4.370	0.208	0.131	0.436	34.266	0.130	1.508
3360	1.061	0.943	3.239	0.181	0.079	0.261	38.019	0.087	1.241
3370	1.645	0.964	3.648	0.209	0.093	0.297	36.707	0.091	1.194
3380	2.000	1.521	5.382	0.247	0.148	0.482	33.166	0.150	1.521
3390	1.863	1.663	5.798	0.226	0.141	0.593	29.232	0.162	2.020
3400	1.372	1.349	4.537	0.220	0.107	0.444	33.044	0.116	1.519
3410	0.980	1.388	4.892	0.211	0.103	0.474	33.685	0.144	1.688
3420	1.104	1.665	5.121	0.216	0.107	0.581	32.061	0.167	1.846
3430	-	1.419	4.412	0.196	0.089	0.479	33.665	0.133	1.698
3430	0.913	1.499	4.587	0.200	0.090	0.480	35.115	0.132	1.667
3440	-	1.357	4.300	0.219	0.084	0.425	35.560	0.133	1.462
3450	1.128	1.563	4.928	0.240	0.103	0.527	34.741	0.145	1.946
3460	-	1.540	4.679	0.227	0.116	0.507	32.366	0.146	2.023
3470	1.160	2.415	8.126	0.273	0.233	0.899	27.685	0.214	2.383
3480	1.527	2.712	9.602	0.323	0.281	1.087	38.088	0.279	3.092
3490	1.312	2.558	8.543	0.260	0.167	0.934	26.452	0.211	2.318
3500	1.550	2.407	8.531	0.358	0.197	0.877	35.385	0.205	2.862
3510	1.398	2.114	8.023	0.259	0.176	0.755	29.201	0.180	2.336
3520	1.446	2.383	8.435	0.258	0.195	0.839	28.517	0.187	2.505
3530	1.559	3.549	10.968	0.309	0.118	1.389	20.489	0.263	3.110
3540	1.410	2.503	8.286	0.270	0.108	0.965	25.590	0.216	2.652
3545	1.595	2.995	8.935	0.279	0.231	1.079	25.760	0.224	2.980
3545	1.481	3.057	9.123	0.254	0.157	1.150	23.885	0.216	2.934
3545	1.717	3.443	9.985	0.290	0.174	1.289	21.867	0.277	3.238
3550	1.580	2.452	7.520	0.243	0.072	0.850	27.217	0.169	2.367
3560	1.737	1.992	6.155	0.244	0.076	0.697	30.932	0.164	2.113
3560	1.161	1.714	5.587	0.234	0.133	0.594	31.730	0.158	2.013
3560	1.582	1.543	4.901	0.214	0.039	0.489	34.307	0.129	1.549
3570	1.039	2.020	6.324	0.253	0.073	0.687	30.461	0.170	2.114

3580	1.075	1.749	5.560	0.221	0.069	0.584	32.480	0.135	1.764
3590	2.091	1.812	5.892	0.239	0.084	0.605	32.169	0.136	1.987
3600	1.643	2.343	6.756	0.237	0.065	0.844	29.043	0.179	2.493
3600	-	1.426	4.508	0.213	0.029	0.476	36.061	0.113	1.551
3600	1.130	2.749	8.792	0.254	0.910	1.090	25.014	0.236	2.970
3610	1.001	2.860	9.133	0.256	0.811	1.138	24.017	0.248	3.044
3620	0.954	1.925	6.746	0.254	0.431	0.718	30.590	0.169	2.188
3630	0.961	2.513	8.221	0.254	0.191	0.950	25.153	0.221	2.557
3640	1.065	2.553	8.093	0.278	0.279	0.936	26.702	0.221	2.647
3650	1.020	2.354	7.432	0.252	0.245	0.852	28.581	0.214	2.523
3660	1.176	2.106	6.440	0.237	0.159	0.767	31.232	0.176	2.255
3670	-	1.265	3.871	0.215	0.056	0.420	37.530	0.107	1.510
3690	1.318	1.535	4.654	0.211	0.112	0.543	36.269	0.144	1.854
3700	1.018	1.624	4.922	0.358	0.178	0.815	26.656	0.209	2.448
3712	-	1.694	4.990	0.213	0.209	0.607	33.467	0.151	1.884
3712	-	1.198	3.528	0.207	0.092	0.379	37.771	0.117	1.393
3712	1.073	1.380	3.992	0.228	0.077	0.463	35.547	0.132	1.719
3720	1.359	2.050	6.146	0.233	0.183	0.782	30.771	0.213	2.144
3730	1.080	1.869	5.679	0.263	0.229	0.693	31.617	0.185	1.940
3740	-	1.366	4.377	0.246	0.136	0.491	37.140	0.133	1.645
3750	1.063	1.538	4.540	0.228	0.087	0.496	35.625	0.132	1.742
3760	1.016	2.348	7.080	0.246	0.171	0.885	28.464	0.213	2.373
3770	1.112	2.754	8.345	0.265	0.200	1.098	25.600	0.243	2.536
3780	1.444	2.808	8.418	0.277	0.207	1.114	25.788	0.242	2.557
3780	-	1.489	4.420	0.195	0.059	0.500	34.960	0.165	1.797
3790	1.284	3.189	9.575	0.241	0.244	1.331	21.376	0.295	3.115
3800	1.497	3.005	9.319	0.259	0.295	1.191	22.313	0.258	2.811
3810	1.130	2.335	9.647	0.270	0.149	0.896	24.189	0.183	2.179
3820	1.227	1.969	7.741	0.248	0.275	0.718	29.094	0.179	2.028
3830	-	1.902	7.756	0.244	0.145	0.670	28.033	0.162	1.756
3840	1.368	1.983	7.751	0.242	0.144	0.692	28.649	0.170	1.834
3850	-	2.161	7.760	0.243	0.151	0.782	26.954	0.186	2.337

3855	1.411	2.902	9.774	0.273	0.192	1.098	20.670	0.233	2.718
3860	1.820	3.438	11.507	0.307	1.421	1.203	15.594	0.272	4.714
3880	1.808	4.803	15.444	0.328	0.110	1.862	8.523	0.359	6.081
3890	0.992	4.250	13.415	0.299	0.225	1.619	12.744	0.321	5.490

4.

5. Table 1b: Results of Showing Trace Elements for Hottman-Furthmeyer #1

Depth (ft)	Zn (ppm)	As (ppm)	Rb (ppm)	Sr (ppm)	Y (ppm)	Zr (ppm)	Nb (ppm)	Mo (ppm)	Ta (ppm)	Pb (ppm)	Th (ppm)
3150	24.8	0	37.7	630.7	13.6	71.0	5.9	0	26.2	44.4	0
3160	27.7	7.0	44.8	580.6	14.7	69.9	8.3	5.4	32.2	14.5	20.8
3170	33.7	6.9	43.9	643.7	14.5	76.4	6.8	3.5	28.6	13.5	18.1
3180	29.7	7.0	44.1	564.2	13.6	72.3	8.0	4.7	28.7	21.1	18.7
3190	26.9	5.7	48.8	573.6	16.3	75.6	7.3	6.2	27.6	9.0	16.6
3200	32.4	5.9	49.1	537.0	20.9	98.7	6.2	0	31.6	11.5	11.6
3210	43.5	9.6	66.8	547.8	21.6	115.4	9.0	7.0	38.9	18.5	23.7
3220	45.0	10.4	80.3	656.0	20.5	112.7	10.2	0	40.6	8.9	14.1
3230	42.4	9.3	77.8	596.8	23.3	123.6	10.1	6.8	42.6	10.2	23.9
3240	28.1	7.4	46.5	733.7	16.3	66.8	7.0	6.0	35.5	10.9	27.5
3250	32.4	7.9	51.4	630.5	16.2	81.0	7.7	5.8	30.8	9.6	19.4
3260	19.2	3.5	29.3	802.9	9.9	54.0	6.1	4.6	17.3	9.8	11.8
3270	13.7	4.8	20.9	864.5	9.7	47.0	3.6	0	24.5	9.1	0
3280	19.3	6.3	29.2	894.5	11.6	60.1	4.7	3.6	21.5	9.4	12.9
3290	18.8	5.6	22.9	703.4	10.9	48.8	5.0	7.5	28.2	6.9	26.3
3300	18.7	0	21.5	676.7	10.1	43.5	5.2	6.2	18.8	9.1	0
3310	45.3	4.6	21.8	1010.9	10.1	41.2	5.5	7.3	17.4	21.2	15.2
3320	70.2	5.6	28.4	552.3	10.4	40.0	4.5	5.0	17.5	10.8	13.3
3330	37.3	4.4	23.6	615.9	10.8	42.7	4.8	4.9	20.7	10.7	0
3340	37.6	4.1	23.6	614.6	11.7	44.8	4.0	6.3	17.6	12.9	13.4
3350	43.5	5.4	30.2	594.5	11.0	57.5	4.8	7.4	20.9	11.2	0
3360	15.0	0	20.0	585.5	9.0	41.2	3.1	3.4	15.4	9.8	0
3370	27.9	4.6	23.5	607.7	10.1	49.1	4.8	5.2	23.8	19.9	17.9
3380	26.5	6.1	31.7	565.5	12.0	71.6	5.8	4.6	23.1	11.4	0

3390	46.0	8.5	53.4	476.3	14.5	70.0	7.1	5.3	33.1	8.1	15.8
3400	24.6	6.1	30.1	549.5	14.6	56.2	4.6	5.0	25.3	13.2	12.1
3410	27.0	5.3	39.3	643.3	11.9	57.1	6.9	5.9	27.8	12.4	13.8
3420	30.4	5.9	50.7	589.5	13.3	58.0	5.6	5.6	26.6	11.4	16.9
3430	26.8	6.1	51.6	463.7	13.5	65.7	7.8	0	29.4	7.6	14.0
3430	40.1	0	41.1	556.6	11.3	51.7	7.3	5.6	30.8	60.0	22.6
3440	20.4	0	37.6	580.0	10.2	51.2	4.6	0	26.7	28.5	15.9
3450	25.2	0	42.6	543.0	10.1	52.9	6.8	0	30.4	19.8	18.9
3460	56.3	6.7	60.5	438.6	16.5	70.4	7.3	8.7	34.5	11.3	20.8
3470	60.7	10.4	65.5	525.1	17.4	94.2	9.9	8.7	32.5	36.8	19.3
3480	62.7	11.4	68.3	649.6	20.0	83.4	11.9	11.1	45.6	16.4	38.7
3490	44.5	5.1	61.1	566.3	14.7	90.0	7.7	7.5	27.6	17.7	17.5
3500	48.3	9.9	56.4	767.9	19.1	75.2	9.9	9.7	31.4	28.3	30.1
3510	110.8	9.5	49.8	625.5	15.9	76.1	6.6	4.5	25.1	8.6	16.5
3520	31.3	0	51.9	666.2	14.1	80.4	6.1	6.5	36.7	61.8	24.4
3530	42.5	7.7	85.7	513.4	19.6	112.7	8.3	5.0	39.5	9.0	13.4
3540	37.9	5.6	63.9	521.3	15.0	87.6	8.6	5.1	34.4	9.9	15.2
3545	36.1	11.2	68.5	532.4	18.0	76.2	9.1	4.3	37.8	11.3	12.2
3550	28.9	6.2	55.3	543.9	11.5	73.3	7.3	4.2	31.2	5.7	15.5
3560	37.9	4.0	53.1	524.3	13.1	63.9	7.5	4.1	33.4	8.5	17.2
3570	26.5	5.7	49.3	477.0	14.9	69.4	8.0	3.6	29.1	7.9	13.4
3580	26.2	4.3	43.4	620.3	13.1	65.4	5.8	0	28.9	7.7	13.6
3590	27.7	5.8	42.6	618.3	15.0	64.0	6.9	5.9	23.9	6.7	18.1
3600	29.7	6.4	57.4	565.2	14.8	70.6	7.7	3.6	36.6	4.7	19.4
3610	34.8	5.2	68.3	657.3	14.9	112.4	9.3	5.5	38.6	21.1	18.5
3620	36.1	3.9	51.7	568.4	14.0	85.7	7.3	11.5	36.4	19.2	16.7
3630	78.6	7.8	68.5	435.5	17.0	90.7	6.8	6.4	36.8	9.8	14.2
3640	40.7	4.1	75.2	464.5	19.2	96.8	9.7	4.9	44.9	13.3	16.8
3650	42.3	6.8	69.4	514.4	16.9	99.2	7.5	7.7	34.0	12.6	15.2
3660	34.9	6.7	62.7	574.5	16.2	100.2	8.5	4.8	32.0	8.5	16.5
3670	19.2	4.7	35.0	650.8	11.8	59.0	4.7	0	22.8	8.4	0
3690	27.8	7.7	41.7	724.0	15.2	66.1	6.9	5.3	38.8	6.7	20.1

3700	34.9	6.3	62.3	652.3	18.1	87.6	6.5	4.5	27.0	13.5	12.7
3712	41.9	6.9	45.8	712.8	13.9	69.6	6.0	0	32.3	7.4	14.0
3720	33.1	5.8	55.7	574.0	13.2	77.5	7.7	7.9	29.9	9.2	13.4
3730	36.5	10.6	50.1	642.8	14.0	72.1	6.2	7.0	35.4	9.1	15.1
3740	28.1	10.0	37.4	559.1	12.7	52.4	6.9	8.7	27.5	12.2	13.7
3750	22.7	8.1	39.5	683.2	12.6	58.0	7.7	7.3	31.7	16.3	15.1
3760	32.8	5.3	60.0	625.6	14.4	78.6	8.4	4.8	36.3	8.6	0
3770	74.2	5.4	65.9	549.8	14.5	87.4	7.7	0	35.2	11.4	12.0
3780	64.8	7.6	65.8	556.5	17.5	86.7	7.7	4.0	29.0	9.5	24.8
3790	36.5	7.8	82.3	449.7	18.6	113.5	9.8	4.7	42.8	12.8	13.3
3800	35.8	0	73.8	431.1	17.6	101.6	7.3	5.3	42.2	50.9	16.3
3810	27.3	5.7	53.0	335.9	14.9	74.6	5.8	3.8	27.4	9.6	0
3820	22.2	6.4	46.1	478.6	15.4	73.5	6.7	3.7	26.8	40.2	16.4
3830	27.6	4.9	45.5	426.7	15.3	74.2	6.1	3.9	30.8	26.7	13.9
3840	27.8	0	46.9	394.5	15.9	63.7	6.7	3.6	26.9	35.8	0
3850	25.7	0	54.5	606.7	15.5	74.8	6.3	0	30.9	48.2	0
3855	28.4	8.1	64.9	325.3	15.7	85.0	8.3	4.6	24.4	7.6	16.1
3860	39.6	7.0	59.0	509.3	15.8	91.9	5.8	3.7	36.6	139.7	12.0
3870	33.9	4.5	81.7	291.7	24.0	145.0	9.3	9.0	43.3	15.7	13.3
3880	35.9	6.3	97.9	256.6	24.9	166.4	13.2	8.4	55.9	11.6	12.7
3890	86.3	5.6	86.5	345.4	21.3	145.6	12.1	16.0	43.0	78.9	12.4

6. Table 2a: Results of Yocemento #1 showing Major elements

Depth (ft)	Mg (%)	Mn (%)	Al (%)	Si (%)	P (%)	S (%)	K (%)	Ca (%)	Ti (%)	Fe (%)
3150	-	0.065	2.217	6.832	0.250	0.478	0.807	23.067	0.255	2.716
3160	0.970	0.071	2.001	6.459	0.252	0.237	0.782	24.127	0.221	2.343
3170	-	0.069	2.245	6.918	0.253	0.306	0.865	23.618	0.269	2.598
3180	1.962	0.058	2.435	7.140	0.287	0.151	0.996	16.733	0.318	3.841
3190	0.982	0.061	2.723	8.900	0.230	0.224	0.977	16.192	0.324	3.854
3200	1.204	0.047	3.468	9.839	0.282	0.228	1.387	13.663	0.334	4.045

3210	1.096	0.048	3.386	9.599	0.295	0.244	1.422	13.838	0.391	4.379
3220	2.063	0.038	3.109	9.168	0.280	0.193	1.237	11.253	0.396	4.093
3230	-	0.052	1.834	6.214	0.225	0.138	0.543	24.246	0.239	2.313
3240	-	0.047	1.561	4.939	0.202	0.091	0.496	28.662	0.226	2.265
3250	-	0.052	1.432	4.856	0.179	0.064	0.412	31.140	0.165	1.388
3260	-	0.044	1.528	4.953	0.202	0.082	0.487	28.788	0.223	2.307
3270	-	0.035	1.337	4.487	0.185	0.098	0.313	32.596	0.164	1.330
3280	-	0.032	2.366	6.165	0.231	0.096	0.915	21.985	0.317	4.183
3290	1.003	0.033	1.230	3.950	0.190	0.120	0.428	29.487	0.180	1.837
3300	1.060	0.026	2.100	6.615	0.228	0.140	0.849	21.796	0.271	3.327
3310	-	0.026	0.960	4.211	0.556	0.097	0.945	14.014	0.249	3.021
3320	1.068	0.034	1.570	5.308	0.212	0.163	0.540	23.755	0.227	2.723
3330	1.594	0.029	2.001	7.133	0.233	0.368	0.737	22.153	0.308	2.511
3340	-	0.025	2.063	6.013	0.224	0.081	0.714	24.255	0.291	2.834
3350	-	0.019	1.107	4.381	0.181	0.050	0.334	30.253	0.161	1.406
3360	-	0.034	1.326	4.581	0.195	0.072	0.377	30.260	0.168	1.275
3370	-	0.024	2.803	8.074	0.245	0.081	1.247	17.956	0.329	4.110
3380	1.031	0.029	1.180	4.359	0.223	0.255	0.364	29.777	0.151	1.307
3390	-	0.024	1.159	4.606	0.191	0.092	0.351	29.597	0.145	1.610
3400	-	0.015	1.715	5.059	0.196	0.085	0.568	27.180	0.172	1.487
3410	-	0.022	1.280	4.265	0.196	0.041	0.442	29.869	0.168	1.501
3420	0.981	0.027	1.894	6.559	0.226	0.219	0.807	21.415	0.272	3.107
3430	-	0.017	1.494	5.219	0.203	0.072	0.617	26.388	0.188	2.507
3440	-	0.019	0.968	6.056	0.202	0.093	0.271	28.083	0.104	1.038
3450	-	0.027	1.208	4.697	0.221	0.236	0.452	26.811	0.184	2.459
3460	-	0.030	1.081	3.657	0.212	0.067	0.380	30.534	0.161	1.718
3470	-	0.030	1.183	4.970	0.196	0.105	0.460	30.872	0.166	1.277
3480	-	0.027	0.974	4.202	0.185	0.076	0.313	32.377	0.148	1.429
3490	-	0.036	1.203	5.800	0.194	0.041	0.440	25.130	0.163	1.885
3500	1.087	0.036	1.360	5.548	0.214	0.178	0.506	24.299	0.198	2.338
3510	-	0.039	1.532	8.890	0.225	0.131	0.500	22.150	0.177	1.971
3520	0.981	0.036	1.535	6.453	0.251	0.113	0.617	22.671	0.225	2.908

3540	0.880	0.028	1.540	6.485	0.209	0.031	0.717	23.857	0.253	2.242
3550	-	0.025	1.645	5.651	0.204	0.045	0.662	23.853	0.254	2.855
3560	1.406	0.053	1.588	5.386	0.207	0.123	0.635	20.152	0.224	4.359
3570	2.053	0.030	2.104	7.278	0.259	0.149	0.879	18.470	0.269	3.186
3580	1.031	0.020	1.543	5.520	0.216	0.430	0.734	20.778	0.240	2.388
3590	-	0.023	2.089	6.875	0.232	0.590	0.879	23.244	0.284	5.512
3600	-	0.026	1.589	5.532	0.216	0.222	0.756	20.713	0.251	2.879
3610	-	0.026	1.808	6.986	0.223	0.100	0.750	22.836	0.239	2.795
3620	-	0.030	1.778	7.150	0.232	0.146	0.731	22.039	0.214	1.993
3630	0.962	0.030	1.230	4.885	0.209	0.038	0.397	30.064	0.125	1.105
3640	-	0.025	1.666	5.982	0.396	0.090	1.129	11.899	0.260	3.337
3650	-	0.029	1.413	5.094	0.188	0.076	0.685	27.285	0.243	2.126
3660	-	0.029	1.877	5.118	0.211	0.054	0.709	25.779	0.246	2.730
3670	-	0.019	1.354	3.896	0.195	-	0.525	31.765	0.195	2.148
3680	-	0.025	1.838	5.777	0.225	0.032	0.854	21.102	0.268	3.312
3690	-	0.024	0.903	3.097	0.170	0.039	0.266	32.412	0.162	1.614
3730	-	0.021	0.877	3.139	0.189	0.056	0.292	29.868	0.155	1.643
3740	1.316	0.028	1.632	5.849	0.217	0.197	0.639	24.233	0.228	2.506
3750	0.929	0.037	1.653	5.549	0.203	0.075	0.615	25.482	0.233	2.260
3760	1.029	0.041	1.619	5.150	0.208	0.054	0.653	24.388	0.215	2.415
3770	-	0.034	1.500	5.301	0.183	0.030	0.639	24.555	0.209	2.160
3780	-	0.069	1.270	5.104	0.207	-	0.646	29.267	0.176	1.653
3790	-	0.029	2.092	7.600	0.239	0.040	0.999	19.239	0.292	3.278
3800	-	0.030	2.042	7.475	0.215	0.053	0.941	20.682	0.307	3.240
3810	-	0.022	2.281	9.559	0.270	0.040	1.296	13.017	0.291	3.387
3820	1.113	0.031	2.022	9.422	0.255	0.040	0.878	15.717	0.251	2.511
3840	1.396	0.078	1.686	7.456	0.246	0.145	0.658	16.129	0.171	2.722
3850	1.977	0.075	1.611	7.439	0.296	0.097	0.667	15.148	0.154	1.817
3860	1.889	0.063	1.546	7.140	0.220	0.142	0.517	21.632	0.178	1.928
3870	2.590	0.110	1.383	5.540	0.221	0.058	0.394	21.031	0.111	1.343

7. Table 2b: Results of Showing Trace Elements for Yocemento #1

Depth (ft)	Ni (%)	Zn (%)	As (%)	Cr (%)	Rb (%)	Sr (%)	Y (%)	Zr (%)	Nb (%)	Mo (%)	Ta (%)	Pb (%)	Th (%)	LE (%)
3150	0.003	0.003	0.001	-	0.005	0.073	0.001	0.007	0.001	-	0.003	0.002	0.002	62.858
3160	-	0.002	0.001	0.007	0.004	0.066	0.001	0.007	0.001	0.001	0.003	0.001	0.002	62.443
3170	0.003	0.003	0.001	-	0.004	0.066	0.001	0.007	0.001	-	0.003	0.001	0.002	62.766
3180	0.005	0.005	0.001	-	0.009	0.046	0.002	0.011	0.001	-	0.004	0.001	0.001	65.996
3190	0.003	0.005	0.001	-	0.007	0.042	0.002	0.017	0.001	-	0.004	0.001	0.002	65.448
3200	0.003	0.005	0.001	0.006	0.009	0.041	0.002	0.010	0.001	-	0.005	0.001	0.002	65.417
3210	0.004	0.006	0.001	0.008	0.010	0.049	0.002	0.014	0.001	-	0.006	0.001	0.002	65.198
3220	0.004	0.006	-	0.006	0.009	0.029	0.003	0.015	0.001	-	0.005	0.001	-	68.091
3230	0.003	0.003	0.001	0.006	0.004	0.054	0.001	0.008	0.001	-	0.003	0.001	0.001	64.111
3240	-	0.003	-	0.006	0.004	0.058	0.001	0.007	0.001	-	0.003	0.001	0.001	61.425
3250	-	0.002	0.001	-	0.003	0.065	0.001	0.005	0.001	0.001	0.003	0.001	0.002	60.229
3260	-	0.003	-	0.008	0.004	0.057	0.001	0.007	0.001	-	0.003	0.001	0.002	61.298
3270	0.003	0.002	-	0.007	0.002	0.049	0.001	0.005	-	-	0.002	0.001	-	59.383
3280	0.005	0.005	0.001	0.008	0.010	0.051	0.001	0.007	0.001	-	0.006	0.001	0.001	63.612
3290	-	0.002	-	0.010	0.003	0.052	0.001	0.004	-	0.001	0.002	0.001	0.002	61.463
3300	0.003	0.005	0.001	0.008	0.008	0.040	0.001	0.007	0.001	-	0.005	0.001	0.001	63.509
3310	-	0.004	-	0.008	0.007	0.032	0.001	0.008	0.001	-	0.004	0.001	0.002	75.852
3320	-	0.003	0.001	0.009	0.006	0.041	0.001	0.009	0.001	-	0.003	0.001	0.001	64.326
3330	0.003	0.003	0.001	-	0.005	0.239	0.002	0.012	0.001	-	0.004	0.001	0.003	62.659
3340	-	0.003	0.001	0.008	0.007	0.046	0.001	0.008	0.001	0.001	0.005	0.001	0.002	63.416
3350	-	0.003	-	-	0.003	0.078	0.001	0.004	-	0.001	0.003	0.001	0.002	62.013
3360	0.003	0.002	-	-	0.003	0.058	0.001	0.006	0.001	-	0.002	-	-	61.636
3370	0.004	0.006	0.001	0.010	0.010	0.046	0.002	0.009	0.001	-	0.005	-	0.002	65.035
3380	-	0.003	0.001	0.006	0.003	0.053	0.001	0.007	0.001	-	0.003	0.001	0.001	61.245
3390	-	0.002	-	-	0.003	0.060	0.001	0.006	-	-	0.002	-	0.001	62.148
3400	0.003	0.002	0.001	-	0.004	0.051	0.002	0.010	0.001	-	0.004	0.001	0.002	63.442
3410	0.002	0.003	-	0.008	0.003	0.053	0.001	0.005	-	-	0.003	-	-	62.137
3420	0.004	0.004	0.001	0.006	0.007	0.050	0.002	0.010	0.001	-	0.004	0.001	0.001	64.401
3430	0.003	0.003	-	0.008	0.005	0.051	0.001	0.007	0.001	-	0.003	0.001	-	63.210
3440	0.003	0.002	-	-	0.003	0.045	0.001	0.004	-	0.001	0.002	-	0.001	63.107

3450	0.009	0.052	0.001	0.021	0.004	0.041	0.001	0.006	-	0.003	0.003	0.001	-	63.556
3460	0.003	0.004	-	0.009	0.003	0.073	0.001	0.004	-	0.001	0.003	0.001	0.002	62.054
3470	0.003	0.009	0.001	0.011	0.002	0.062	0.001	0.004	-	0.001	0.002	0.001	-	60.120
3480	-	0.002	0.001	-	0.002	0.065	0.001	0.004	-	-	0.002	-	0.002	60.185
3490	0.002	0.002	-	0.006	0.003	0.051	0.001	0.006	-	-	0.002	-	0.002	65.028
3500	0.002	0.003	0.001	0.008	0.005	0.066	0.002	0.006	0.001	-	0.003	0.001	-	64.140
3510	0.003	0.003	0.001	0.006	0.004	0.059	0.001	0.005	-	-	0.003	-	0.001	64.294
3520	0.003	0.005	0.001	0.007	0.005	0.068	0.001	0.006	0.001	-	0.004	0.001	0.001	64.107
3540	0.003	0.003	-	0.006	0.005	0.038	0.001	0.011	0.001	-	0.003	-	0.001	63.685
3550	-	0.003	0.001	-	0.007	0.038	0.001	0.010	0.001	-	0.004	0.001	0.001	64.740
3560	0.005	0.012	0.001	0.023	0.006	0.069	0.001	0.008	-	0.001	0.003	0.001	-	65.737
3570	0.005	0.005	0.001	-	0.007	0.095	0.001	0.010	0.001	-	0.004	0.001	0.003	65.190
3580	0.003	0.003	0.001	-	0.007	0.044	0.001	0.010	0.001	-	0.005	0.001	0.001	67.022
3590	0.007	0.004	0.001	0.006	0.006	0.051	0.001	0.011	0.001	0.001	0.004	0.002	0.002	60.176
3600	0.023	0.006	0.001	0.042	0.007	0.048	0.002	0.008	-	0.001	0.003	0.002	-	67.668
3610	0.004	0.004	0.001	-	0.005	0.044	0.001	0.006	-	0.001	0.002	0.001	0.002	64.165
3620	0.003	0.003	0.001	-	0.005	0.050	0.001	0.007	0.001	0.001	0.003	0.003	0.001	65.610
3630	0.002	0.002	0.001	0.010	0.002	0.071	0.002	0.003	-	0.001	0.002	0.001	-	60.859
3640	0.005	0.004	-	0.009	0.009	0.042	0.002	0.009	0.001	-	0.005	0.001	0.001	75.126
3650	-	0.003	0.001	-	0.004	0.062	0.001	0.007	0.001	0.001	0.004	0.001	0.002	62.775
3660	-	0.004	0.001	0.007	0.007	0.080	0.002	0.006	-	-	0.004	0.002	0.002	63.131
3670	0.004	0.003	-	0.006	0.004	0.055	0.001	0.004	-	-	0.003	0.001	0.002	59.817
3680	0.003	0.004	0.001	0.006	0.008	0.049	0.002	0.011	0.001	-	0.004	0.002	0.002	66.475
3690	0.003	0.002	-	-	0.003	0.057	0.001	0.005	0.001	-	0.003	0.002	-	61.236
3730	0.002	0.003	0.001	0.006	0.004	0.062	0.001	0.006	0.001	-	0.003	0.002	0.002	63.665
3740	0.002	0.003	0.001	0.008	0.004	0.055	0.002	0.006	-	-	0.003	0.004	-	63.066
3750	0.002	0.002	0.001	0.009	0.005	0.062	0.002	0.008	0.001	0.001	0.004	0.003	0.002	62.865
3760	0.003	0.003	-	0.008	0.005	0.068	0.002	0.007	0.001	-	0.003	0.002	-	64.126
3770	0.004	0.003	0.001	-	0.004	0.066	0.002	0.006	0.001	0.001	0.003	0.004	0.002	65.295
3780	0.002	0.002	0.001	-	0.004	0.042	0.001	0.004	-	-	0.003	0.002	0.002	61.542
3790	0.004	0.003	0.001	0.007	0.007	0.037	0.002	0.010	0.001	-	0.004	0.003	-	65.796
3800	0.003	0.003	0.001	0.009	0.007	0.040	0.002	0.009	0.001	-	0.004	0.002	0.001	64.933

3810	0.005	0.004	0.001	0.005	0.010	0.018	0.002	0.015	0.001	-	0.005	0.001	-	69.770
3820	0.003	0.003	0.001	0.008	0.007	0.022	0.002	0.010	0.001	-	0.003	0.002	0.002	67.699
3840	-	0.003	0.001	-	0.004	0.020	0.001	0.005	-	0.001	0.003	0.001	0.001	69.274
3850	0.003	0.001	-	-	0.004	0.020	0.001	0.006	0.001	-	0.001	0.001	-	70.677
3860	0.002	0.002	0.001	-	0.003	0.031	0.001	0.004	-	-	0.001	0.001	-	64.698
3870	0.002	0.002	-	0.006	0.002	0.017	0.001	0.003	-	-	0.001	0.001	-	67.185

8. Table 3a: Results of Mong Benno #1 showing Major elements

Depth (ft)	Mg	Al (%)	Si (%)	Mn (%)	Fe (%)	P (%)	S (%)	Cl (%)	K (%)	Ca (%)	Ti (%)
3600	1.064	1.469	4.640	0.031	1.859	0.267	0.051	0.002	0.458	29.916	0.189
3610	1.138	1.314	4.385	0.026	1.537	0.273	0.157	0.002	0.329	32.190	0.143
3620	1.103	1.793	6.034	0.026	2.008	0.254	0.092	0.002	0.586	29.009	0.204
3630	0.000	1.478	7.533	0.023	1.434	0.273	0.085	0.002	0.380	26.352	0.130
3630	1.734	1.718	5.684	0.022	1.671	0.280	0.106	0.002	0.480	30.585	0.197
3640	1.752	1.643	5.993	0.020	2.557	0.243	0.103	0.002	0.677	24.863	0.235
3650	0.957	1.356	4.467	0.026	1.442	0.244	0.086	0.002	0.350	33.289	0.160
3660	1.227	1.193	5.290	0.019	2.026	0.252	0.085	0.002	0.410	27.754	0.184
3670	2.404	1.122	5.521	0.030	1.596	0.258	0.136	0.002	0.288	29.064	0.109
3680	1.668	1.091	6.638	0.017	0.863	0.254	0.101	0.002	0.255	28.994	0.107
3690	1.679	1.283	5.211	0.017	1.079	0.260	0.148	0.002	0.356	30.586	0.128
3700	1.877	1.429	4.910	0.028	1.412	0.238	0.225	0.002	0.389	29.889	0.129
3710	1.047	2.207	7.668	0.026	2.774	0.269	0.192	0.002	0.695	22.879	0.247
3720	1.241	1.421	4.874	0.033	1.621	0.236	0.073	0.002	0.398	31.790	0.181
3730	1.290	2.178	6.851	0.032	3.110	0.267	0.058	0.002	0.745	26.163	0.286
3740	0.919	1.815	8.246	0.019	2.184	0.276	0.067	0.002	0.574	23.906	0.214
3750	0.980	1.626	6.857	0.039	1.425	0.275	0.107	0.002	0.511	27.770	0.153
3760	1.024	1.800	6.030	0.023	0.992	0.281	0.074	0.002	0.416	34.267	0.142
3770	1.895	1.445	4.810	0.033	1.435	0.247	0.081	0.002	0.324	30.795	0.120
3780	1.072	1.857	6.573	0.037	2.115	0.256	0.049	0.002	0.518	26.390	0.181
3790	1.819	1.485	6.249	0.022	1.185	0.240	0.061	0.002	0.336	23.179	0.101
3800	1.080	1.646	5.627	0.031	1.892	0.267	0.214	0.002	0.479	32.437	0.180

3810	1.261	1.486	5.099	0.023	1.372	0.248	0.043	0.002	0.452	32.426	0.196
3820	1.370	2.278	6.042	0.024	4.351	0.269	0.067	0.002	0.642	23.833	0.286
3830	2.130	0.564	1.841	0.022	0.480	0.223		0.000	0.023	38.900	0.071
3840	1.429	0.718	5.339	0.018	1.027	0.234	0.019	0.002	0.202	31.733	0.097
3850	0.000	0.630	2.230	0.016	0.669	0.189	0.007	0.002	0.114	38.564	0.084
3850	0.000	0.655	2.516	0.021	0.936	0.198	0.000	0.000	0.158	36.962	0.120
3860	0.000	0.521	1.716	0.020	1.663	0.301	0.053	0.002	0.165	35.800	0.164
3870	1.358	2.027	6.110	0.019	2.283	0.271	0.054	0.002	0.540	30.844	0.204
3880	1.026	1.527	5.997	0.018	1.014	0.230	0.044	0.002	0.356	31.118	0.128
3890	0.000	2.235	7.094	0.031	2.642	0.260	0.055	0.002	0.697	27.841	0.234
3900	1.262	2.199	5.710	0.024	2.361	0.264	0.034	0.002	0.642	29.456	0.219
3910	1.136	2.033	6.802	0.022	1.920	0.255	0.141	0.002	0.590	28.686	0.207
3920	0.000	1.357	4.213	0.023	2.147	0.412	0.053	0.002	0.602	27.110	0.229
3920	1.442	2.706	7.356	0.026	2.902	0.287	0.120	0.002	0.895	24.112	0.272
3930	0.000	1.158	3.899	0.029	2.832	0.384	0.035	0.002	0.563	27.260	0.250
3940	1.310	1.704	5.184	0.020	2.051	0.224	0.037	0.002	0.454	31.096	0.218
3950	1.061	2.049	6.467	0.028	1.814	0.262	0.080	0.002	0.663	28.592	0.226
3960	1.119	2.260	6.398	0.023	3.222	0.263	0.111	0.002	0.651	27.673	0.251
3970	1.259	3.069	8.366	0.029	2.940	0.308	0.114	0.002	0.954	23.676	0.302
3980	1.412	3.554	11.509	0.023	3.030	0.326	0.066	0.002	1.320	20.632	0.321
3990	1.214	2.190	7.638	0.044	2.003	0.286	0.021	0.002	0.750	27.147	0.244
4000	0.000	1.217	4.066	0.050	1.116	0.234	0.000	0.000	0.411	34.670	0.170
4010	1.395	2.671	8.772	0.048	2.521	0.266	0.000	0.000	0.924	22.930	0.290
4020	0.956	3.111	9.794	0.052	2.662	0.281	0.000	0.000	1.017	24.055	0.294
4030	1.290	2.708	9.288	0.040	2.815	0.296	0.028	0.002	0.934	22.744	0.299
4040	0.904	2.154	7.585	0.025	3.873	0.523	0.054	0.002	1.243	15.187	0.324
4050	1.609	3.458	11.508	0.043	3.330	0.316	0.039	0.002	1.271	17.938	0.347
4060	1.019	2.166	7.981	0.050	1.338	0.298	0.000	0.000	0.547	29.553	0.194
4070	1.288	2.703	10.655	0.039	1.982	0.334	0.052	0.002	0.833	21.036	0.240
4080	1.438	2.937	11.975	0.024	2.841	0.301	0.037	0.002	1.181	18.315	0.281
4100	1.806	1.697	9.751	0.033	1.697	0.350	0.046	0.002	0.476	22.820	0.172
4110	1.603	1.766	10.330	0.031	1.353	0.332	0.000	0.000	0.478	24.377	0.146

4120	1.461	1.680	11.484	0.029	1.368	0.327	0.007	0.002	0.464	21.093	0.165
4130	1.596	1.997	11.396	0.051	2.008	0.335	0.059	0.002	0.626	19.350	0.187
4140	1.599	2.467	13.907	0.036	2.603	0.352	0.048	0.002	0.822	16.874	0.228
4150	0.914	2.114	10.575	0.031	3.052	0.302	0.205	0.003	0.674	18.881	0.248
4160	0.998	2.383	10.601	0.048	2.238	0.300	0.051	0.002	0.762	20.673	0.257
4170	1.630	3.219	11.086	0.051	3.406	0.305	0.058	0.002	1.137	17.480	0.338
4182	1.143	5.775	18.050	0.010	4.949	0.423	0.035	0.002	2.301	3.512	0.423
4190	1.203	3.691	13.912	0.075	14.656	0.308	0.059	0.002	1.099	3.941	0.179
4200	0.797	3.570	21.740	0.012	3.917	0.412	0.042	0.002	1.022	4.048	0.318
4210	1.303	4.493	17.232	0.012	3.666	0.362	0.044	0.002	1.513	5.236	0.325
4220	0.822	4.351	15.593	0.031	3.660	0.386	0.070	0.002	1.392	13.180	0.378
4230	1.388	4.321	18.194	0.009	3.264	0.413	0.073	0.002	1.612	5.444	0.312
4240	0.822	4.085	22.172	0.010	3.547	0.457	0.057	0.002	1.261	2.018	0.296
4250	1.228	2.928	24.263	0.007	1.662	0.475	0.044	0.002	0.839	1.103	0.170
4260	0.000	2.327	25.747	0.007	1.259	0.422	0.030	0.002	0.645	2.492	0.142
4270	0.845	2.759	23.006	0.010	2.142	0.471	0.025	0.002	1.073	3.164	0.177
4280	2.773	1.818	17.398	0.018	1.562	0.352	0.056	0.002	0.496	10.265	0.148
4281	1.065	3.873	15.429	0.035	3.101	0.353	0.182	0.002	1.434	9.889	0.323
4285	2.451	1.641	18.514	0.012	1.290	0.361	0.000	0.000	0.537	8.002	0.127

9. Table 3b: Results of Showing Trace Elements for Mong Benno #1

Depth (ft)	Cr (ppm)	Ni (ppm)	Zn (ppm)	As (ppm)	Rb (ppm)	Sr (ppm)	Y (ppm)	Zr (ppm)	Nb (ppm)	Mo (ppm)	Ta (ppm)	Pb (ppm)	Th (ppm)
3600	58.0	34.9	27.3	-	43.4	494.1	12.4	56.5	3.5	-	30.2	9.3	-
3610	-	29.4	23.2	4.4	29.2	559.7	9.1	42.8	5.0	-	30.5	9.8	18.2
3620	82.5	24.4	31.3	9.1	42.2	424.7	12.0	54.2	6.6	6.9	36.2	8.9	16.5
3630	74.3	26.8	24.6	8.0	31.3	421.8	11.1	42.5	4.6	5.6	33.0	8.1	21.1
3640	73.0	21.5	37.0	7.4	58.9	358.0	11.1	100.1	6.9	6.9	34.9	4.8	17.7
3650	-	25.4	22.6	4.1	26.2	443.2	8.6	38.5	-	-	17.7	8.7	-
3660	74.7	31.8	33.8	3.7	56.3	397.8	13.5	53.9	5.6	5.7	39.1	6.6	-
3670	-	26.5	16.5	4.4	25.3	410.3	9.2	34.0	-	5.5	20.2	6.7	13.1
3680	70.1	23.3	17.0	-	15.5	452.0	7.5	30.2	3.1	-	-	8.0	-
3690	57.6	28.8	21.7	4.9	20.6	420.7	9.0	42.7	4.3	7.5	21.2	9.5	-

3700	56.2	20.9	26.7	4.0	23.1	396.8	8.7	43.4	3.6	8.1	19.4	12.3	-
3710	57.8	39.1	57.4	12.2	74.8	349.5	15.5	83.8	8.9	9.0	39.1	15.9	19.8
3720	97.8	23.7	49.2	-	33.8	810.2	13.2	48.7	4.7	7.2	24.9	8.6	-
3730	62.5	29.4	41.2	8.1	62.5	575.6	14.4	73.2	7.6	7.9	34.8	10.2	19.5
3740	56.4	-	30.3	-	52.4	495.0	12.6	59.6	5.3	3.5	33.3	6.8	-
3750	-	-	25.6	5.3	33.1	580.9	12.8	46.1	3.2	3.6	31.7	5.9	14.4
3760	77.6	-	23.1	-	16.9	824.5	10.0	33.7	3.4	4.1	23.1	6.0	14.2
3770	59.8	-	17.0	4.6	18.5	994.2	7.5	29.9	-	-	18.1	5.4	-
3780	-	-	31.4	4.6	35.5	804.7	15.4	59.8	4.2	-	22.9	-	-
3790	-	-	26.6	5.6	27.3	767.9	8.9	35.6	4.0	3.6	26.2	6.9	16.2
3790	-	-	15.5	4.7	17.3	439.7	10.0	28.7	4.5	-	24.0	-	20.8
3800	102.0	21.4	32.0	5.4	32.4	557.5	11.6	67.3	4.8	3.6	29.4	6.8	15.3
3810	-	-	26.7	5.9	34.8	596.1	11.6	53.0	4.3	-	29.8	5.2	16.6
3820	69.8	-	53.4	8.7	88.6	313.0	20.0	81.1	7.4	-	45.4	5.8	18.3
3830	-	-	12.9	4.7	6.3	516.1	5.5	16.7	3.1	3.5	-	-	12.4
3840	63.3	-	15.9	-	18.0	487.6	8.3	32.8	3.7	4.9	23.1	11.2	14.1
3850	-	-	21.0	3.9	13.8	504.8	8.4	25.9	4.1	7.3	15.6	6.6	12.7
3860	62.1	-	37.8	4.7	29.3	591.3	10.3	30.7	4.2	5.4	32.0	-	20.1
3870	60.7	-	34.9	7.8	57.2	517.7	12.4	66.4	6.6	4.1	46.3	9.3	16.5
3880	-	-	21.9	3.7	21.6	578.7	9.4	39.2	4.7	4.8	19.4	7.2	19.0
3900	81.4	24.4	32.4	5.0	44.2	763.6	11.7	57.2	5.7	-	29.7	4.9	16.9
3910	-	-	22.3	6.5	50.6	764.9	16.2	153.1	7.8	-	31.1	6.9	-
3920	90.4	21.2	36.4	14.7	54.7	728.5	12.2	78.6	6.5	4.2	31.0	12.8	16.2
3930	124.9	35.2	32.0	5.7	62.3	701.2	14.3	84.1	7.1	14.0	32.2	9.9	19.9
3940	58.2	27.4	28.6	10.9	42.5	723.0	10.6	69.0	5.3	-	29.3	9.0	15.1
3950	-	-	31.6	4.6	46.3	589.5	11.6	78.8	6.5	-	31.6	14.2	-
3960	79.1	25.2	30.4	8.4	46.1	568.7	13.5	83.8	6.9	-	46.5	11.8	14.3
3970	-	36.2	49.7	7.8	71.8	454.3	13.6	98.9	8.7	3.8	46.0	7.7	15.7
3980	84.9	36.2	36.7	7.2	66.5	568.3	15.3	93.4	5.6	4.5	46.2	10.8	11.8
3990	69.1	-	21.7	6.8	16.5	521.6	10.6	35.7	-	5.9	18.0	7.9	16.2
4000	65.0	24.5	23.8	3.7	31.3	538.7	14.4	38.0	5.0	7.9	28.2	6.3	22.7
4020	116.0	46.9	33.8	3.7	53.3	488.4	19.5	78.0	5.2	-	37.6	8.4	11.9

4030	64.9	40.5	36.3	7.5	63.1	471.0	16.3	83.3	6.5	-	45.2	10.5	21.3
4040	55.4	25.3	42.3	5.5	93.1	305.2	20.2	127.7	10.4	-	59.6	10.8	13.8
4050	98.8	37.2	34.0	5.4	61.8	517.9	19.8	123.6	8.9	3.8	35.6	11.1	15.0
4060	89.1	-	20.6	-	22.2	610.8	10.8	45.4	-	-	28.2	7.8	-
4070	84.4	23.6	25.3	4.1	43.2	638.9	18.0	76.2	6.7	3.9	36.8	7.3	18.7
4080	94.2	32.5	31.9	4.3	75.7	340.0	15.5	90.2	7.1	4.7	45.7	6.5	23.7
4100	80.8	32.4	25.8	4.2	39.7	478.4	18.7	96.9	4.4	-	19.7	10.2	-
4120	-	-	21.4	4.2	29.9	290.7	12.6	50.2	4.3	5.1	25.3	4.6	-
4130	97.8	19.6	35.8	8.3	49.7	288.2	15.9	70.0	6.5	-	29.1	9.3	13.1
4140	65.4	41.3	32.1	6.4	55.7	334.2	22.3	100.6	6.0	5.9	31.6	5.7	16.1
4150	-	26.8	37.5	-	76.7	318.7	16.7	94.6	9.0	7.0	46.6	10.0	-
4160	77.7	29.1	37.1	5.0	60.7	368.7	22.6	112.9	7.6	-	34.8	8.8	12.3
4170	71.4	33.2	34.9	7.0	54.8	467.2	19.8	81.7	9.0	8.3	31.8	6.5	21.6
4182	119.3	57.2	32.5	13.4	96.4	198.9	34.1	206.0	14.0	4.5	76.3	15.2	17.0
4190	2428.0	32.1	26.2	8.4	64.0	167.2	30.3	160.2	9.5	135.0	41.5	11.3	-
4200	75.7	30.4	21.9	5.5	51.0	151.3	25.9	199.7	9.4	-	33.2	11.4	13.6
4210	67.1	36.3	26.5	10.1	61.0	173.6	26.3	152.6	10.3	-	38.8	7.1	-
4220	86.5	39.6	28.0	9.2	59.9	210.7	61.7	129.0	7.9	4.0	36.3	6.3	-
4230	76.3	164.9	29.3	200.5	66.3	201.4	20.2	120.4	9.6	4.0	39.5	7.6	10.5
4240	48.0	32.7	24.0	5.8	48.9	140.5	25.2	116.6	9.0	3.8	42.6	8.0	-
4250	50.6	23.0	11.7	3.7	31.6	107.5	14.2	79.1	6.5	5.4	19.6	4.4	-
4260	-	21.4	16.0	4.3	44.7	226.7	34.5	94.7	6.2	4.0	26.2	-	15.2
4270	51.2	18.3	17.9	3.2	43.5	123.8	15.1	55.8	5.2	3.9	21.9	3.7	-
4280	55.6	26.1	14.5	4.2	33.4	204.9	8.7	48.4	-	-	16.3	-	-
4281	55.0	37.4	32.8	9.5	88.7	330.2	24.4	183.9	11.6	4.4	45.9	18.4	18.1
4285	50.6	27.3	15.4	-	36.3	151.8	12.8	60.5	4.5	6.0	24.3	4.6	-

10. Table 4a: Results of Yocemento #1 showing Major elements Major Elements

Depth (ft)	Mg (%)	Al (%)	Si (%)	P (%)	S (%)	K (%)	Ca (%)	Ti (%)	Cr (%)	Fe (%)
3150	0.000	2.217	6.832	0.250	0.478	0.807	23.067	0.255	0.000	2.716
3160	0.970	2.001	6.459	0.252	0.237	0.782	24.127	0.221	0.007	2.343

3170	0.000	2.245	6.918	0.253	0.306	0.865	23.618	0.269	0.000	2.598
3180	1.962	2.435	7.140	0.287	0.151	0.996	16.733	0.318	0.000	3.841
3190	0.982	2.723	8.900	0.230	0.224	0.977	16.192	0.324	0.000	3.854
3200	1.204	3.468	9.839	0.282	0.228	1.387	13.663	0.334	0.006	4.045
3210	1.096	3.386	9.599	0.295	0.244	1.422	13.838	0.391	0.008	4.379
3220	2.063	3.109	9.168	0.280	0.193	1.237	11.253	0.396	0.006	4.093
3230	0.000	1.834	6.214	0.225	0.138	0.543	24.246	0.239	0.006	2.313
3240	0.000	1.561	4.939	0.202	0.091	0.496	28.662	0.226	0.006	2.265
3250	0.000	1.432	4.856	0.179	0.064	0.412	31.140	0.165	0.000	1.388
3260	0.000	1.528	4.953	0.202	0.082	0.487	28.788	0.223	0.008	2.307
3270	0.000	1.337	4.487	0.185	0.098	0.313	32.596	0.164	0.007	1.330
3280	0.000	2.366	6.165	0.231	0.096	0.915	21.985	0.317	0.008	4.183
3290	1.003	1.230	3.950	0.190	0.120	0.428	29.487	0.180	0.010	1.837
3300	1.060	2.100	6.615	0.228	0.140	0.849	21.796	0.271	0.008	3.327
3310	0.000	0.960	4.211	0.556	0.097	0.945	14.014	0.249	0.008	3.021
3320	1.068	1.570	5.308	0.212	0.163	0.540	23.755	0.227	0.009	2.723
3330	1.594	2.001	7.133	0.233	0.368	0.737	22.153	0.308	0.000	2.511
3340	0.000	2.063	6.013	0.224	0.081	0.714	24.255	0.291	0.008	2.834
3350	0.000	1.107	4.381	0.181	0.050	0.334	30.253	0.161	0.000	1.406
3360	0.000	1.326	4.581	0.195	0.072	0.377	30.260	0.168	0.000	1.275
3370	0.000	2.803	8.074	0.245	0.081	1.247	17.956	0.329	0.010	4.110
3380	1.031	1.180	4.359	0.223	0.255	0.364	29.777	0.151	0.006	1.307
3390	0.000	1.159	4.606	0.191	0.092	0.351	29.597	0.145	0.000	1.610
3400	0.000	1.715	5.059	0.196	0.085	0.568	27.180	0.172	0.000	1.487
3410	0.000	1.280	4.265	0.196	0.041	0.442	29.869	0.168	0.008	1.501
3420	0.981	1.894	6.559	0.226	0.219	0.807	21.415	0.272	0.006	3.107
3430	0.000	1.494	5.219	0.203	0.072	0.617	26.388	0.188	0.008	2.507
3440	0.000	0.968	6.056	0.202	0.093	0.271	28.083	0.104	0.000	1.038
3450	0.000	1.208	4.697	0.221	0.236	0.452	26.811	0.184	0.021	2.459
3460	0.000	1.081	3.657	0.212	0.067	0.380	30.534	0.161	0.009	1.718
3470	0.000	1.183	4.970	0.196	0.105	0.460	30.872	0.166	0.011	1.277
3480	0.000	0.974	4.202	0.185	0.076	0.313	32.377	0.148	0.000	1.429

3490	0.000	1.203	5.800	0.194	0.041	0.440	25.130	0.163	0.006	1.885
3500	1.087	1.360	5.548	0.214	0.178	0.506	24.299	0.198	0.008	2.338
3510	0.000	1.532	8.890	0.225	0.131	0.500	22.150	0.177	0.006	1.971
3520	0.981	1.535	6.453	0.251	0.113	0.617	22.671	0.225	0.007	2.908
3540	0.880	1.540	6.485	0.209	0.031	0.717	23.857	0.253	0.006	2.242
3550	0.000	1.645	5.651	0.204	0.045	0.662	23.853	0.254	0.000	2.855
3560	1.406	1.588	5.386	0.207	0.123	0.635	20.152	0.224	0.023	4.359
3570	2.053	2.104	7.278	0.259	0.149	0.879	18.470	0.269	0.000	3.186
3580	1.031	1.543	5.520	0.216	0.430	0.734	20.778	0.240	0.000	2.388
3590	0.000	2.089	6.875	0.232	0.590	0.879	23.244	0.284	0.006	5.512
3600	0.000	1.589	5.532	0.216	0.222	0.756	20.713	0.251	0.042	2.879
3610	0.000	1.808	6.986	0.223	0.100	0.750	22.836	0.239	0.000	2.795
3620	0.000	1.778	7.150	0.232	0.146	0.731	22.039	0.214	0.000	1.993
3630	0.962	1.230	4.885	0.209	0.038	0.397	30.064	0.125	0.010	1.105
3640	0.000	1.666	5.982	0.396	0.090	1.129	11.899	0.260	0.009	3.337
3650	0.000	1.413	5.094	0.188	0.076	0.685	27.285	0.243	0.000	2.126
3660	0.000	1.877	5.118	0.211	0.054	0.709	25.779	0.246	0.007	2.730
3670	0.000	1.354	3.896	0.195	0.000	0.525	31.765	0.195	0.006	2.148
3680	0.000	1.838	5.777	0.225	0.032	0.854	21.102	0.268	0.006	3.312
3690	0.000	0.903	3.097	0.170	0.039	0.266	32.412	0.162	0.000	1.614
3730	0.000	0.877	3.139	0.189	0.056	0.292	29.868	0.155	0.006	1.643
3740	1.316	1.632	5.849	0.217	0.197	0.639	24.233	0.228	0.008	2.506
3750	0.929	1.653	5.549	0.203	0.075	0.615	25.482	0.233	0.009	2.260
3760	1.029	1.619	5.150	0.208	0.054	0.653	24.388	0.215	0.008	2.415
3770	0.000	1.500	5.301	0.183	0.030	0.639	24.555	0.209	0.000	2.160
3780	0.000	1.270	5.104	0.207	0.000	0.646	29.267	0.176	0.000	1.653
3790	0.000	2.092	7.600	0.239	0.040	0.999	19.239	0.292	0.007	3.278
3800	0.000	2.042	7.475	0.215	0.053	0.941	20.682	0.307	0.009	3.240
3810	0.000	2.281	9.559	0.270	0.040	1.296	13.017	0.291	0.005	3.387
3820	1.113	2.022	9.422	0.255	0.040	0.878	15.717	0.251	0.008	2.511
3840	1.396	1.686	7.456	0.246	0.145	0.658	16.129	0.171	0.000	2.722
3850	1.977	1.611	7.439	0.296	0.097	0.667	15.148	0.154	0.000	1.817

3860	1.889	1.546	7.140	0.220	0.142	0.517	21.632	0.178	0.000	1.928
3870	2.590	1.383	5.540	0.221	0.058	0.394	21.031	0.111	0.006	1.343

11. Table 4b: Results of Yocemento #1 showing Trace and Rare earth elements

Depth (ft)	P (ppm)	Cr (ppm)	Ni (ppm)	Zn (ppm)	As (ppm)	Rb (ppm)	Sr (ppm)	Y (ppm)	Zr (ppm)	Nb (ppm)	Mo (ppm)	Ta (ppm)	Pb (ppm)	Th (ppm)
3150	2502.3	-	33.8	32.9	7.3	52.2	733.8	12.9	74.6	7.5	-	31.1	15.5	18.3
3160	2517.4	67.4	-	24.6	6.7	44.7	660.4	12.4	66.7	6.6	5.4	27.9	8.2	15.5
3170	2532.6	-	27.2	33.7	7.4	40.8	656.5	13.4	66.3	5.2	4.4	28.8	9.1	24.3
3180	2865.7	-	46.8	51.2	7.9	88.3	457.7	18.0	106.1	12.4	-	37.5	10.8	12.3
3190	2300.7	-	31.9	49.7	7.2	66.8	417.4	22.7	173.9	9.7	-	44.9	10.2	20.2
3200	2817.3	62.6	27.3	52.3	13.3	90.6	414.0	22.1	99.2	9.0	3.5	47.7	10.1	17.3
3210	2951.5	78.3	43.3	61.9	6.3	102.3	485.1	21.5	139.6	13.1	4.8	63.7	11.9	17.3
3220	2799.0	62.5	43.8	61.7	-	95.0	289.7	25.3	147.6	10.3	-	46.1	8.4	-
3230	2247.6	59.3	26.4	25.6	6.8	38.3	541.5	13.5	82.5	6.2	3.9	30.0	13.0	12.4
3240	2020.4	60.6	-	29.8	4.9	40.6	581.0	14.1	73.8	5.3	-	28.8	5.2	14.5
3250	1788.8	-	-	18.4	5.7	25.5	650.1	10.2	50.2	6.0	6.1	25.6	7.8	22.0
3260	2019.1	80.9	-	32.5	4.8	39.9	570.7	14.0	73.8	7.1	3.6	33.7	6.1	18.0
3270	1849.9	69.3	34.5	22.1	-	24.8	485.4	9.6	47.8	-	-	22.7	9.0	-
3280	2307.8	83.0	50.5	53.7	7.0	95.0	510.1	14.8	74.4	10.1	-	57.4	6.1	15.0
3290	1899.5	100.3	-	22.6	3.6	32.4	520.8	11.4	40.7	5.0	5.9	22.3	8.3	16.7
3300	2275.8	78.1	28.8	47.9	5.6	76.1	396.5	13.1	74.8	6.9	-	49.0	6.4	14.2
3310	5563.4	83.8	-	41.5	4.0	69.8	322.7	13.9	80.9	9.5	5.0	38.3	11.2	15.4
3320	2122.4	92.6	-	26.0	5.0	57.7	406.5	14.7	88.7	5.7	-	32.4	5.5	11.0
3330	2333.3	-	32.9	34.2	7.2	52.8	2392.9	15.2	116.8	9.4	4.6	41.5	11.6	28.3
3340	2241.8	79.0	-	29.9	8.7	74.4	464.2	13.2	79.5	8.2	5.7	52.6	9.4	17.8
3350	1812.1	-	-	25.3	4.5	27.8	784.3	10.2	39.3	4.5	7.8	29.7	5.9	17.4
3360	1951.7	-	29.8	23.7	4.6	26.7	578.5	9.3	58.8	5.4	3.6	20.8	-	-
3370	2452.9	98.0	38.4	55.1	6.9	101.4	461.2	19.4	88.4	7.3	-	54.2	-	21.9
3380	2227.4	59.9	-	25.1	5.4	32.1	530.3	13.1	69.4	5.5	4.5	30.2	7.8	14.0
3390	1912.6	-	-	21.9	3.4	29.1	604.3	11.3	61.1	4.3	-	20.2	-	12.9

3400	1961.2	-	31.2	25.0	7.7	42.6	506.9	16.8	101.7	6.2	-	44.7	13.3	16.6
3410	1962.2	82.6	21.4	25.4	4.2	33.1	529.8	10.8	47.3	3.7	-	29.5	-	-
3420	2263.6	60.4	36.0	36.6	9.1	74.6	497.7	16.9	95.2	7.1	-	37.4	7.8	11.3
3430	2033.5	80.7	31.3	30.9	4.4	54.6	505.8	11.4	65.8	7.2	4.4	31.5	10.0	-
3440	2018.9	-	26.7	19.2	3.1	25.1	445.4	8.4	39.2	-	5.1	19.7	-	12.2
3450	2208.9	209.0	90.3	522.8	9.5	41.7	413.4	13.0	64.8	-	30.4	29.3	13.0	-
3460	2117.7	94.0	32.8	37.9	4.9	33.7	727.1	10.0	41.8	4.6	5.3	28.9	6.8	15.6
3470	1957.4	106.8	30.2	88.5	5.1	20.1	615.1	9.0	35.6	3.8	14.5	21.2	7.8	-
3480	1853.9	-	-	22.1	5.5	22.1	648.1	7.7	40.7	3.4	-	22.1	-	15.9
3490	1940.1	60.8	23.1	24.0	-	33.1	508.7	12.3	60.2	4.3	7.2	21.7	-	17.8
3500	2136.0	80.5	24.0	25.8	5.4	52.9	661.2	15.2	58.4	5.5	-	33.4	8.5	-
3510	2246.7	62.5	27.1	26.6	5.8	36.6	594.8	10.0	54.9	3.4	-	28.3	-	11.1
3520	2510.5	67.6	25.8	47.3	9.7	53.3	682.7	13.1	59.2	5.8	-	36.7	6.8	12.1
3540	2091.6	64.0	26.1	29.7	3.4	54.3	383.1	14.3	108.9	6.4	-	28.7	-	13.1
3550	2035.4	-	-	33.6	5.0	65.3	383.5	14.7	97.0	7.4	3.4	36.2	7.5	14.0
3560	2067.9	228.9	45.7	117.3	9.6	55.6	686.9	14.7	75.6	4.7	6.8	29.1	10.3	-
3570	2590.2	-	50.9	46.0	5.4	70.8	953.1	14.3	101.8	8.3	-	40.5	12.2	27.1
3580	2161.7	-	26.0	31.1	8.0	67.4	443.2	13.9	103.9	8.6	-	46.2	8.6	14.7
3590	2317.4	61.0	68.5	36.5	7.0	55.3	509.7	14.5	110.5	7.7	6.0	42.3	21.9	19.5
3600	2162.9	419.1	232.0	63.5	10.7	70.0	480.4	15.2	84.2	4.7	14.4	33.3	20.5	-
3610	2229.8	-	39.2	39.9	10.0	46.8	441.8	12.3	59.6	4.1	13.4	24.6	9.5	20.6
3620	2316.3	-	26.9	31.2	9.0	51.8	496.1	13.8	70.9	7.7	10.2	31.9	28.3	12.0
3630	2088.4	96.1	24.6	24.2	5.5	19.4	708.1	15.6	30.4	3.9	6.6	16.9	6.7	-
3640	3960.3	88.3	52.5	44.5	4.1	85.7	422.6	15.7	93.7	9.0	-	49.9	12.3	13.3
3650	1879.2	-	-	33.7	5.0	42.4	618.6	14.2	68.8	6.6	6.1	38.3	6.3	24.4
3660	2112.9	73.7	-	38.4	6.5	65.0	802.6	15.2	56.3	4.8	-	43.6	22.0	16.9
3670	1946.4	59.5	39.8	31.8	3.7	44.4	554.6	10.0	43.9	4.1	-	32.7	6.8	18.4
3680	2246.2	64.1	32.5	37.6	7.7	81.6	490.2	16.2	108.9	8.9	3.6	36.7	15.5	15.1
3690	1699.7	-	27.9	22.9	-	33.7	574.9	9.0	49.2	5.3	-	25.2	21.0	-
3730	1889.9	58.3	24.7	32.9	8.1	38.4	620.9	13.7	62.5	6.2	4.9	34.5	24.2	21.7
3740	2169.2	77.6	21.9	27.3	8.9	37.9	552.6	15.4	59.9	4.8	4.5	27.6	38.5	-
3750	2033.5	85.6	23.0	22.7	8.5	49.0	619.2	18.0	75.4	6.7	5.1	36.6	25.5	21.7

3760	2078.9	78.4	31.3	32.0	4.4	50.0	680.3	17.4	74.4	6.3	-	29.2	21.4	-
3770	1829.8	-	36.0	29.4	6.0	39.6	660.3	15.9	58.9	6.7	6.4	32.8	39.5	15.1
3780	2073.0	-	23.8	24.7	6.3	43.3	421.7	14.0	44.2	4.9	3.5	31.1	20.1	18.7
3790	2389.4	66.7	38.1	26.8	5.7	74.8	367.0	17.3	99.1	7.7	-	38.8	32.2	-
3800	2153.2	92.4	32.5	29.3	7.6	72.2	402.4	16.7	90.3	7.3	-	35.3	19.1	12.6
3810	2703.9	53.6	45.3	38.3	6.3	105.0	177.0	20.5	154.1	11.6	-	49.2	12.3	-
3820	2552.3	84.6	31.5	26.2	5.5	71.5	219.2	18.8	95.2	7.6	-	33.0	19.7	15.0
3830		-	-	-	-	47.3	161.3	-	-	-	-	-	-	-
3840	2460.4	-	-	26.4	6.1	41.4	196.3	9.5	52.4	4.6	5.1	26.7	10.9	13.5
3850	2961.9	-	27.1	14.8	-	37.1	202.5	7.6	59.9	5.7	-	14.3	14.4	-
3860	2200.7	-	24.9	23.8	5.3	25.1	313.8	9.0	40.8	-	-	13.3	12.1	-
3870	2213.2	56.9	20.7	16.8	4.3	16.1	169.6	6.0	28.7	-	-	14.7	10.4	-

12. Table 5a: Results of Rhian #3 showing Major elements Major Elements

Depth (ft)	Mg (%)	Al (%)	Si (%)	K (%)	Ca (%)	Ti (%)	Mn (%)	Fe (%)
3310	1.549	2.439	7.051	0.788	26.722	0.243	0.048	2.641
3320	1.380	2.471	7.203	0.585	28.598	0.244	0.031	1.821
3330	1.342	2.499	7.687	0.722	25.313	0.280	0.036	2.340
3340	0.939	1.771	6.316	0.868	19.916	0.254	0.027	2.548
3350	1.870	3.081	9.710	1.052	15.409	0.292	0.046	4.012
3360	1.332	3.147	9.787	1.144	18.452	0.231	0.030	2.916
3370	2.260	3.197	9.785	0.999	19.737	0.261	0.037	2.662
3380	1.490	2.726	10.215	0.890	19.792	0.286	0.044	2.195
3390	1.402	3.535	10.582	1.255	16.853	0.337	0.039	3.401
3400	1.430	2.889	10.003	0.946	20.488	0.262	0.031	2.270
3410	2.575	4.253	12.665	1.757	11.560	0.364	0.031	3.927
3420	1.821	1.635	5.428	0.438	30.493	0.174	0.034	1.525
3430	1.677	2.224	6.713	0.626	27.061	0.204	0.022	2.171
3440	1.612	1.474	4.924	0.515	28.064	0.204	0.026	1.464
3450	1.852	3.727	11.408	1.655	14.920	0.322	0.026	4.135
3460	1.319	2.581	7.556	0.788	23.023	0.233	0.032	2.646
3470	1.403	3.657	12.086	1.470	13.991	0.363	0.029	3.483
3490	1.824	2.804	8.956	1.058	19.599	0.285	0.027	3.068

3500	1.690	2.912	8.730	1.025	20.761	0.278	0.034	2.500
3509	1.390	2.732	8.389	0.970	22.633	0.309	0.027	2.941
3510	1.164	3.179	9.347	1.108	19.378	0.339	0.024	4.205
3520	1.802	3.590	11.147	1.384	16.406	0.341	0.032	3.229
3530	1.916	4.159	13.157	1.801	11.258	0.351	0.030	4.480

13. Table 5b: Results of Showing Trace and Rare Earth Elements in Rhian #3

Depth (ft)	P (ppm)	Ti (ppm)	Cr (ppm)	Ni (ppm)	Zn (ppm)	As (ppm)	Rb (ppm)	Sr (ppm)	Y (ppm)	Zr (ppm)	Nb (ppm)	Mo (ppm)	Ta (ppm)	Pb (ppm)	Th (ppm)
3310	2543.43	2433.82	56.25	23.01	43.69	9.17	55.93	400.79	14.26	71.24	4.37	-	47.05	9.31	-
3320	2760.28	2438.27	72.08	20.57	31.01	8	34.93	464.39	12.82	65.93	5.38	4.29	38.9	10.08	12.24
3330	3217.51	3236.34	74.56	31.54	56.81	10.4	62.07	362.73	19.91	149.9	8.91	4.09	37.75	9.35	12.31
3340	2746.2	2220.33	90.74	20.34	35.44	15.75	54.09	336.2	12.94	76.44	5.62	4.11	29.66	10.86	-
3350	3051.46	2640.43	78.74	26.75	38.64	7.38	57.1	338.35	15.68	102.54	7.45	-	27.14	8.97	14.17
3360	3262.07	2306.71	58.27	25.42	49.47	8.21	60.69	375.77	13.98	77.14	7.7	4.57	34.14	38.82	20.5
3370	3303.09	2520.35	74.13	21.03	40	10.16	49.64	449.81	14.05	87.71	4.83	4.62	28.6	12.04	-
3380	3188.46	3171.76	73.28	55.71	111.87	10.56	78.39	364.55	20.91	124.65	8.07	14.39	43.54	19.81	16.02
3390	2990.69	3366.63	98.99	39.03	68.84	12.48	81.57	418.91	18.53	128.71	8.6	4.66	41.75	68.23	11.27
3400	3196.58	2622.28	99.5	23.73	36.4	6.72	50.39	427.25	18.05	110.96	8.5	4.23	30.59	5.32	-
3410	3843.6	3638.7	91.27	46.06	65.36	9.31	103.06	388.13	22.78	146.55	11.32	-	50.91	12.09	14.09
3420	2367.96	1742.31	81.99	30.72	37.84	3.43	30.08	466.4	13.95	67.54	4.26	-	16.72	8.57	-
3430	2091.08	2037.86	111.76	25	23.85	11.67	49.98	380.22	15.86	72.86	4.87	-	33.58	6.35	14.52
3440	3826	2042.51	105.32	26.29	51.56	4.29	30.52	557.63	10.57	49.62	3.88	4.85	33.42	-	-
3450	3710.23	3216.62	189.53	95.48	282.88	15.16	81.77	285.4	21	136.88	9.02	31.49	40.12	21.96	12.07
3460	2874.2	2328.01	205.57	130.05	163.23	16.23	57.99	327.57	15.55	75	6.74	40.45	49.92	34.55	-
3470	3609.85	3631.41	226.49	87.13	204.22	14.18	86.26	286.1	21.49	138.59	9.29	23.77	48.27	27.02	15.8
3490	2865.73	2847.08	198.88	92.61	153.74	19.48	59.89	459.16	17.73	96.93	6.11	34.23	34.96	26.05	13.03
3500	2996.81	2783.43	138.74	51.25	140.31	6.91	68.6	667.3	18.61	99.18	7.38	20.69	41.22	14.51	-
3509	2400.35	3328.92	91.63	38.33	48	6.65	86.98	212.44	17.35	156.03	10.08	-	41.83	7.06	-
3510	2866.46	3392.62	58.89	46.66	36.03	6.01	82.75	380.95	15.81	126.01	9.06	5.04	38.01	10.45	14.23
3520	3072.52	3405.4	94.1	48.08	48.84	8.55	76.63	448.25	19.67	136.4	10.14	6.5	38.24	11.49	16.52

3530	3417.21	3510.72	84.1	45.8	81.9	6.11	107.28	276.69	19.22	156.76	10.94	-	51.96	7.26	11.3
3872	3870.58	3801.78	75.07	40.5	44.2	5.46	100.25	238.2	26.76	249.15	12.61	-	53.03	7.07	12.86

14. Table 6a: Results of Showing Major Elements in Worcester #3

Depth (ft)	Mg (ft)	Al (ft)	Si (ft)	K(ft)	Ca (ft)	Mn (ft)	Fe (ft)
3100	3.08	5.90	16.55	2.26	2.87	0.03	4.35
3050	2.46	5.40	14.52	1.89	5.71	0.04	3.82
3060	4.27	5.61	14.79	1.97	6.89	0.07	3.35
3070	2.43	5.18	13.27	1.65	4.79	0.03	4.15
3080	3.07	5.37	14.42	1.40	4.43	0.05	6.32
3100	3.23	5.36	14.59	1.82	4.32	0.04	3.94
3120	2.17	5.48	14.87	2.16	3.02	0.02	3.76
3130	2.85	4.94	13.87	1.65	7.47	0.04	3.23
3140	2.55	3.37	9.26	0.80	17.75	0.05	2.59
3150	2.28	3.39	9.27	1.07	20.83	0.06	2.38
3160	2.19	3.04	8.60	0.71	21.80	0.05	2.20
3170	2.12	2.39	6.49	0.61	25.41	0.05	2.18
3180	1.30	2.64	7.79	0.80	24.10	0.04	3.18
3200	1.89	2.70	7.31	0.77	23.86	0.05	2.70
3210	3.24	2.68	7.77	0.87	17.58	0.08	3.85
3220	2.20	3.50	9.91	0.95	21.07	0.04	2.76
3230	1.47	2.85	7.33	0.53	27.58	0.04	1.69
3240	3.22	3.53	10.26	1.30	14.08	0.05	3.96
3250	1.85	2.77	8.27	0.75	25.79	0.06	2.09
3260	1.57	2.48	7.80	0.79	23.45	0.05	2.33
3270	2.10	3.33	9.61	1.14	17.93	0.05	3.33
3280	2.30	3.40	10.10	1.37	14.78	0.03	3.89
3200	2.72	2.77	8.01	0.79	23.15	0.05	2.60
3400	2.09	3.36	11.09	1.35	11.29	0.03	4.36
3410	2.15	2.98	9.96	1.14	19.64	0.04	3.00
3420	1.95	1.45	5.89	0.39	27.43	0.03	1.11
3430	2.11	2.15	7.29	0.63	22.29	0.03	2.39
3440	1.93	2.34	8.50	0.62	25.82	0.03	1.32

3450	1.82	2.04	6.74	0.66	26.36	0.03	2.33
3460	1.18	2.17	6.59	0.87	21.87	0.02	2.77
3470	1.55	2.29	8.08	0.70	23.79	0.03	2.47
3480	1.65	3.11	9.84	1.23	15.38	0.02	3.78
3490	1.80	2.61	8.48	0.83	23.31	0.04	2.95
3500	2.20	2.92	8.76	1.00	20.58	0.04	4.41
3509	0.98	2.05	6.53	0.65	27.12	0.03	2.35
3510	1.47	3.04	9.66	1.06	20.65	0.03	2.62
3520	0.98	2.32	7.86	0.70	24.13	0.03	2.12
3530	1.22	2.17	10.10	0.63	23.45	0.03	1.60
3540	1.67	2.83	10.79	0.99	19.11	0.03	2.55
3550	1.50	4.59	13.25	1.98	9.78	0.03	4.41
3560	1.67	2.80	8.21	0.94	22.08	0.03	2.99
3570	1.39	3.90	11.79	1.45	14.85	0.03	3.23
3580	1.52	3.63	11.84	1.61	10.91	0.02	3.97
3500	1.38	2.59	8.26	0.93	23.15	0.03	2.66
3562	1.52	2.54	7.63	0.82	23.18	0.03	2.76
3600	1.68	3.41	11.08	1.24	17.02	0.03	2.95
3610	2.40	4.03	12.36	1.69	13.28	0.03	4.20
3620	1.91	3.78	11.76	1.52	14.42	0.07	3.17
3630	3.01	4.28	14.05	1.74	7.77	0.03	3.40
3640	1.93	4.27	14.42	2.00	9.23	0.03	4.39
3650	3.13	5.47	16.34	2.51	1.96	0.03	5.62
3660	1.98	3.37	10.46	1.26	18.41	0.03	3.75
3670	2.78	4.56	14.26	1.96	10.12	0.05	3.70
3680	1.85	3.94	11.17	1.48	14.57	0.03	4.12
3658	2.23	3.87	12.21	1.54	14.55	0.03	3.08
3700	2.25	4.19	13.31	1.86	11.33	0.03	3.92
3710	3.40	5.01	15.82	2.17	3.79	0.05	4.23
3720	3.61	5.00	15.81	2.14	5.14	0.03	4.29
3730	3.28	4.73	14.74	2.03	7.14	0.03	4.29
3740	3.40	4.15	12.39	1.72	8.91	0.03	5.06
3750	3.05	4.92	15.93	2.15	7.53	0.03	3.71
3760	2.25	5.08	15.90	2.36	4.66	0.03	4.33

3770	2.57	4.96	16.24	2.22	3.28	0.02	4.56
3780	2.05	3.32	9.95	1.21	18.12	0.04	3.22
3790	1.89	4.24	13.16	1.73	10.33	0.03	4.83
3800	2.64	4.51	14.58	1.91	8.56	0.04	3.79
3810	1.35	3.02	10.37	1.80	7.83	0.03	4.43
3820	2.63	4.51	15.37	2.14	8.20	0.04	3.56
3830	2.13	4.16	13.88	1.74	10.85	0.05	2.98
3840	2.94	3.88	12.84	1.66	10.91	0.04	3.00
3850	3.20	4.16	13.87	1.82	8.00	0.04	4.37
3860	4.41	3.02	10.54	1.09	12.90	0.05	3.01
3870	3.17	4.08	12.65	1.78	9.91	0.04	3.95

15. Table 6b: Results of Showing Trace and Rare Earth Elements in Worcester #3

Depth (ft)	P (ppm)	Ti (ppm)	Cr (ppm)	Ni (ppm)	Zn (ppm)	As (ppm)	Rb (ppm)	Sr (ppm)	Y (ppm)	Zr (ppm)	Nb (ppm)	Mo (ppm)	Ta (ppm)	S (ft)	Pb (ppm)	Th (ppm)
3100	4205.23	4503.79	72.49	59.31	64.85	50.67	144.54	116.11	37.04	238.94	13.07	-	69.78	0.29	20.93	-
3050	4028.02	3726.17	-	44.80	61.25	11.87	110.55	162.51	36.76	164.91	12.14	3.26	67.96	0.78	14.38	12.24
3060	3844.56	3893.44	80.02	47.84	66.51	17.04	89.17	261.14	27.87	149.70	10.63	3.09	45.29	0.33	42.90	14.46
3070	4937.41	4359.06	57.29	36.58	63.33	22.95	114.80	141.46	36.87	182.88	13.77	-	59.41	0.29	19.44	12.53
3080	4176.71	4019.08	116.77	45.44	64.88	12.52	98.23	210.82	30.20	173.48	12.53	3.50	66.45	0.69	15.11	15.68
3100	3813.96	3938.19	-	35.14	60.65	11.23	111.04	152.96	26.67	179.18	13.44	-	59.88	0.18	12.82	17.19
3120	3757.77	3605.16	69.01	33.27	50.39	47.94	135.05	207.87	38.23	163.48	13.39	4.45	64.41	0.27	17.27	17.45
3130	3245.02	4071.07	-	32.04	54.63	8.17	84.65	374.07	22.75	171.17	10.48	-	49.99	1.77	11.68	13.03
3140	3269.35	2956.76	82.42	-	34.56	3.83	48.71	367.05	16.43	123.28	8.31	-	40.00	1.77	12.39	11.56
3150	3019.09	2808.34	65.33	31.26	39.64	6.59	47.76	442.32	14.81	67.44	5.44	-	36.61	0.94	12.13	-
3160	2914.48	2673.40	-	-	34.74	9.90	40.23	502.62	18.21	95.44	7.72	5.50	38.21	0.23	10.58	16.93
3170	2566.38	2448.00	-	29.22	35.23	9.25	47.58	707.33	14.68	86.74	6.07	-	23.28	0.11	4.97	17.49
3180	2658.73	3063.47	84.27	22.99	45.11	7.14	60.12	425.30	17.63	103.38	9.53	-	40.86	0.31	10.99	19.07
3200	2767.28	2646.48	67.07	42.12	42.65	8.75	57.24	727.20	16.52	87.09	7.36	4.15	34.86	0.27	9.30	-
3210	2816.74	3203.41	62.87	29.21	69.76	10.22	88.17	183.04	23.60	118.09	10.84	3.99	48.45	0.20	8.55	12.35
3220	2836.15	3004.88	70.92	28.29	42.42	6.42	48.04	433.43	15.42	93.61	6.34	-	37.37	0.28	7.05	-
3230	2709.13	2801.94	-	27.87	28.19	8.66	34.29	367.09	12.25	69.77	3.73	-	32.18	0.13	9.03	13.94
3240	3249.99	3574.67	70.08	26.21	60.56	8.39	88.15	270.36	21.64	120.17	10.42	3.33	53.86	0.14	10.86	14.84
3250	2866.35	2392.60	74.42	27.85	30.77	6.91	39.42	389.69	13.62	75.94	5.02	3.76	27.84	0.26	5.79	-

3260	2959.01	2669.05	92.31	25.44	49.97	7.40	48.97	352.89	18.13	97.33	5.53	5.20	36.43	0.14	6.08	14.76
3270	2965.41	3377.68	90.80	61.96	49.38	8.67	83.51	359.69	25.48	123.84	9.54	-	56.75	0.16	7.67	18.38
3280	3033.45	3274.40	83.39	37.19	55.86	9.65	112.23	218.47	22.34	114.77	10.38	4.01	56.37	0.39	11.98	13.25
3200	2942.40	2632.71	64.26	22.13	37.68	5.58	44.29	401.59	12.82	81.30	5.09	-	27.33	0.30	8.06	13.09
3400	3355.44	3887.77	61.15	40.95	54.90	9.19	94.03	326.10	19.63	189.73	11.63	3.37	48.02	0.36	6.54	11.49
3410	2964.86	2885.03	87.96	39.11	49.45	7.75	62.08	446.14	15.52	99.00	6.67	-	43.59	0.14	16.61	14.38
3420	2484.02	1667.22	63.35	19.86	50.80	5.10	20.86	444.35	10.38	54.07	2.86	4.32	16.32	0.56	-	-
3430	2324.93	2243.54	-	26.40	40.97	3.72	44.15	721.52	13.88	100.80	5.94	3.80	28.20	0.15	5.68	13.97
3440	2576.12	1698.07	60.25	20.39	26.32	5.09	28.93	529.50	8.48	44.57	-	-	25.11	0.25	17.53	-
3450	2676.80	2420.40	84.09	43.19	39.44	-	48.22	401.72	12.28	72.83	6.80	10.45	31.24	0.09	11.33	-
3460	3497.18	2434.36	249.54	155.49	505.61	18.06	62.83	323.90	22.09	89.93	4.16	53.22	29.01	0.36	34.22	-
3470	2611.42	2283.91	-	29.94	131.65	7.84	46.70	418.05	14.67	83.47	5.36	18.18	27.19	0.23	12.48	13.54
3480	2960.12	3392.69	142.20	45.10	224.04	9.87	96.20	409.58	18.83	137.04	11.86	18.24	60.51	0.17	14.23	18.84
3490	2790.94	2734.26	98.21	49.77	683.88	8.28	49.38	533.17	14.73	71.62	5.26	10.33	38.62	0.19	9.86	-
3500	2976.28	3054.80	70.37	27.05	46.52	7.92	64.26	356.40	17.49	107.53	9.83	6.94	42.56	0.46	7.38	16.06
3509	2626.84	2226.08	96.58	29.09	65.15	10.02	45.07	473.64	12.00	77.22	4.37	5.24	38.90	0.18	9.55	13.30
3510	2941.46	2953.65	-	23.80	38.53	4.98	59.88	442.27	14.21	112.08	7.89	-	34.99	0.14	16.61	-
3520	2449.27	2302.60	78.14	22.69	32.48	7.47	55.63	458.76	14.54	94.84	5.89	-	29.99	0.12	8.17	14.61
3530	2754.86	1992.28	84.53	19.19	30.57	-	34.64	327.94	10.71	69.18	4.77	4.85	17.55	0.09	-	-
3540	3176.93	2664.16	88.37	34.73	46.04	7.88	59.73	369.80	16.17	100.72	8.25	3.38	34.11	0.24	7.36	10.79
3550	3520.28	4063.60	90.94	50.38	67.45	4.78	126.12	255.11	21.89	146.15	11.51	3.44	50.34	0.14	16.67	-
3560	2733.27	2939.63	53.59	30.90	54.92	7.23	75.63	427.99	18.28	113.06	10.73	4.61	47.66	0.19	11.21	11.63
3570	3224.62	3346.57	53.48	43.43	51.49	4.92	87.95	387.67	18.22	140.36	10.03	-	38.57	0.12	10.46	17.11
3580	3261.89	3901.04	68.24	27.19	51.31	8.68	102.02	192.74	22.42	223.18	11.63	3.40	41.94	0.20	11.01	14.49
3500	2630.35	2817.38	57.14	-	33.81	5.68	62.99	320.14	15.66	126.69	8.15	-	34.04	0.13	6.04	14.12
3562	2614.03	2943.54	62.44	19.69	56.18	5.75	70.66	411.53	15.91	109.98	7.70	4.01	36.14	0.17	10.06	-
3600	2585.73	3054.52	78.36	30.74	46.71	6.91	82.19	355.10	18.89	131.15	9.05	-	42.17	0.11	9.73	10.67
3610	3048.03	3699.57	50.57	40.56	55.36	7.88	94.85	340.07	23.00	172.89	11.41	3.45	44.56	0.12	8.53	17.47
3620	3355.00	3484.03	65.59	23.20	48.42	6.19	82.89	317.87	20.61	128.48	10.23	4.23	46.50	0.45	8.04	10.85
3630	3607.94	3423.30	-	32.47	53.45	6.49	77.97	348.27	18.31	130.10	10.45	-	38.83	0.22	-	-
3640	3478.55	3762.07	82.86	42.44	60.66	7.74	110.93	418.45	21.36	161.89	11.04	4.76	59.21	0.15	10.37	15.08
3650	4470.04	4270.68	73.14	57.42	86.04	12.10	128.06	156.59	27.35	184.50	15.55	4.30	63.75	0.23	20.81	18.88
3660	2866.22	3576.22	80.33	34.51	49.76	4.48	85.50	470.43	16.35	128.17	7.41	-	45.30	0.11	8.30	-
3670	3569.88	3705.35	66.41	43.89	56.13	6.67	94.58	399.11	23.25	151.84	10.24	4.01	46.29	0.54	5.45	16.64

3680	3102.55	4182.85	86.21	38.33	62.38	5.43	94.35	433.68	18.28	184.20	9.32	-	48.01	0.75	11.43	12.35
3658	3606.13	3606.47	62.33	36.37	46.95	10.35	97.72	416.77	19.21	152.37	12.77	-	45.17	0.21	11.24	15.02
3700	3619.89	3508.61	110.06	34.64	53.50	4.67	100.39	384.81	21.73	158.17	9.55	4.21	49.55	0.24	9.44	14.19
3710	4224.71	4893.25	87.42	33.23	73.58	8.78	106.19	350.70	45.43	1093.60	16.82	11.94	53.36	0.28	5.53	20.81
3720	4126.99	3964.57	64.51	41.59	66.21	11.16	111.15	237.26	25.66	188.22	12.74	-	61.61	0.15	9.61	-
3730	3697.68	4027.28	78.74	60.25	61.40	7.31	107.24	299.01	32.08	172.23	12.62	-	55.62	0.15	9.20	-
3740	3933.67	4088.58	71.48	38.91	73.45	11.05	99.64	269.29	25.02	179.62	10.07	4.14	53.39	0.12	8.36	17.22
3750	4235.19	3975.48	72.88	38.85	54.84	7.40	101.25	303.72	23.30	166.83	12.33	-	48.23	0.13	9.05	-
3760	4120.48	3743.19	110.82	47.42	80.73	13.11	113.86	308.58	21.19	171.49	12.53	-	57.75	0.10	10.12	14.50
3770	4399.29	4026.17	80.66	39.89	64.38	10.99	117.68	146.89	22.88	220.28	14.37	3.40	42.90	0.12	13.93	11.58
3780	3011.90	3068.01	75.74	26.09	47.92	10.86	79.85	295.68	21.12	135.42	10.51	-	51.14	0.16	11.48	17.47
3790	3274.54	4054.95	91.15	36.87	51.04	8.92	112.52	347.46	22.22	169.90	11.41	3.64	53.03	0.10	13.39	12.02
3800	3573.67	4084.94	98.62	37.92	47.91	9.91	106.84	364.75	24.75	182.61	12.37	-	59.74	0.10	12.25	13.30
3810	4988.45	3759.46	73.64	45.08	51.93	8.23	111.72	264.83	24.70	187.96	12.40	-	59.46	0.12	9.59	13.60
3820	3484.52	3883.79	-	40.71	47.94	5.62	107.53	333.08	28.85	194.11	13.86	3.67	46.09	0.12	10.43	16.33
3830	3773.46	3680.95	56.33	-	46.69	-	94.22	349.89	26.83	222.23	12.76	-	41.06	0.04	11.40	-
3840	3748.53	3115.92	-	39.24	36.92	5.47	91.76	303.99	18.07	144.50	9.53	3.86	37.27	0.08	6.42	-
3850	4069.34	3756.64	76.22	21.88	44.79	7.73	105.69	283.40	20.29	167.35	10.98	-	45.40	0.11	9.30	12.01
3860	4881.14	2783.17	51.79	39.86	39.55	6.24	71.86	202.04	16.10	130.84	8.90	4.61	44.04	0.05	6.83	14.17
3870	3895.84	3767.69	60.84	46.25	55.31	9.46	101.21	406.40	21.78	146.15	11.49	-	56.36	0.31	10.68	19.14

16. Table 7: Results Showing Mineral Content of the sediments in Hottman-Furthmeyer #1

Depth (ft)	Qtz + Carbonates (%)	Quartz (%)	Chlorite (%)	Illite (%)	Calcite (%)	Dolomite (%)	Feldspar (%)	Albite (%)	SiO2 (%)	UNIDENTIFIABLE (%)	Total (%)
3150	45.4	21.4	6.1	19.3	19.6	4.4	4.4	7.4	7.1	10.3	100
3160	36.1	16.3	5.8	23.4	15.9	3.9	3.8	11.2	8.7	10.9	99.9
3170	42.9	18.5	4.8	21.4	19.7	4.7	3.7	8.8	7.9	10.5	100
3180	39.9	17.5	6.3	20.4	16	6.4	5	9.6	7.6	11	99.8
3190	33.6	15.9	5.6	25.6	12.4	5.3	4.5	9.9	9.5	11.1	99.8
3200	39.6	17.2	5.1	21.5	16.7	5.7	4.9	9.5	8	11.4	100
3210	41.6	20.3	6	20	15.8	5.5	4	11	7.4	10.1	100
3220	31.7	16.3	6	23.4	10.5	4.9	6	13.6	8.7	10.5	99.9
3230	39	20.8	4.9	22.2	12.2	6	5	11.6	8.2	9.1	100
3240	36.5	15.1	7	20.4	17	4.4	5.5	10.4	7.6	12.6	100

3250	45.5	18.6	3.2	21.7	20.4	6.5	3.6	6.4	8	11.5	99.9
3260	38.8	16	6	24.3	18.7	4.1	1.9	7.6	9	12.4	100
3270	39.1	16	5.1	18.6	19.6	3.5	7.7	8.7	6.9	13.8	99.9
3280	41.8	16.8	6.1	18.1	21.2	3.8	6.2	8.2	6.7	13	100
3290	42	15.9	4.9	19.9	23.1	3	4.4	8.7	7.4	12.6	99.9
3300	42.6	16.1	6.6	17.4	23.2	3.3	4.6	8.9	6.4	13.4	99.9
3310	42.7	16.4	4.2	20.6	22.9	3.4	4	8.9	7.6	12	100
3320	34.8	12.2	4.2	22.9	19.1	3.5	4.7	11.5	8.5	13.4	100
3330	41.4	15.1	4.5	20.4	18.1	8.2	4.3	9.3	7	13.1	100
3340	38.5	14	5.9	18.7	18.9	5.6	5.6	9.7	6.9	14.7	100
3350	42.1	16	6.1	19.9	21.3	4.8	4.5	11.1	3.2	13.1	100
3360	40.2	15	4.3	20.2	20.4	4.8	4.3	10.4	7.5	13.3	100
3370	42.1	16.5	6.7	17.8	20.6	5	4	9.2	6.6	13.5	99.9
3380	39.9	16.2	7.1	17.5	18.5	5.2	3.8	12.3	7	12.6	100
3390	44.5	17.9	7.3	17.6	21.5	5.1	4.4	8.6	6.5	11.1	100
3400	44.8	17.1	6.3	16.7	23.3	4.4	4.9	9.5	5.7	12.2	100
3410	40.2	15.2	7	19	21.4	3.6	5.6	7.4	7	13.7	99.9
3420	43.7	15.4	4.4	19.1	24.6	3.7	5.3	9	7.1	11.4	100
3430	37	13.9	5.2	18.7	20.2	2.9	7.9	10.5	6.9	13.9	100
3430	36.8	15.4	6.2	24.9	18.5	2.9	3.1	7.4	9.2	12.3	99.9
3440	44.2	15.2	5.9	17.5	26.5	2.5	4.3	9.8	6.5	11.7	99.9
3450	39.3	14.9	6.6	20.2	21.8	2.6	5.5	7.3	7.5	13.8	100
3460	38.2	14.6	4.8	21	21	2.6	4.1	11.1	7.3	13.5	100
3470	40.5	18.8	5.2	20.3	17.8	3.9	4.6	11.7	7.5	10.1	99.9
3480	38	16.4	4.9	19.1	17.2	4.4	4	14.8	7.1	12.1	100
3490	40.7	18.8	5.6	20.1	17.7	4.2	4.6	10.3	7.4	11.3	100
3500	41.8	18.8	4.1	20.2	19.1	3.9	6	9.1	7.5	11.2	99.9
3510	41.3	19	5.1	20.4	18.4	3.9	5.3	9.2	7.6	11.1	100
3520	39.1	17.3	4.9	20	16.8	5	4.9	12	7.4	11.7	100
3530	34.8	17.8	5.1	23.8	13.6	3.4	5.8	10.9	8.8	10.9	100
3540	36.3	16.3	5.5	21.9	16.6	3.4	4.5	12.3	8.1	11.4	100
3545	39.8	18.2	4.1	21.2	17.5	4.1	5.1	11.3	7.9	10.8	100
3545	33.4	16.4	4.9	23.5	13.3	3.7	7.3	11.3	8.7	10.9	100
3545	38.2	18.5	3.8	23.3	16.4	3.3	5.9	10.2	8.6	10	100

3550	40.9	18.6	3.2	20	16.7	5.6	6	11.6	8	10.2	99.9
3560	43.4	18.7	3.2	21.8	19.3	5.4	4.4	8.9	8.1	10.3	100
3560	41.4	17.1	4.6	18.4	20.8	3.5	5.6	10.7	6.8	12.5	100
3560	39.7	15.6	6.3	19.7	18.8	5.3	6.3	7.6	6.8	13.6	100
3570	38.3	17.9	5.4	19.2	16.1	4.3	4.2	14.8	7.1	11.1	100
3580	41.6	16.5	5.2	20.7	19.8	5.3	4	9	7.7	11.8	100
3590	40.2	16.7	6.6	19.4	16.8	6.7	3.4	10.4	7.2	12.9	100
3600	34	13.1	5.1	24.7	16.9	4	4.8	10	9.2	12.4	100
3600	39	14.7	5.8	18.5	19.6	4.7	6.5	10.2	5.9	14	99.9
3600	31.7	16	5.7	25.7	12.9	2.8	5.2	11	9.5	11.2	100
3610	29.1	14.3	6.1	28.2	11.6	3.2	4.1	9.9	10.5	12.1	100
3620	37.4	15.5	5.6	22.2	19.5	2.4	4.3	10.8	8.2	11.4	99.9
3630	40	19	6.4	22.1	17.4	3.6	3.1	9.2	8.2	11	100
3640	35.2	15.4	5.7	23.4	16.4	3.4	6.3	8.4	8.7	12.5	100
3650	42.6	19	7.1	20.5	19.7	3.9	4.6	6.6	7.6	11	100
3660	34.4	14.6	5.3	22.3	17.5	2.3	5.3	11	8.3	13.4	100
3670	42.3	17.6	5.3	19	22.2	2.5	5.7	8.6	7.1	11.9	99.9
3690	38.7	16.3	5.3	20.5	19.8	2.6	5.3	10.2	7.6	12.5	100
3700	33.7	14.9	4	25.3	16.7	2.1	5.9	9.2	9.4	12.4	99.9
3712	40.9	16.2	5.1	20.3	21.3	3.4	5.3	7.8	7.5	13.2	100
3712	36.5	13.8	7.6	18.5	19	3.7	5.6	11.5	6.9	13.4	100
3712	36.1	15.6	6.1	19.5	17.5	3	7	10.8	7.2	13.3	100
3720	33.7	14.3	5.8	22.1	16.4	3	5.6	11.7	8.2	13	100
3730	40	17.2	5.6	21.6	20.1	2.7	4.2	8.3	8	12.3	100
3740	40.2	16.5	5.2	20.8	21.1	2.6	4	9.2	7.7	12.9	100
3750	39.5	15.4	5.4	20.8	21.1	3	5	8.6	7.7	13.1	100
3760	35.6	16	5.4	21.5	16.8	2.8	5.1	12.2	7.5	12.6	99.9
3770	30.4	14.7	5.6	22.3	13.6	2.1	7.7	14.1	8.3	11.6	100
3780	34.3	16.2	5.4	24.7	15.3	2.8	4.5	11.1	9.1	10.9	100
3780	36.5	14.2	5.8	21.7	19.6	2.7	5.2	8.9	8.1	13.8	100
3790	31.1	16.6	4.8	28.2	11.9	2.6	5.4	9.1	10.4	10.9	99.9
3800	37.5	17	6.8	22.7	17.3	3.2	4.8	9.3	8.4	10.5	100
3810	40.3	20.9	5.8	21.4	17.5	1.9	4.8	9.6	7.9	10.2	100
3820	38.7	17.2	6	19.9	18.6	2.9	5.9	10.1	7.4	12.1	100

3830	39.5	18	5.3	19.4	18.9	2.6	6.6	10	7.2	12	100
3840	39.8	18.8	5.7	21.9	18.6	2.4	5.3	8.9	8.1	10.4	100
3850	41.5	19.6	6.9	17.6	18.8	3.1	6.3	10.9	5.8	11.2	100
3855	37.9	18.3	6.4	21.2	16.4	3.2	6.6	8.9	7.8	11.2	100
3855	33.6	18.5	7.5	23.3	12.8	2.3	5.1	11.4	8	11.1	100
3860	35.2	21.3	6.8	21	10.2	3.7	5.9	13.3	7.8	9.8	99.8
3860	38.1	20.5	6.3	21.8	15.3	2.3	5.7	9.8	8.1	10.2	100
3860	39.1	21.5	5.6	25	14.5	3.1	3.3	8.9	9.3	8.8	100
3860	38	24.6	4.3	24.1	10.3	3.1	6	10.2	8.9	8.4	99.9
3870	32.4	19.4	7	27.8	10.2	2.8	5.5	8.1	10.3	9.1	100
3880	29.9	20.4	6.2	25.6	7.6	1.9	5.8	12.5	10.1	9.8	99.9
3890	33.5	19.9	4.8	26.7	10.4	3.2	5.7	9.6	9.9	9.8	100

17. Table 8: Results Showing Mineral Content of the sediments in Yocemento #1

Depth (ft)	Qtz + Carbonates (%)	Quartz (%)	Chlorite (%)	Illite (%)	Montmorillonite (%)	Calcite (%)	Dolomite (%)	Feldspar (%)	Albite (%)	SiO2 (%)	UNIDENTIFIABLE (%)	Total (%)
3150	39.4	15.5	5.4	20.9	-	20.2	3.7	6.9	6.5	7.7	13.2	100
3160	40.4	15.4	3.6	23.4	-	19.8	5.2	0.3	9.6	9.7	13	100
3170	37.3	14.9	5	24.1	-	18.8	3.6	3.6	8.3	8.9	12.7	99.9
3180	37.9	13	4.9	17.7	-	21.1	3.8	6.3	12.7	6.6	13.9	100
3190	36.1	15.6	5.8	20.8	-	16.1	4.4	6.9	10.8	7.7	11.9	100
3200	35.2	15.7	4	21.2	-	15.3	4.2	5.7	14.1	7.9	12	100
3210	36.2	17	4.3	21.4	-	14.6	4.6	5.4	14	7.9	10.8	100
3220	34.8	13.2	6.8	18.9	-	18	3.6	5.3	11.8	7	15.4	100
3230	33.3	12.9	5.7	23.3	-	17.3	3.1	5.8	9	8.6	14.3	100
3240	37.1	13.9	5.9	18.7	-	19.9	3.3	4.5	12.6	6.9	14.1	99.8
3250	40.2	12.9	6.5	18.8	-	24.2	3.1	5.9	10.1	7	11.6	100
3260	34.5	14.4	5.9	22.1	-	17.3	2.8	4.7	12	8.2	12.5	99.9
3270	39.1	12.5	7.5	21	-	23.5	3.1	5	6.4	7.8	13.2	100
3280	39.5	12.2	5.3	22.6	-	25.2	2.1	4.7	8.1	8.4	11.3	99.9
3290	36.4	11	5.7	24.7	-	21.7	3.7	4.1	7	9.2	13	100
3300	36.7	11.2	4.1	18.4	-	22.4	3.1	5.5	8.3	6.4	11.5	99.9
3310	34.2	11.5	6.8	21.9	-	19.2	3.5	6.8	7.9	8.1	14.2	99.9
3320	40.1	11.6	7	19.3	-	24.8	3.7	5.4	9.2	7.2	12	100

3330	34.5	12.7	6.3	22.9	-	19.1	2.7	5.2	8	8.5	14.6	100
3340	39.2	12.8	5.8	17.7	-	22.8	3.6	3.6	11.5	9.1	13.1	100
3350	38.7	11.2	5.5	18.5	-	23.7	3.8	5.1	12.1	6.8	13.2	99.9
3360	38.7	12.4	4.7	21.8	-	22.9	3.4	5	8.5	8.1	13.2	100
3370	37.5	11.4	5.4	19.4	0.4	21.7	4.4	7.6	9	7.2	13.5	100
3380	34.2	10.6	6.5	21.3	0.4	19.8	3.8	5.4	10.9	7.9	13.3	99.9
3390	34	10.4	6.1	20	0.3	21.1	2.5	6.3	6.8	7	13.6	100
3400	39.7	12.2	7.6	17.6	0.4	24.6	2.9	5.9	10.3	6	12.5	100
3410	43.3	13.9	6.2	20.9	0.3	25.1	4.3	4	5.8	7.8	11.9	100
3420	41.4	13.1	5.3	19.1	0.4	24.6	3.7	4.7	10.2	7.1	11.9	100
3430	45.2	14.8	5.7	19.2	0.2	26.7	3.7	5	6.2	7.1	11.2	99.8
3440	41.1	14.3	4.6	19.6	0.3	23.5	3.3	4.3	9.6	7.3	12.5	99.9
3450	36.9	11.7	6	20.9	0.3	21.3	3.9	6.9	6.8	8.4	13.2	100
3460	44.6	13.5	5.5	19.1	0.4	28.1	3	6.1	4.8	7.6	12	100
3470	24.2	7.5	15.3	18.6	1.7	14.3	2.4	2.6	7.9	3.2	26.5	100
3480	22.8	5.7	10.8	15.5	2.4	13.2	3.9	8.2	7.3	6.2	26.6	99.8
3490	20.9	7.2	13.6	17.3	0.8	10.4	3.3	6.8	6.5	3.9	29.7	100
3500	47.7	16.8	4.5	20.8	0.3	28.3	2.6	3.1	7.4	4	12.1	99.9
3510	41.3	16.6	5.7	19.9	0.8	21.9	2.8	3.4	6.9	8.6	13.4	100
3520	36.8	14.6	4.5	21.6	0.3	19.3	2.9	5.3	10	8.6	12.9	100
3540	44.2	13.9	5.9	18.8	0.4	25.4	4.9	3.9	6.9	7.5	12.3	99.9
3550	36.2	13.2	5.4	19.9	0.9	20.2	2.8	8.2	6.6	8.5	14.3	100
3560	41.6	14	7.7	20.7	0.6	20.5	7.1	1.5	9.6	3.6	14.6	99.9
3570	36	17.2	7.2	26.9	0	14.1	4.7	4.8	8.3	3.4	12	98.6
3580	36.7	15.4	7.2	22.7	0.4	17.9	3.4	7	10.4	2.2	13.4	100
3590	41.5	12.6	7.2	22.1	0.5	22.6	6.3	4.2	6	4.1	14.4	100
3600	42.5	13.4	5.1	22.3	0.4	25.9	3.2	4.2	8.4	4.6	12.7	100
3610	22.2	9.8	3.8	13.1	0.4	11.2	1.2	17.6	16.4	4.3	16.8	94.6
3620	37.9	14.4	4.1	22.6	0.6	20.1	3.4	3.2	12.6	5.2	13.8	100
3630	43.6	15.8	1.7	20.5	1.4	24.9	2.9	6	9.1	4.7	13	100
3640	39	15	8	20.2	0	20.2	3.8	4.3	8.2	7.5	13	100
3650	35.9	12.4	7.6	19.6	0.3	20.4	3.1	5.5	9.4	8.2	13.5	100
3660	33.1	12.7	6.2	23.9	0.3	18.3	2.1	4.1	9.7	8.9	13.8	100
3670	37.1	12.9	6.6	24.2	0.3	20.2	4	3.8	5.6	9	13.4	100
3680	34	12.7	6.1	21.6	0.3	18.5	2.8	4.1	12.3	8	13.4	99.8

3690	35.1	10.6	6.1	22.2	0.3	21.8	2.7	4.7	10.1	8.2	13.3	100
3730	31.8	13.7	5.9	24.5	0.3	13.5	4.6	5	11.4	9.1	12.2	100
3740	33.5	15.6	5.3	25	0.3	14.9	3	4.3	10.7	9.3	11.6	100
3750	34.2	11.4	5.1	24.5	0.3	18.6	4.2	4.5	8.6	9.1	13.7	100
3760	42.1	12.8	5.7	19.6	0.4	23.3	6	3.2	8.5	7.3	13.4	100
3770	39.2	15.3	7.1	16.3	0.2	17.8	6.1	4.2	11.6	6.1	14	100
3780	36.5	12	5.3	24	0.2	21.1	3.4	6.3	5.9	8.9	12.9	100
3790	40.9	18.9	4.2	22.1	0.3	18.7	3.3	4.6	9.2	8.2	10.6	100
3800	37.6	14.4	6.9	22	0.3	19.7	3.5	5.2	6.8	8.2	13	100
3810	37.2	20.5	7.2	22.1	0.3	14.7	2	8.3	7.1	8.2	9.6	100
3820	37.5	18.8	5.9	21.2	0.2	16.6	2.1	5.3	6.5	7.4	10.3	100
3830	41	18.2	4.7	20.9	0.3	18.5	4.3	5.8	8.6	7.9	10.8	100
3840	42.3	16.3	6	20.4	0.3	11.7	14.3	6	5.4	7.6	12.1	100
3850	43.6	16.7	5.2	19.4	0.3	10.2	16.7	4.7	7.9	7.2	11.7	100
3860	48.1	14.8	5.4	16.1	0.3	7.2	26.1	5.3	6.6	6	12.2	100
3870	41.1	14.2	5.4	17.8	0.3	8.5	18.4	5.2	9.8	6.6	13.8	100

18. Table 9: Results Showing Mineral Content of the sediments in Mong Benno #1

Depth (ft)	Qtz + Carbonates (%)	Quartz	Chlorite (%)	Illite (%)	Calcite (%)	Dolomite (%)	Feldspar (%)	Albite (%)	SiO2 (%)	UNIDENTIFIABLE (%)	Total (%)
3600	37.9	17.3	7.1	18.4	17.0	3.6	6.2	11.9	6.8	11.7	100.0
3610	43.5	19.5	4.3	19.2	18.1	5.9	5.5	9.3	7.1	11.0	99.9
3620	39.4	16.6	7.4	16.4	16.7	6.1	6.1	10.4	7.7	12.8	100.0
3630	38.6	16.5	4.8	23.5	15.8	6.3	4.6	8.0	8.7	11.8	100.0
3640	42.9	19.6	6.8	19.3	16.7	6.6	5.6	6.8	7.2	11.5	100.0
3650	39.7	17.8	5.5	20.7	16.8	5.1	5.8	8.6	7.7	11.9	99.9
3660	40.8	17.4	4.7	17.2	18.7	4.7	6.3	10.8	7.5	12.6	99.9
3670	43.7	18.4	5.4	16.5	17.7	7.6	6.6	10.1	6.1	11.5	99.9
3680	39.5	18.4	5.0	21.4	14.9	6.2	5.2	10.1	7.9	11.0	100.0
3690	38.4	13.4	7.0	19.2	18.4	6.6	4.9	8.3	7.1	14.0	99.9
3700	39.6	18.4	4.6	19.8	17.1	4.1	6.0	10.1	7.3	11.5	99.9
3710	37.2	19.3	6.1	19.0	13.0	4.9	5.5	14.6	7.1	10.5	100.0
3720	38.3	16.9	4.9	19.6	18.2	3.2	4.8	14.1	7.3	11.0	100.0
3730	36.2	17.2	4.8	22.9	15.2	3.8	4.0	11.9	8.5	11.6	99.9
3740	33.7	17.2	5.8	21.6	12.4	4.1	6.9	11.8	8.0	12.2	100.0

3750	43.5	20.7	4.7	18.5	19.2	3.6	5.8	9.8	6.8	10.8	99.9
3760	33.8	17.1	6.9	23.0	11.3	5.4	4.2	11.9	8.5	11.6	99.9
3770	31.8	18.1	6.1	24.2	9.7	4.0	5.8	11.3	9.0	11.7	99.9
3780	32.2	18.0	6.9	24.0	10.8	3.4	5.0	8.7	10.7	11.6	100.0
3790	36.3	16.2	6.1	23.2	17.0	3.1	7.2	6.6	8.6	12.0	100.0
3800	30.6	15.4	7.1	20.6	12.7	2.5	8.7	11.7	8.2	13.1	100.0
3810	35.2	15.2	5.9	21.8	16.6	3.4	4.9	10.4	8.1	13.9	100.0
3820	36.1	16.4	5.3	22.0	15.0	4.7	5.3	9.1	9.8	12.4	100.0
3830	39.5	18.4	5.7	21.4	13.5	7.6	4.5	7.6	7.9	12.3	100.0
3840	32.6	15.8	5.1	26.9	14.0	2.8	4.5	8.8	10.0	12.3	100.0
3850	33.8	19.4	6.9	20.8	11.3	3.1	8.7	10.7	7.7	11.4	100.0
3860	39.5	16.6	7.1	17.9	19.2	3.7	8.1	7.9	6.6	12.8	99.9
3870	40.3	17.4	4.2	25.1	19.6	3.3	4.1	10.8	3.4	12.0	99.9
3880	35.0	16.1	4.2	24.4	15.1	3.8	7.1	7.7	9.0	12.5	99.9
3890	31.3	18.7	6.6	21.9	9.6	3.0	6.9	12.9	8.1	11.1	99.9
3900	37.2	20.5	6.2	22.0	13.8	2.9	4.9	11.3	8.2	10.1	99.9
3910	37.5	23.1	6.7	22.6	10.7	3.7	5.6	10.9	8.4	8.3	100.0
3920	29.8	16.9	6.1	15.0	10.8	2.1	2.3	8.0	5.3	10.4	100.0
3930	34.3	19.5	5.9	21.0	12.3	2.5	6.3	14.9	7.8	9.8	100.0
3940	37.7	19.7	4.4	22.8	14.5	3.5	7.9	9.6	7.9	9.9	100.0
3950	37.8	20.5	6.6	20.0	14.1	3.2	5.8	12.8	6.8	10.1	99.9
3960	38.2	20.5	5.7	20.1	14.4	3.3	5.7	11.3	7.5	10.7	100.0
3970	38.7	21.1	7.7	18.9	14.9	2.7	6.0	11.6	7.0	10.1	100.0
3980	38.2	26.3	3.9	25.9	9.4	2.5	5.3	9.1	9.6	7.1	100.0
3990	39.5	22.9	6.8	18.4	13.7	2.9	5.4	12.7	6.8	9.6	100.0
4000	41.2	24.3	2.8	21.7	14.2	2.7	4.9	11.6	8.0	8.8	100.0
4010	32.9	20.5	4.5	27.6	9.8	2.6	5.7	8.5	10.2	9.4	99.8
4020	29.8	21.4	4.8	30.6	6.4	2.0	5.9	8.9	11.3	8.6	99.9
4030	25.9	15.8	10.0	24.0	7.6	2.5	5.8	9.8	8.9	15.6	100.0
4040	36.3	25.5	4.9	22.7	8.4	2.4	6.0	13.8	8.4	7.8	99.9
4050	32.1	21.6	4.0	28.9	8.1	2.4	7.0	9.0	10.7	8.3	100.0
4060	34.3	17.7	4.3	27.0	14.9	1.7	5.0	9.8	10.0	9.8	100.0
4070	37.7	25.1	3.9	24.7	9.8	2.8	5.9	12.1	8.3	7.4	100.0
4080	32.1	23.8	6.9	25.7	6.4	1.9	7.6	9.8	9.5	8.3	99.9

4100	38.1	22.8	4.9	26.5	11.3	4.0	4.6	7.9	9.8	8.2	100.0
4110	35.1	18.4	3.2	28.0	13.2	3.5	8.1	6.4	9.1	10.1	100.0
4120	32.9	22.6	6.1	24.2	7.1	3.2	6.4	12.3	9.0	9.1	100.0
4130	35.0	23.8	6.0	25.6	8.2	3.0	5.8	9.9	9.5	8.2	100.0
4140	49.1	26.7	3.1	18.9	4.8	17.6	3.3	12.9	7.1	5.7	100.0
4150	39.1	23.4	6.0	24.9	12.3	3.4	4.6	8.1	9.2	8.1	100.0
4160	34.8	22.2	5.1	25.9	10.6	2.0	6.2	9.2	9.6	9.1	99.9
4170	32.1	22.8	4.4	30.6	7.2	2.1	5.3	7.9	11.3	8.4	100.0
4182	28.8	22.4	4.1	34.2	4.3	2.1	4.4	7.7	12.6	8.2	100.0
4190	26.3	21.2	4.4	36.1	3.5	1.6	4.3	7.3	13.4	8.2	100.0
4200	27.3	22.5	4.6	32.3	3.4	1.4	8.2	7.8	12.0	7.8	100.0
4210	32.5	27.5	2.6	29.6	3.3	1.7	4.5	13.0	11.0	6.9	100.0
4220	26.8	19.4	5.1	29.5	5.2	2.2	5.4	5.4	10.9	10.6	100.0
4230	28.5	22.9	5.4	28.5	3.8	1.8	6.4	11.1	10.6	8.5	100.0
4240	29.3	23.5	4.3	31.6	3.5	2.3	6.5	8.1	11.7	8.4	99.9
4250	35.1	28.9	3.9	28.5	3.9	2.3	6.7	8.0	10.6	7.2	100.0
4260	23.7	17.3	5.8	34.1	4.7	1.7	5.5	7.2	12.6	10.3	100.0
4270	33.0	22.6	4.1	33.8	6.1	4.3	3.4	7.8	10.5	7.4	100.0
4280	30.2	18.0	2.9	33.9	10.5	1.7	5.8	6.1	12.6	8.5	100.0
4182	31.7	23.8	5.0	29.8	5.7	2.2	4.7	9.7	11.0	8.1	100.0
4182	29.2	22.1	4.4	31.6	5.0	2.1	5.4	10.6	11.0	8.0	100.0
4285	33.3	24.1	5.1	30.3	5.4	3.8	4.6	9.7	9.6	7.3	99.9
4285	32.5	21.1	3.5	32.0	4.4	7.0	4.3	7.3	11.8	8.6	100.0

19. Table 10: Results Showing Mineral Content of the sediments in Rhian #3

Depth (ft)	Qtz + Carbonates	Quartz %	Chlorite %	Illite %	Calcite %	Dolomite %	Feldspar %	Albite %	SiO2 %	Unidentifiable %	Total (%)
3300	38.80	20.80	6.50	22.10	13.70	4.30	5.00	10.10	7.60	9.90	100.00
3310	39.80	22.10	4.50	21.80	14.20	3.50	4.50	12.00	8.10	9.30	100.00
3320	39.50	23.50	5.40	18.90	12.60	3.40	6.70	13.00	7.00	9.50	100.00
3330	38.40	22.20	5.50	21.90	13.00	3.20	7.20	9.20	8.10	9.50	99.80
3340	33.30	19.80	4.50	28.40	11.00	2.50	4.80	9.50	10.50	9.00	100.00
3350	37.40	19.80	5.00	23.10	15.40	2.20	5.60	11.00	8.60	9.20	99.90
3360	36.90	23.40	6.60	25.10	10.90	2.60	4.70	8.10	9.20	9.40	100.00
3370	27.80	16.50	3.90	23.60	8.90	2.40	4.00	8.00	8.70	9.70	100.00

3380	37.20	23.10	5.50	22.80	11.10	3.00	5.60	11.20	8.50	9.20	100.00
3390	35.20	22.50	5.40	24.00	9.10	3.60	6.30	12.30	8.90	8.10	100.00
3400	40.30	23.90	3.30	21.40	11.80	4.60	6.80	11.50	7.90	8.70	99.90
3410	38.20	22.90	5.40	22.60	11.30	4.00	4.70	11.10	8.40	8.80	100.00
3420	35.70	18.80	5.50	23.60	11.80	5.10	4.60	11.50	8.80	10.30	100.00
3430	38.20	22.30	4.60	21.80	11.30	4.60	7.20	10.80	8.10	9.20	99.90
3440	33.70	17.90	6.20	24.00	10.70	5.10	5.80	11.00	8.90	10.40	100.00
3450	36.70	23.20	5.30	20.80	9.40	4.10	6.60	14.40	7.70	8.60	100.00
3460	37.90	24.00	5.10	25.60	9.70	4.20	3.90	9.90	9.50	8.20	100.00
3470	38.10	24.90	3.60	24.30	9.60	3.60	4.80	12.00	9.00	8.20	100.00
3490	32.90	23.30	4.30	27.00	6.30	3.30	6.60	11.30	10.00	7.90	100.00
3500	39.10	24.80	5.00	20.00	11.10	3.20	7.00	13.50	7.40	8.10	100.00
3509	37.80	23.50	5.00	19.00	10.90	3.40	7.50	14.60	7.00	8.50	100.00
3510	33.10	21.30	4.10	24.80	9.10	2.70	6.80	13.30	9.20	8.70	100.00
3520	34.40	20.30	6.60	21.80	11.50	2.60	7.30	12.50	8.10	9.40	100.00
3530	34.70	20.50	3.50	25.70	11.30	2.90	5.00	12.60	9.50	9.00	100.00

20. Table 11: Results Showing Mineral Content of the sediments in Worcester #1

Depth (ft)	Quartz %	Chlorite %	Illite %	Calcite %	Dolomite %	Feldspar %	Albite %	SiO2 %
3010	24.8	4.6	28.2	3.3	4.3	6	10.3	10.6
3060	26.8	3.4	28.8	3.2	2.6	7.6	9.3	10.7
3070	21.9	5.4	31.5	3.3	3.9	5.3	9.1	11.6
3080	23.8	4.8	32	3.1	3.4	6.6	6.6	11.8
3100	25.5	3.1	27.4	6.1	4.8	5	10.3	10.2
3120	25	4	29	4.5	4.4	6.1	8.7	10.7
3130	25.9	5.2	25.5	4.7	4.1	6	12.3	9.5
3140	21.9	4.1	27.5	6.2	3.1	5.3	13.7	10.2
3150	24.2	5	23.8	9	4.6	6.9	9.9	8.8
3160	21.9	5.6	23.6	8.5	3.5	6.2	13.4	8.7
3170	20.9	6.1	22.2	11.3	5.1	5.9	11.4	8.3
3180	21.6	5.3	23.2	13.9	3.8	6.1	9	8.6
3200	22.3	6	24	11	4.3	5.4	9.3	8.9
3210	19.3	5.8	24.1	10.4	3.4	6.9	10.6	8.9

3220	22.9	4.7	24.6	9.3	4	4.5	12.7	9.1
3230	19.7	6.4	26.5	7.4	3.1	4.8	12.3	9.8
3240	21.8	5.7	23.5	11.4	4.1	5.2	10.6	8.7
3250	21.5	4.7	25.1	9	3.8	6.9	10.5	9.3
3260	20.3	6.6	20.1	16.4	3.9	5	9.7	7.4
3270	24.6	4.8	22	9.9	3.9	4.9	13.6	8.2
3280	16	5.8	20.1	18	2.8	4.5	13.3	7.5
3280	21.3	7	19.1	13.4	4.4	5	13.3	7.1
3200	23.7	4.1	21.2	11.3	4.5	5.7	13.1	7.9
3400	23.2	5.2	22.7	11.8	4.4	4.7	10.9	8.4
3410	23	4.9	22.5	10.7	3.6	6.5	12.5	8.3
3420	21.2	5.1	22.8	12.7	5.1	5.2	10.2	8.4
3430	21.4	6.4	20.9	14.1	4.1	6.1	10.4	7.7
3440	24.2	3.1	21.7	13.4	3.9	5.9	11.4	8.1
3450	21.7	4.3	19.4	20.1	3.8	4.2	10.4	7.2
3460	20	5.9	25.1	12.3	4.8	4	8.3	9.3
3470	20.2	3.7	23.3	13.3	3.5	5.7	12.6	8.6
3480	15	11	20.2	9	3.1	6.1	11.4	7.5
3490	24	4.2	21.5	12.9	4.2	3.9	13.1	8
3500	19.6	4.8	21	16.5	3.7	6.3	9.5	7.8
3509	16.2	4.8	26.1	15.6	3.4	3.9	10.1	9.7
3510	23	5.9	22.7	11	3.3	5.5	11.2	9.1
3520	23.9	5.6	23.3	10.7	2.6	5.7	11.2	8.6
3530	20.5	4.1	23.8	11.9	4.2	5	12.5	8.8
3540	20.1	4.6	27	9.3	2.9	4.8	12.5	10
3550	21.6	4.1	25.2	8.4	3.1	5.3	14.8	9.3
3560	24.2	3.1	23.9	11.2	3.4	5.9	11.4	8.8
3570	20.4	5.3	25.4	14.3	2.9	3.3	9.9	9.4
3580	19.7	5.4	22.9	13.6	2.5	5.6	10.9	8.5
3580	20.4	5.4	23.7	11.9	2.9	5	12.7	8.8
3562	19	3.9	23.9	13.1	2.4	6.2	13.1	8.8
3600	18.7	5.1	20.1	17.1	3.3	6.8	11.7	7.5
3610	17.2	10.5	21.5	6.7	2.5	5.6	12.9	8
3620	22.1	4	25.8	7.3	3.5	7.1	12.2	9.6

3630	23.2	4.2	22.7	12.9	4.8	6.5	8.1	8.4
3640	23.7	5.6	21.3	7.1	4.2	5.6	16.4	7.9
3650	22.2	4.6	21.9	10.3	3.5	6.3	13.8	8.1
3660	22.9	4.1	24.6	9.2	3.3	5.5	12.7	9.1
3670	23.8	4.7	23.5	8.2	3.8	5.8	13.2	8.7
3680	21.2	6.7	19	13	5.7	4.1	13.2	7.7
3690	23	4.6	22.6	11.7	4.4	6.5	15.8	2.6
3700	21.8	5.4	23.4	8.5	3.5	5.1	15.1	8.7
3710	25.2	5.1	27.1	3.7	3.2	6	12.2	10
3720	21.5	7.3	25.1	6.7	3.1	5.1	13.4	9.3
3730	23.7	5.5	23.3	8.2	3.7	5.7	12.9	8.6
3740	20.5	3.5	29.3	4.9	2.3	5.8	14.2	10.9
3750	25	4.8	24.5	5.2	2.8	6.1	15.3	9.1
3760	23	5.2	24.6	7.6	2.6	6.5	12.8	9.1
3770	20.5	4.5	29.2	4.6	2.6	5.6	14.2	10.8
3780	22.3	3.5	28	4.7	3.2	6.3	13.9	10.4
3790	22.7	5.2	24.5	7.8	2.5	5.5	14.1	9.1
3800	23.9	5.3	25.5	7.5	3.8	5.6	11.5	9.4
3810	21.6	4.2	27.1	7.4	2.8	6	12	10.1
3820	19.9	3.9	28.5	7.1	2.8	7.1	11	10.6
3830	22.1	4.3	29.5	6.6	3.5	4.5	10.5	10.9
3840	19	4.8	23.8	5.7	11.5	5.4	11.7	8.8
3850	21.8	6.6	23.5	3.9	10.8	7.1	9	8.7
3860	22.8	6.1	20.4	5.5	11.6	6.4	10.8	7.6
3870	31.2	5.1	13.7	3.2	15.4	6.1	13	5.1

**Fort Hays State University
FHSU Scholars Repository
Non-Exclusive License Author Agreement**

I hereby grant Fort Hays State University an irrevocable, non-exclusive, perpetual license to include my thesis ("the Thesis") in *FHSU Scholars Repository*, FHSU's institutional repository ("the Repository").

I hold the copyright to this document and agree to permit this document to be posted in the Repository, and made available to the public in any format in perpetuity.

I warrant that the posting of the Thesis does not infringe any copyright, nor violate any proprietary rights, nor contains any libelous matter, nor invade the privacy of any person or third party, nor otherwise violate FHSU Scholars Repository policies.

I agree that Fort Hays State University may translate the Thesis to any medium or format for the purpose of preservation and access. In addition, I agree that Fort Hays State University may keep more than one copy of the Thesis for purposes of security, back-up, and preservation.

I agree that authorized readers of the Thesis have the right to use the Thesis for non-commercial, academic purposes, as defined by the "fair use" doctrine of U.S. copyright law, so long as all attributions and copyright statements are retained.

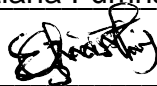
To the fullest extent permitted by law, both during and after the term of this Agreement, I agree to indemnify, defend, and hold harmless Fort Hays State University and its directors, officers, faculty, employees, affiliates, and agents, past or present, against all losses, claims, demands, actions, causes of action, suits, liabilities, damages, expenses, fees and costs (including but not limited to reasonable attorney's fees) arising out of or relating to any actual or alleged misrepresentation or breach of any warranty contained in this Agreement, or any infringement of the Thesis on any third party's patent, trademark, copyright or trade secret.

I understand that once deposited in the Repository, the Thesis may not be removed.

Thesis: Using Geochemical Composition to determine Paleoenvironmental Conditions and Source Inputs in Paleozoic Rocks within the Central Kansas Uplift, USA

Author: Christiana Fumnanaya Eziashi

Signature: _____



Date: 7/23/2022